ACTA PROTOZOOLOGICA

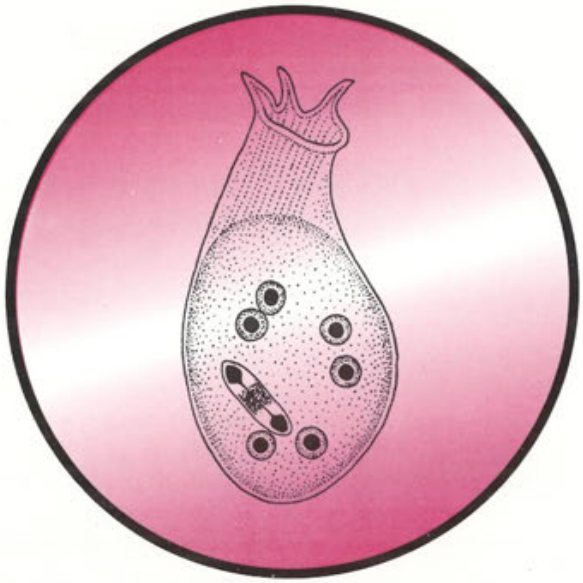

NENCKI INSTITUTE OF EXPERIMENTAL BIOLOGY
WARSAW, POLAND
1996
VOLUME 35 NUMBER 1
ISSN 0065-1583

Polish Academy of Sciences
Nencki Institute of Experimental Biology

ACTA PROTOZOOLOGICA

International Journal on Protistology

ACTA PROTOZOOLOGICA appears quarterly.

The price (including Air Mail postage) of subscription to ACTA PROTOZOOLOGICA at 1996 is: US $ 180.- by institutions and US $ 120. - by individual subscribers. Limited number of back volumes at reduced rate are available. For matters regarding ACTA PROOTOZOLOGICA, contact Managing Editor, Nencki Institute of Experimental Biology, ul. Pasteura 3, 02-093 Warszawa, Poland; Fax: (4822) 225342; E-mail: jurek@ameba.nencki.gov.pl

Front cover: *Stephanopogon colpoda.* In: I. B. Raikov - Kariologiya prosteishikh. Izd.Nauka, Leningrad 1967

Printed at the MARBIS, ul. Kombatantów 60, 05-070 Sulejówek, Poland

Acta Protozoologica (1996) 35: 1 - 2

Stanisław Dryl
(1922-1995)

Professor Dr Stanisław Dryl passed away in Warsaw on October 3rd, 1995. He was widely known among protozoologists for his investigations on the behaviour, excitability and electrophysiology of ciliates, especially *Paramecium*. Dr Dryl was first Deputy Editor (1963-70) and then Editor-in-Chief (1971-89) of **Acta Protozoologica**, having been involved in this international journal since its foundation by the Nencki Institute in 1963. He made contributions to the development of protozoology which made this journal proud to recognise.

Stanisław Dryl was born in Łódź, on March 14th, 1922. He graduated from secondary School in May 1939. During the Second World War he joined the Polish Underground Army AK (with the nickname "Rudy") and participated in the Warsaw Uprising as an Officer Cadet of the 21st Company AK, the Trojan group.

Settled in Warsaw Stanisław Dryl commenced medical studies at the clandestine Warsaw University and completed at Poznań University in 1946. He was simultaneously studying pharmacy in Poznań and continued to do so at the University in Łódź. He divided his time between duties as a part-time doctor in the 1st Clinic of Internal Diseases of the Medical Academy and work at the Nencki Institute of Experimental Biology in Łódź. As a result of his work at the Nencki Institute, Stanisław Dryl presented a thesis "The dependence of chemotropism in *Paramecium caudatum* on chemical changes in the medium" in 1951 and the degree of Ph.D. was conferred on

him. Dr Dryl moved to Warsaw when the Nencki Institute occupied its new buildings in 1953, and was appointed as an Assistant Professor in 1960.

Dr Dryl was nominated to be the head of the Department of Biology in 1961, and Department of Cell Biology (from 1971-84). He headed the Laboratory of the Physiology of the Cell Membrane of this department (1971-91). He was accorded the title of Associate Professor in 1970, and the title of Full Professor in 1979.

Research visits abroad and participation in scientific conferences and meetings played an important part in the academic activities of Dr Dryl. As a holder of a one-year scholarship of the Rockefeller Foundation he worked in the Laboratory of Genetics of Protozoa, Indiana University, Bloomington (1958-59) headed by Dr T. M. Sonneborn. Dr Dryl was awarded the W. Roehr scholarship to work in the Laboratory of the Physiology of Invertebrates, Institute of Zoology, University of Tokyo in 1963. This was a rewarding visit, as a result of which important papers were published with the well-known researchers Drs H. Kinosita and Y. Naitoh on the membrane potential in *Paramecium caudatum*. Three years later (in 1966) he received a scholarship from the National Science Foundation to continue his research in the Laboratory of Genetics and Physiology of Protozoa, at the University of Pennsylvania. During his stay in Philadelphia, he conducted research with Dr J. R. Preer on the motor response of *Paramecium aurelia* infected with kappa particles. In addition to these research periods he repeatedly visited the USA, Japan, France, Great Britain, Germany, Denmark, Spain and Italy, to lecture in well known scientific centers about his own research and that of his coworkers. He was a member of the Society of Protozoologists (USA) (since 1959) and a member of the Groupement des Protistologues de Langue Francaise since 1965. He participated three times in Gordon Conferences in Santa Barbara as well as in International Congresses of Protozoology (1961-89). At the Congress held in London (1965) Dr Dryl, together with Dr A. Grębecki, presented a leading paper on "Recent Advances in Research on Excitability of Ciliates", while at the Congress in Clermont-Ferrand (1973) he was President of a Round Table on "Ciliary and Flagellar Movement" and reviewed this subject in a joint paper with Dr T. L. Jahn. Together with Dr J. Zurzycki he organized an International Symposium on "Motile Systems of Cells" in Cracov (1971). Dr Dryl was a member of the International Commission of Protozoology (ICP) from 1973 to 1993. At the Congress in New York in 1977 the ICP entrusted the Polish protozoologists with the honour (and responsibility) to organize the VIth International Congress of Protozoology in Warsaw. Dr Dryl was elected the President of this Congress and the Chairman of the ICP for the period 1979-83. The VI International Congress of Protozoology (5-11 July, 1981) was held at Warsaw proved to be very successful, resulting in many scientific and social contacts, for which Dr Dryl deserves much credit.

Particularly important among Dr Dryl's studies and publications are those concerned: 1. Studies on the quantitative analysis of chemotactic and galvanotactic responses in *Paramecium* and *Stylonychia*; 2. Technique of macrophotographic registration of movement of Protozoan cells; 3. Quantitative research on relation between the membrane potential and ciliary reversal in *Paramecium* (together with Kinosita and Naitoh) and in other ciliates (in his own laboratory).

Comprehensive scientific monographs have had a particular impact on the development of research on ciliary activity and chemosensory transduction in ciliates, especially in *Paramecium*. In this field the input of Dr Dryl is really important. A treatise by Drs Dryl and Grębecki entitled: "Progress in the Study of Excitation and Response in Ciliates" was published in Protoplasma in 1966. In the comprehensive monograph "*Paramecium*: A Current Survey", edited by W. J. Van Wagtendonk, and published by Elsevier in 1974, Dr Dryl contributed a major chapter "Behaviour and Motor Response of *Paramecium*". A monographic 115-page survey by M. J. Doughty and S. Dryl on "The Control of Ciliary Activity in *Paramecium*: An Analysis of Chemosensory Transduction in a Eukaryotic Unicellular Organism" was published in Progress in Neurobiology (vol. 16, No 1, 1981).

All of us who have known Stanisław Dryl realize what a good man he was. He was free from any envy, and always ready to help unselfishly anybody who needed it. His death has left all his friends in Poland, and all over the world, grieving deeply.

Leszek Kuźnicki

ACTA
PROTOZOOLOGICA

Acta Protozoologica (1996) 35: 3 - 12

Review Article

Strategies for Cell-substratum Dependent Motility among Protozoa

Terry M. PRESTON and Conrad A. KING

Biology Department, University College London, London, England

Summary. Protozoa exhibit 2 major types of cell-substratum dependent motility, amoeboid locomotion and gliding. The latter is typified by essentially uni-directional progression at speeds in the order of micrometres per second, accompanied by neither distortion of cell shape nor overt cytoskeletal turnover. A consideration of the biophysical problems which constrain the gliding of protists identifies three fundamental requirements of this motile behaviour: (1) cell surface binding sites with which to attach to a substratum, (2) transmembrane connectors to link up with a cortical motor apparatus consisting of, (3) linear trackways along which the force-producing motor proteins may shuttle with their cargo. Simple calculations show that the energy required to power gliding in these cells is extremely small (of the order of 10^{-19} W in the case of the sporozoite of Plasmodium) and could be delivered by a very small number of motor proteins with the properties of myosins, kinesins or dyneins. This result tells us that the task of identifying the macromolecular assemblage of the hypothetical cell-surface linear motor (King 1988) will be a daunting one. Evidence for the presence of these essential elements of gliding motility is discussed in the case of 5 well known protistan examples - the sporozoites of *Plasmodium* and *Eimeria*, the trophozoite of *Gregarina*, the spindle cells of the net slime mould *Labyrinthula*, and the flagella of *Chlamydomonas*.

Key words: *Acanthamoeba*, amoeboid locomotion, *Chlamydomonas* flagella, *Dictyostelium*, *Eimeria* sporozoites, gliding locomotion, *Gregarina* trophozoite, *Labyrinthula* spindle cells, *Listeria*, *Naegleria*, *Plasmodium* sporozoites, sporozoite locomotion.

INTRODUCTION

Two general strategies for locomotion by unicells can be recognised: I - motility in the bulk liquid phase of the medium classically by using flagella or cilia. Protozoan motility using cilia and flagella has been extensively studied and reviewed (Ricci 1989) and will not be considered here. II - motility requiring the presence of a substratum (Preston et al. 1990 b) which can be further subdivided into: (i) crawling motility where (apart from the special case of the Hypotrich ciliates which creep about by means of their cirri (compound cilia) (Ricci 1990) there is continual change in the cell shape (cytoskeleton); (ii) gliding motility where there is apparently no overt change in cell shape.

There is a huge diversity of crawling motility displayed among the amoebae and detailed studies on *Dictyostelium* and *Acanthamoeba* have provided important insights into crawling motility in general including that of metazoan cells. A key feature of crawling locomotion is the extensive remodelling of the cell/cytoskeleton taking place during movement. This underlying activity in the cytoplasm has been demonstrated well using computer based studies on chick heart fibroblasts where although overt cell movement is only 0.02 μms^{-1} cytoplasmic bulk flow may reach 2 μms^{-1} (Brown and Dunn 1989). Although crawling movement has been studied for well over a century a universal hypothesis is lacking (Zigmond 1993). In order

Paper presented at the Symposium Motility, Behaviour and Orientation at the IX International Congress of Protozoology, July 25th - August 1st, 1993, Berlin, Germany

Address for correspondence: T. M. Preston, Biology Department, University College London, Gower Street, London WC1E 6BT, England; Fax:(+) 171 380 7096; E-mail: t.preston@ucl.ac.uk

for movement to occur in association with the substratum it is essential that traction can be developed via cell-substratum interactions. These can be highly specific requiring the interaction of special substratum molecules (e.g. fibronectin) with particular cell receptors (e.g. integrins) (Hynes 1992). However for many amoebae crawling on a glass slide this level of specificity does not exist. For instance *Naegleria* amoebae in de-ionised water (specific conductance <2 μScm^{-2}) can move across a coverslip at speeds of about 0.2 μms^{-1} (Preston and King 1978, Preston et al. 1990b) which is an order of magnitude faster than a vertebrate fibroblast.

Gliding motility has been a greatly ignored area of study and consequently we will concentrate on outlining the problems posed by and the solutions arrived at by protists employing this style of progression. Below we explore the factors which dominate this form of motility.

BIOPHYSICAL CONSIDERATIONS

Reynolds number and the world of small creatures

In order to achieve an understanding of the problems faced by microscopic organisms as they move through their environment we have to superimpose upon the light microscope images a filter of biophysical appreciation. Our views of motility are clearly influenced by visual experiences witnessed by our multicellular human form! For microscopic organisms moving in an aqueous medium, biophysical considerations are very different. These are generally expressed in terms of Reynolds number, which compares the viscous forces in the medium to the inertial forces generated by a motile organism. In its simplest form large organisms moving fast (in absolute terms) generate considerable inertial force in aqueous media, whereas small organisms moving slowly (in absolute terms) generate little inertial force. Mathematically this can be expressed as follows:

$$\text{Reynolds number (Re)} = \frac{\text{Inertial force}}{\text{Viscous force}} = \frac{v^2 r L^2}{v \eta L} = \frac{v r L}{\eta}$$

where: v = velocity, ρ= density of liquid (H_20), L = size of body (length) and η = viscosity (H_20), given that for H_20, $\rho = 10^3$ kg m^{-3} and $\eta = 10^{-3}$ Nsm^{-2}.

At low Re values (<1.0) inertial forces become insignificant, laminar flow occurs and the aqueous medium appears to behave like syrup or treacle. This contrasts with high Re values (>100; for example *Homo sapiens* swimming, Re = 10^6) where inertial forces are important and turbulent flow predominates (in these situations considerations of streamlining are important).

For a hypothetical protist of length 10 µm moving at a velocity of 1 μms^{-1} through water (density = 1.0, viscosity = 0.01 poise) would have a Re value of 10^{-5}. (These values are similar to those observed for the gliding sporozoite of *Plasmodium*).

Thus inertial forces are negligible and viscous forces predominate. The importance of these calculations stress that gliding can only occur when the unicell is developing traction and force generation on a substratum since there is almost zero inertial force in this microscopic world. This is clearly at variance to our concept of the gliding of a paper aeroplane or a rowing boat.

BIOLOGICAL MOTORS

Considerable advances have been achieved with respect to biological motors. A simple generalisation is the requirement for a cytoskeletal trackway along which a motor protein moves in a stepwise fashion using the hydrolysis of ATP as the energy source.

Motors based on microtubules

Microtubules are linear polymers composed of heterodimers of tubulin essentially organised as 13 axially orientated protofilaments producing a hollow cylinder with an exterior diameter of 24 nm. Each microtubule has an intrinsic polarity with a (+) and a (-) end (Preston et al. 1990b). The biological motors associated with microtubules are of two general kinds (a) kinesins, (b) dyneins. With certain exceptions each class of motor moves unidirectionally along a microtubule, the kinesins towards the (+) end and the dyneins towards the (-) end. Considerable knowledge has been gained on kinesin interaction with single microtubules. In general the ATPase activity of motor proteins is stimulated on interaction with the associate linear polymer. The step distance of kinesin on the microtubule is 8 nm (Svoboda et al. 1993) which represents the length of the tubulin α-β heterodimer.

Motors based on microfilaments

Microfilaments are linear polymers composed of monomeric actin essentially organised as a double helix. Again this polymer has intrinsic polarity with (+) and (-) ends; however only one type of motor protein has so far been discovered - the myosins - which move only toward the (+) end of the actin filament. The myosin

family of molecules is complex (initial phylogenetic DNA sequence studies suggested at least 7 discrete classes (Cheney et al. 1993), currently there are at least 11 members. Muscle myosin (myosin II) can form antiparallel arrays leading to the production of large bipolar filaments (muscle "thick filaments"). Myosin I molecules cannot form bipolar filaments since their tails lack the necessary conformation. Myosin I has been shown to be associated with the following motile phenomena - (a) contractile vacuole in *Acanthamoeba* (Doberstein et al. 1993) (b) organelle transport (Adams and Pollard 1986) (c) superprecipitation of actomyosin (Fujisaki et al. 1985). There is circumstantial evidence linking this motor to protrusive activity at the front end of crawling cells (Fukui et al. 1989). There is a difference of opinion concerning the step distance of myosin on F-actin (greater than 100 nm (Ishijima et al. 1991)) while measurements on individual molecules with optical tweezers suggest a value of 11 nm (Finer et al. 1994).

An alternative strategy to provide force might be through the agency of polymerisation of microfilaments at a localised site of G-actin addition. A prime example of this is provided by the bacterium *Listeria* moving within host cells. Motile *Listeria* are always associated with a "comet-like" tail of host F-actin associated with the posterior end of the microbe which provides the nucleation site for actin polymerisation. By this means the intracellular parasite can move at speeds of 0.1-1.0 μms^{-1} (Southwick and Purich 1994).

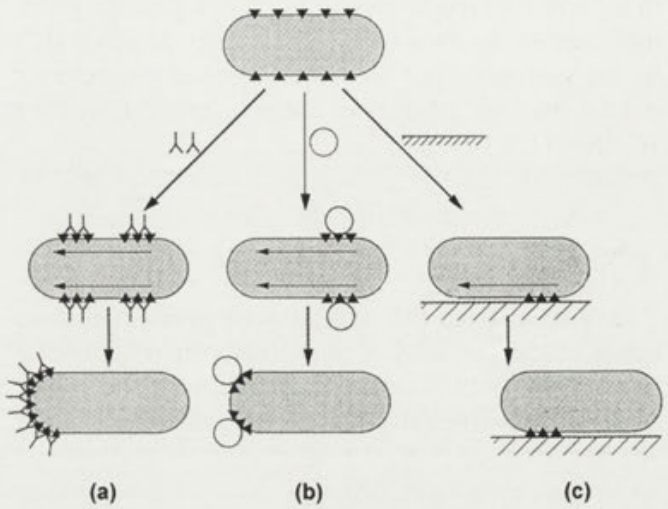

Fig. 1. A unified model for various forms of cell-surface motility. (a) Capping of surface antigen with antibody (⅄). (b) Translocation (and capping) of microbeads. (c) Overt gliding on a substratum. Closed triangles (▲) represent cell surface components which could be specific as in (a) or relatively non-specific as in the case of polystyrene beads (b) or a glass substratum (c). In the last case (c), since the substratum is immoveable, it is the cell that would move forward. The arrows within the cell outline indicate the hypothesised cell surface motors organised with an anterior-posterior polarity

CONCEPT OF CELL-SURFACE LINEAR MOTOR IN GLIDING CELLS

Observations on several gliding organisms point out that exogenous particles can be transported over the cell surface at velocities comparable with those attained during gross cell gliding suggesting that a common mechanism might be operating. A third manifestation of cell-surface associated movement is provided by the redistribution of surface antigenic binding sites on crosslinking by antibody or, in the case of *Acanthamoeba*, bacterial flagella (Preston and King 1984). Superficially there appears to be very little re-modelling of the cytoskeleton during the above types of motility. Therefore the movement-associated machinery might be more stable and so more amenable to analysis. These ideas have been embodied in the unified model of cell-surface associated motility of King 1988 (Fig. 1). All the three manifestations of this model are displayed by the sporozoite stage of *Plasmodium* - overt gliding and bead translocation (King 1988), and capping of circumsporozoite proteins (Stewart and Vanderberg 1991).

ENERGETICS OF GLIDING MOTILITY IN *Plasmodium* SPOROZOITES

The *Plasmodium* sporozoite (approximately 12 µm long x 0.8 mm diameter) can glide across a glass surface at speeds of around 1 μms^{-1}

1. Viscous drag (**F'**) concerns the problem of overcoming the viscous forces of the medium in order to move through it and can be approximated from Stokes' equation -

$$F' = 6\pi\eta rv$$

For a *Plasmodium* sporozoite the radius of the cell (r) = 0.4 x 10^{-6}m; viscosity of water $\eta = 10^{-3}Nsm^{-2}$; velocity (v) = 1 x $10^{-6}ms^{-1}$, hence **F'**= 7.5 x 10^{-15}N.

Since the sporozoite is clearly not a sphere but similar to a cylinder of length about 12 μm, this value might be increased by a factor of 10. The energy required (**E'**) by the sporozoite per second to move at this velocity = **F'** x distance moved per second , hence **E'**= 7.5 x 10^{-15}N x (1 x 10^{-6}ms^{-1}) Js^{-1}

$$= 7.5 \times 10^{-21} \text{ Js}^{-1}$$
$$= 0.75 \times 10^{-20} \text{ Js}^{-1}$$

2. Viscous force (**F"**) concerns the problem of shear forces in the thin film of aqueous medium between a moving cell and the underlying substratum and can be estimated from the following expression:

$$\mathbf{F''} = \frac{A\eta v}{h}$$

For a gliding sporozoite (**A**) = surface area of cell contact with the substratum. From reflection interference microscopy (RIM) (King 1995 unpublished) this contact has the following dimensions - width 0.3 μm and length 10 μm, hence (**A**) = 3 x 10^{-12} m^2 (h), the cell-substratum separation distance is estimated from RIM to be about 30 nm.

$$\mathbf{F''} = \frac{(3\times10^{-12})\times10^{-3}\times10^{-6}}{30\times10^{-9}} = 0.1\times10^{-12}\,\text{N}$$

It is important to note that shear forces may be reduced by the presence of molecules in the intervening gap between the ventral surface of the cell and the substratum. This may be significant in the case of the gliding motility of unicells. Nevertheless it needs to be underlined that cell-substratum interaction (traction) is essential for translational movement. The energy required (E") by the sporozoite per second to move at this velocity while overcoming viscous force = **F"** x distance moved per second, hence **E"**= (0.1 x 10^{-12}) x 1 x 10^{-6}

$$= 0.1 \times 10^{-18} \text{ Js}^{-1}$$
$$= 1 \times 10^{-19} \text{ Js}^{-1}$$

Therefore the total energy theoretically required by the gliding sporozoite to overcome the sum of viscous drag and viscous force is approximately 1.1 x 10^{-19} Js^{-1}. How does this compare with the known values of energy release from the hydrolysis of ATP? The maximum energy available from the hydrolysis of 1 molecule of ATP-> ADP + P_i is **1 x 10^{-19} J.** Surprisingly these calculations suggest that the hydrolysis of 1 molecule of ATP per second could power gliding of the sporozoite! Furthermore it informs us that huge arrays of cortical motor molecules are not required. Therefore the motor, although it may be stable may be difficult to discern ultrastructurally.

CELL-SUBSTRATUM INTERACTIONS

Classically this would require the interaction between the extracellular domains of molecules present in the plasmalemma and a substratum. These cell surface molecules would need to be anchored to the underlying cortical cytoskeleton in order to transmit force from the motor machinery to the substratum. Since the cell shape doesn't change during gliding one can imagine the cytoskeleton being "rigid" /stable. The technique of Reflection Interference Microscopy (Preston and King 1978) enables the cell-substratum interactions to be observed in moving cells. This technique is particularly useful for discerning intervening gap distances between 20-200 nm and any morphological differentiation in the cell contact.

SUMMARY OF GENERAL CONSIDERATIONS

Gliding protists need: (i) cell surface binding sites with which to attach to a substratum, (ii) transmembrane connectors to link up with motor proteins in the cortex, (iii) linear trackways along which the motor proteins may shuttle with their cargo.

What is the evidence for any of these components from the study of gliding protists?

Plasmodium

The sporozoite of *Plasmodium* has a thin, sickle-shaped cell profile. Its gliding motility has been extensively described (Stewart and Vanderberg 1988). One problem of studying the motile behaviour of this cell is the difficulty by light microscopy of identifying the anterior from the posterior end of the sporozoite! The general speed of movement is in the order of 1 μms^{-1}. However when the motility rates are studied over short time intervals then the rates of movement are much more erratic (Fig. 2). Since the gliding sporozoite has almost no inertial force (see previous Biophysical considerations paragraph), this erratic behaviour is a reflection of the variability of the force generation system acting on the substratum. As gliding proceeds, trails of the major

surface protein (circumsporozoite protein - CSP) are left behind on the substratum. This observation, the deposition of cell-surface material on the substratum, may be a feature of all gliding motility. Addition of anti-CSP antibody to sporozoites results in the formation of a bulky cap (capping) of material at the posterior end of the cell.

Although bi-directional movement of microbeads over the sporozoite has been observed (King 1988), usually beads are transported in an anterior-posterior sense resulting in a cap of beads at the extreme posterior end similar to that described in *Gregarina*. Bead translocation rates observed over short time intervals show the general erratic pattern seen in overt gliding, but the translocation rates are usually higher at about 12 μms^{-1}

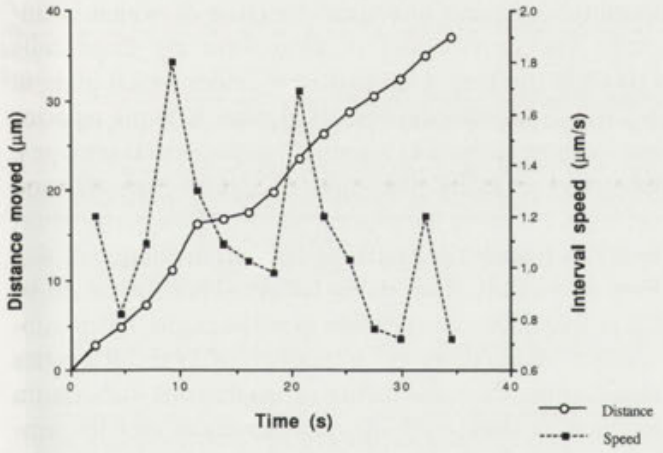

Fig. 2. Analysis of the gliding of a single *Plasmodium berghei* sporozoite across a glass substratum at 22°C. The open circles represent the total distance moved by the sporozoite from time = 0. Measurements were taken every 2.5 s. The closed squares represent the motility rates measured over the previous 2.5 s, expressed as μms^{-1}

(King, in preparation).

Dynamic cell-substratum interactions between the underside of the gliding sporozoite and a glass substratum can be demonstrated by RIM (Fig. 3). Gliding, but not the secretion of CSP (Stewart and Vanderberg 1991), can be inhibited by cytochalasin. This suggests the involvement of actin-based motility machinery.

The cloning and sequencing of two actin genes from *P. falciparum* has enabled the amino acid sequences of the two actin proteins to be deduced (Wesseling et al. 1988). One of these genes, *pf-actin I*, is expressed at all stages of the life cycle whereas the other, *pf-actin II*, is expressed only during the sexual phase occurring within

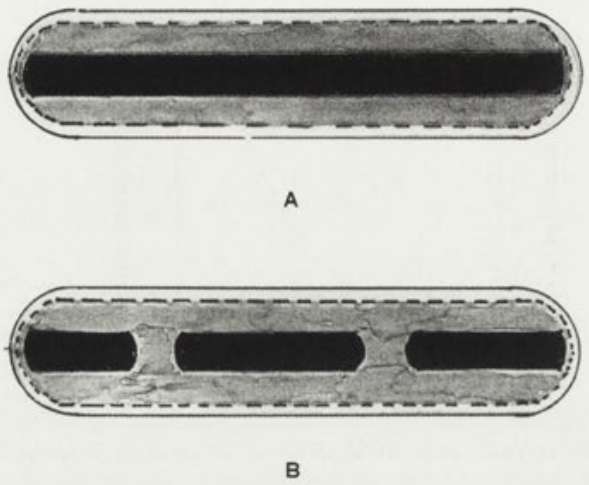

Fig. 3. RIM studies on gliding sporozoites of *Plasmodium*. The diagrams below depict the contact pattern obtained from the ventral surface of the sporozoite moving on a glass substratum. The width:length ratio of the sporozoite has been exaggerated. The general form of contact is shown in A. The solid outer line represents the cell profile. The dotted line represents the boundary to the contact area that can be detected by RIM. The solid central region represents the region of closest approach to the substratum. The central region of contact may not be continuous, as shown in B. The following can be deduced from such RIM images: **i** - the closest cell-substratum approach gives a separation distance of between 20-40 nm (say 30 nm), **ii** - the area of cell-substratum contact area in the closest approach zone = 10 µm x 0.3 µm = 3.0 μm^2 for A and 3.0 µm x 0.85 µm= 2.55 μm^2 for B

the female mosquito vector. It is of interest to note that only one actin gene has been found in *Cryptosporidium parvum* (Nelson et al. 1991) - an apicomplexan using only one host during its life cycle.

What is the biological function of gliding in this organism? Two obvious possibilities are to provide the means for (i) migration across the mosquito haemocoel and (ii) migration from the mammalian blood vascular system into the liver tissues.

Eimeria

The *Eimeria* sporozoite has a shape reminiscent of a twisted banana (12 µm long x 2 µm wide). A corset of microtubules positioned in the anterior two thirds of the cell gives a gyre to the cell form (Russell and Sinden 1982). There is a uni-directional movement progressing in cell length units at speeds of 2-10 μms^{-1} when moving over a planar glass substratum. As gliding proceeds trail material can be detected on the substratum (Entzeroth et al. 1989).

Translocation of 2 µm latex beads over the surface of the sporozoite can be observed (Fig. 4). It is important to note that the beads are translocated to the extreme

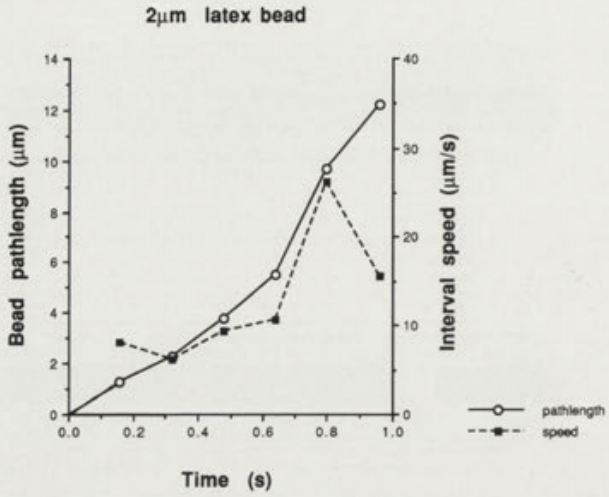

Fig. 4. Analysis of the movement of a 2 μm latex bead over the surface of a "non-gliding" sporozoite of *Eimeria tenella*. The bead initially attached at the front end of the cell and ended up at the extreme posterior end of the cell. The open circles represent the total distance moved by the bead from time = 0. Measurements were carried out every 0.16 s. The closed squares represent motility rates measured over the previous 0.16 s, expressed as μms^{-1}

posterior end thereby negating a major role for microtubule-associated motors in this phenomenon. Addition of the positively-charged ligand, cationised ferritin, results in the formation of a cap at the posterior of the sporozoite (Russell and Sinden 1981).

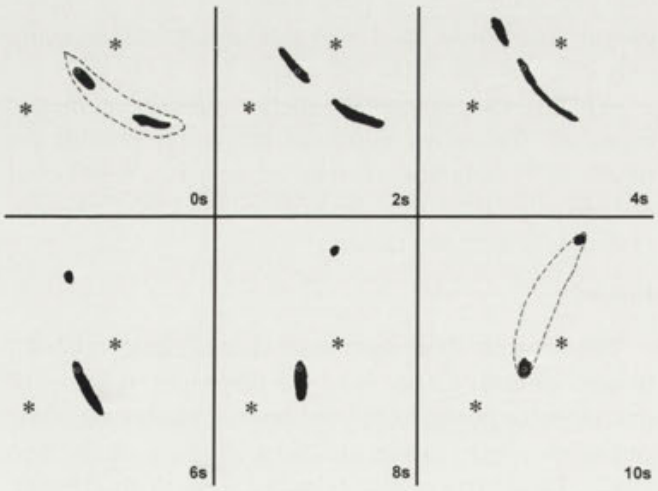

Fig. 5. RIM study on a moving *Eimeria tenella* sporozoite. The cell contact pattern made by the ventral surface of the cell with the glass substratum is shown in black.(*) - 2 fixed laboratory coordinates. Dotted line represents the cell profile (time = 0 and time = 10 s. O - Point contact maintained throughout the 10 s period. A hypothetical motor acting at this point could account for the cell length movement in the 10 s interval. This was a particularly slow-moving sporozoite and the general sequence depicted here would normally occupy a period of 1 s or less

Dynamic cell-substratum interactions can be demonstrated by RIM. Figure 5 shows a tracing of the sequence of contacts made with the substratum over a 10 s period. What is the nature of the linear motor in *Eimeria*? Motility is inhibited by cytochalasin (Baines 1988) indicating the involvement of an actin-based system. Actin has been demonstrated by immunoblotting (Baines and King 1989b) and there is evidence for actomyosin in cytoplasmic extracts (Preston and King 1992).

Concerning the biological function of gliding motility in *Eimeria* it may allow the sporozoites to escape from the sporocyst into the gut lumen and thereafter to invade the host intestinal epithelial cells.

Gregarina

Many parasitic gregarines demonstrate gliding motility, the exact biological function of which is unclear. The trophozoites of *Gregarina* are large cells (100-300 μm long x up to 40 μm wide) which glide at 1-5 μms^{-1} in a uni-directional manner with the anterior end leading, rather like microscopic motorised sausages. Observed casually the motion appears smooth and uniform, however measurements of velocity over short intervals reveals the fundamentally erratic nature of this form of motility. This might reflect either the nature of the power output or variation in the strength of cell-substratum interactions or a mixture of both. RIM has revealed the dynamic nature of trophozoite-substratum interactions during gliding. Contact areas vary in number, position and endurance. Nothing equivalent to the stable differentiated focal adhesion of *Naegleria* or *Acanthamoeba* is found. The structure of the cortex revealed by TEM is complex. Essentially the surface is thrown into numerous, closely-packed parallel folds extending along the anterior-posterior axis of the cell. The tips of these folds will be the sites of interaction with the substratum during gliding. These tips consist of two sets of membranes, a clearly defined plasma membrane and a double internal cytomembrane between which occur undefined filamentous structures. Internal to the double cytomembranes are found further filaments which have some of the properties of intermediate filaments (Schrevel et al. 1983).

Latex or glass beads added to these cells attach to them and are transported along their surface towards the posterior. Large diameter beads equivalent in mass to the trophozoites themselves are also transported at a similar speed. The bead-cell contact area here is very small which demonstrates the remarkable power output

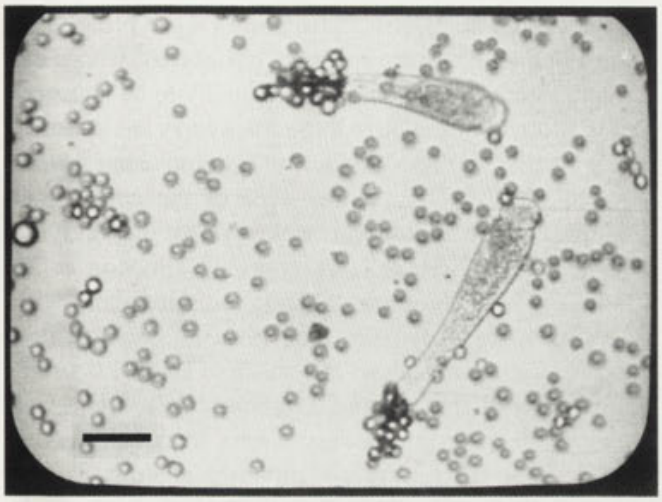

Fig. 6. Light micrograph of two *Gregarina* trophozoites moving on a glass substratum in the presence of 9.5 µm latex beads. Bar - 50 µm. A gliding cell comes in contact with a bead and following on from the initial adhesion event the bead is translocated backwards. When this happens several times it results in the formation of a bulky "cap" of beads at the posterior end of the cell

Fig. 7. Scanning electron micrograph of the posterior end of a *Gregarina* trophozoite which had been fixed after capping 2 µm latex beads. Note the surface folds of the gregarine pellicle

from the trophozoite motor. The beads follow a linear pathway which parallels the major axis of the gregarine. At the posterior the particles accumulate as a cap (Figs. 6, 7) implying the presence of a cell surface secretion binding them together. Whether this secretion is a highly hydrated polysaccharide is unknown but its optical properties preclude its detection by RIM.

Gliding and bead translocation share common features including unidirectional movement at similar rates and a sensitivity to both phenothiazine drugs and cytochalasins and an indifference to microtubule poisons. Cortical microtubules are present in the trophozoites but immunofluorescence microscopy reveals them to be arranged orthogonally to the major axis of the cell thus excluding them from a trackway function (Baines 1988). Cytochalasin inhibition points to the dynamic involvement of F-actin in these motile phenomena. Actin has been detected in trophozoites by immunofluorescence and located to the pellicle by immunogold TEM (Baines and King 1989a). Intriguingly both α-actinin and myosin (M_r = 175 kDa) have been found in *Gregarina blaberae* by immunofluorescence to be confined to longitudinal bands paralleling the cortical folds (Ghazali and Schrevel 1993). A hypothetical model of the cell-surface linear motor based on several lines of experimental evidence has been proposed and is shown in Fig. 8. Here the trackway is constituted by F-actin and the mobile elements by myosin. Conventional preparative techniques for electron microscopy have so far failed to reveal in thin sectioned trophozoites definite F-actin microfilaments in the cortex. Examination of rapid freeze-substituted trophozoites is needed

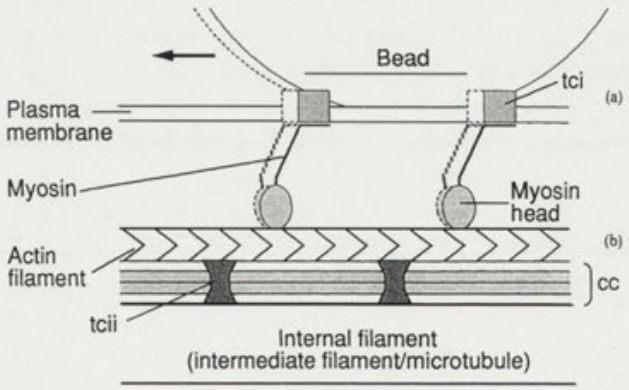

Fig. 8. A model for the cell surface linear motor in *Gregarina*.Transmembrane components (**tci**) span the plasma membrane and link the external ligand (in this case a bead) to the cytoplasmic motor. It is proposed that the tail region of myosin can link either directly or indirectly with "**tci**". Actin filaments are postulated to be associated with the cortical cytomembranes (**cc**) and interact with myosin head groups. The power stroke is developed by the myosin head group undergoing a conformational change on release of bound ADP + P_i. This change is depicted by the broken line image of myosin and would result in the movement of "**tci**" plus bead to the left. It is possible that another set of transmembrane components (**tcii**) link the actin filaments to the internal filaments (from King 1988)

either to confirm this or to demonstrate that indeed very few trackways are needed.

These three protists are related (Phylum Apicomplexa) and so are likely to have a common mechanism for generating gliding motility. The final two examples to be considered are phylogenetically distant from these and from each other.

Labyrinthula

Labyrinthula is a net slime mould that grows commonly on the surface of algae or marine plants such as *Zostera marina* in which it may produce a wasting disease (Muehlstein et al. 1988). This protist demonstrates during its life cycle three forms of cell motility. First there is the zoospore whose flagella are dispensed with on settling down onto a suitable substrate after a free swimming existence (Amon and Perkins 1968). The formation of a new colony involves rapid growth and extension of the cytoplasmic "net" by means of the extension across the substratum of exploratory filopodia from the periphery, adhesion of these extensions and the filling in of the axillary space by cytoplasmic protrusion (Preston and King, in preparation). This process is analogous to that which occurs at the advancing edge of many amoeboid or crawling cells or even the growth cone of neurones. Furthermore it is likely to be controlled by an actin-based cytoskeleton. This form of extension would permit *Labyrinthula* to breach plant surfaces (or that of animals such as crustacea) through abrasions and invade deeper tissue.

As the colony develops, a third form of motility is expressed - gliding - and this involves the spindle-shaped cells. These cells, 12 µm long x 4 µm broad, may glide along, and may be entirely confined by, what were termed "slime trails". Thought originally to be an amorphous extracellular matrix these trackways are in reality an amalgam of filopodia and other cytoplasmic extensions synthesized by pioneer cells of the colony that combine to form cylindrical trackways within which the gliding of fusiform cells is confined (Preston et al. 1990a). Gliding is predominantly unidirectional with cells migrating away from their place of origin within the colony to the periphery at a speed of about 1.0 μms^{-1}. Examination of colonies of *Labyrinthula* by RIM and scanning electron microscopy shows the trackways to be tethered to the substratum, although at a distance off it, by numerous filopodia. Fine, lateral processes from these interact to establish a reticulate network of fibrils on the substratum which effectively anchors each "slime trail" (Preston et al. 1990a). The overall effect is rather like a microscopic overhead urban monorail system. This is corroborated by RIM of living colonies grown on coverslips which confirms that the fusiform cells when gliding do not come into contact with the glass surface but distort the trackway and its tethering filopodia.

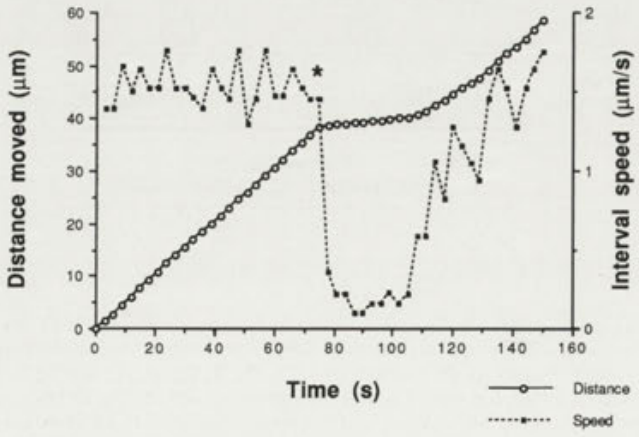

Fig. 9. *Labyrinthula* - Analysis of the gliding of a fusiform cell within the trackway of a colony. These cells appear to glide with uniform velocity within the trackway unless they encounter an obstruction (*). If the average velocity is measured over short intervals (here three seconds) it can be seen to be erratic

While gliding appears to be a smooth process when examined over short time periods it is seen to be erratic (Fig. 9) reflecting the discontinuous nature of the power output of the motile machinery. What can be said of the mechanism of gliding here? Fusiform cells when removed from the trackways onto glass or plastic by micro-manipulation no longer move, suggesting that the motile powers rest with the trackways. From this comes the simplest hypothesis that the fusiform cells attach to the trackway surface membrane and are transported like cargo by a surface located linear motor present in the trackways. So far we cannot exclude the possibility that the entire colony represents a syncytium, in which case the shuttling of spindle cells would be merely an exaggerated form of **intra**cellular transport, analogous to that occurring in axons. Since by means of immunofluorescence microtubules can only be detected in dividing cells within the colony, but not in the trackways themselves, we can exclude molecular motors associated with these elements as candidates to power gliding. On the other hand F-actin, recorded by HMM labelling ultrastructurally (Nakatsuji and Bell 1980), is abundant in the trackways as detected by fluorescence microscopy (Preston et al. 1990a), and immunochemistry. Actomyosin can be detected in sucrose-soluble high speed extracts of cultures together with a myosin I like protein

(detected by immunoblotting with anti-peptide antibodies designed to recognise common myosin I domains (Preston et al. 1992 and in preparation). Whether this mini-myosin is associated with gliding or with the amoeboid-like motile properties of the colony is not known at present.

Chlamydomonas flagella

In addition to generating wave forms providing the propulsive force enabling cells to swim through the bulk phase of the medium the flagella of *Chlamydomonas* have provided an excellent model system for studies on cell surface motility (Bloodgood 1989, 1990). Three manifestations of this phenomenon are displayed, not by the cell body but exclusively by the flagellar membrane-substratum-dependent motility, particle translocation and redistribution of surface components (Fig 11).

The alga can develop cell-substratum adhesions (confirmed by RIM - Fig. 10) with a glass slide by means of the flagella which orientate at 180° on the substratum. In this configuration *Chlamydomonas* can glide across the glass interface in a bidirectional manner at speeds of 1-2 μms^{-1}. Remarkably this motile property, presumably permitting anchorage and an alternative means of progression within soil interstices, persists in non-swimming paralysed flagella (*pf*) mutants.

Latex microbeads can be translocated at speeds of 1-2 μms^{-1} over the flagellar surface. Transport occurs in a linear fashion with respect to the distal-proximal axis of the flagellum. Furthermore beads can be seen passing each other moving in different directions even within local regions of a given flagellum.

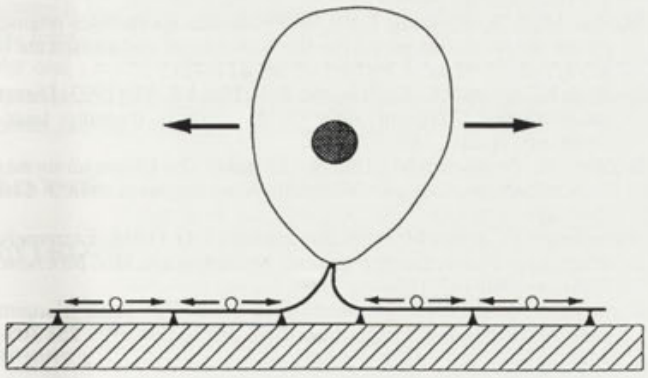

Fig. 10. Flagellar surface motility in *Chlamydomonas*. Diagram to show the bidirectional transport of attached beads and the flagella-substratum interactions during gliding. Potential force generation sites could develop at regions of close contact found at the areas of adhesion (arrowheads)

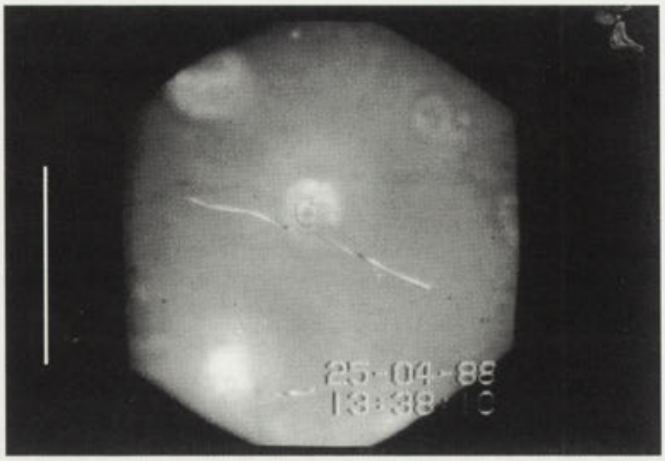

Fig. 11. Cell-substratum contact pattern of a gliding *Chlamydomonas* cell. Note the clear contact pattern made by the two flagella while the cell body is a much further distance off the substratum. Bar - 10 µm

Finally, redistribution on the flagellar surface membrane of component glycoproteins (Mr = 340 kDa) can be induced by the addition of the lectin Concanavalin A (Con A). Addition of fluorescently-tagged Con A to the cell sample initially results in uniform labelling of the flagellar surface followed by redistribution to form a "cap" of highly fluorescent material at the tip of the flagellum.

These three processes appear to be driven by the same force generation system and are important for the successful orientation of (+) and (-) gametes in the early stages of conjugation before the docking of the fertilisation tube. What of the motor system involved? Motility here is insensitive to the presence of cytochalasins, drugs which are generally inhibitors of actin-dependent motor systems. Therefore it is more likely that doublet microtubules of the axoneme could provide the trackway for the operation of a linear motor system analogous to that described for axonal transport. Whether all the 9 doublets, or simply a restricted number, take part is not yet known.

The polarity of the microtubule doublets is uniform with the minus end towards the flagellar base and plus end towards the tip. This demands that **either** there co-exist two distinct microtubule-associated motors already described from *Chlamydomonas* - an anterograde (e.g. kinesin (Bernstein et al. 1994, Walther et al. 1994, Fox et al. 1994, Johnson et al. 1994) and a retrograde (e.g. dynein) motor **or,** there might be

a novel single motor whose vectoral properties might be reversible, as in *Reticulomyxa* (Schliwa et al. 1991). It is envisaged that the hypothetical translocator molecule(s) might be recruited to cross link the cytoplasmic aspect of some cell surface components to the underlying microtubule trackway.

REFERENCES

Adams R. J., Pollard T. D. (1986) Propulsion of organelles isolated from *Acanthamoeba* along actin filaments by myosin I. *Nature* **322:** 754-756

Amon J. P., Perkins F. O. (1968) Structure of *Labyrinthula* sp. zoospores. *J. Protozool.* **15:** 543-546

Baines I. (1988) Studies on the motility and cytoskeleton of two Apicomplexan Protozoans (*Gregarina* and *Eimeria*). Ph.D. Dissertation, University of London

Baines I., King C. A. (1989a) Demonstration of actin in the protozoan - *Gregarina*. *Cell. Biol. Int. Rep.* **13:** 679-686

Baines I, King C. A. (1989b) Demonstration of actin in the sporozoites of the protozoan *Eimeria*. *Cell. Biol. Int. Rep.* **13:** 639-641

Bernstein M., Beech P. L. Katz S. G., Rosenbaum J. L. (1994) A new kinesin-like protein (Klp1) localized to a single microtubule of the *Chlamydomonas* flagellum. *J. Cell Biol.* **125:** 1313-1326

Bloodgood R. A. (1989) Gliding motility: can regulated protein movements in the plasma membrane drive whole cell locomotion? *Cell. Motil. Cytoskel.* **14:** 340-344

Bloodgood R. A. (1990) Gliding motility and flagellar glycoprotein dynamics in *Chlamydomonas*. In: Ciliary and Flagellar Membranes. (Ed: R. A. Bloodgood) Plenum Press, New York, 91-128

Brown A. F., Dunn G. A. (1989) Microinterferometry of the movement of dry matter in fibroblasts. *J. Cell Sci.* **92:** 379-389

Cheney R. E., Riley M. A., Mooseker M. S. (1993) Phylogenetic analysis of the myosin superfamily. *Cell. Motil. Cytoskel.* **24:** 215-223

Doberstein S. K., Baines I. C., Wiegand G., Korn E. D., Pollard T. D. (1993) Inhibition of contractile vacuole function *in vivo* by antibodies against myosin-I. *Nature* **365:** 841-843

Entzeroth R., Zgrzebski G., Dubremetz J.-F. (1989) Secretion of trails during gliding motility of *Eimeria nieschulzi* (Apicomplexa, Coccidia) sporozoites visualized by a monoclonal antibody and immuno-gold-silver enhancement. *Parasitol. Res.* **76:** 174-175

Finer J. T., Simmons R. M., Spudich J. A. (1994) Single Myosin Molecule Mechanics - Piconewton Forces and Nanometre Steps. *Nature* **368:** 113-119

Fox L. A., Sawin K. E., Sale W. S. (1994) Kinesin-related proteins in eukaryotic flagella. *J. Cell Sci.* **107:** 1545-1550

Fujisaki H., Albanesi J. P., Korn E. D. (1985) Experimental evidence for the contractile activities of *Acanthamoeba* myosins IA and IB. *J. Biol. Chem.* **260:** 11183-11189

Fukui Y., Lynch T. J., Brzeska H., Korn E. D. (1989) Myosin I is located at the leading edges of locomoting *Dictyostelium* amoebae. *Nature* **341:** 328-331

Ghazali M., Schrevel J. (1993) Myosin-like protein (M_r 175,000) in *Gregarina blaberae*. *J. Eukaryot. Microbiol.* **40:** 345-354

Hynes R. O. (1992) Integrins: versatility, modulation and signalling in cell adhesion. *Cell* **69:** 11-25

Ishijima A., Doi T., Sakurada K., Yanagida T. (1991) Sub-piconewton force fluctuations of actomyosin in vitro. *Nature* **352:** 301-306

Johnson K. A., Haas M. A., Rosenbaum J. L. (1994) Localization of a kinesin-related protein to the central pair apparatus of the *Chlamydomonas reinhardtii* flagellum. *J. Cell Sci.* **107:** 1551-1556

King C. A. (1988) Cell motility of sporozoan Protozoa. *Parasitol. Today* **4:** 315-319

Muehlstein L. K., Porter D., Short F. T. (1988) *Labyrinthula* sp., a marine slime mold producing the symptoms of wasting disease in eelgrass, *Zostera marina*. *Marine Biol.* **99:** 465-472

Nakatsuji N., Bell E. (1980) Control by calcium of the contractility of *Labyrinthula* slimeways and of the translocation of *Labyrinthula* cells. *Cell. Motil. Cytoskel.* **1:** 17-29

Nelson R. G., Kim K., Gooze L., Petersen C., Gut J. (1991) Identification and isolation of *Cryptosporidium parvum* genes encoding microtubule and microfilament proteins. *J. Protozool.* **38:** 52S-55S

Preston T. M., King C. A. (1978) An experimental study of the interaction between the soil amoeba *Naegleria gruberi* and a glass substrate during amoeboid locomotion. *J. Cell Sci.* **34:** 145-158

Preston T. M., King C. A. (1984) Binding sites for bacterial flagella at the surface of the soil amoeba *Acanthamoeba*. *J. Gen. Microbiol.* **130:** 1449-1458

Preston T. M., King C. A. (1992) Evidence for the expression of actomyosin in the infective stage of the sporozoan protist *Eimeria*. *Cell. Biol. Int. Rep.* **16:** 377-381

Preston T. M., King C. A., Cooper L. C. (1990a) Cytosquelette et motilité chez *Labyrinthula*. *J. Protozool.* **37:** 58A

Preston T. M., King C. A., Hyams J. S. (1990b) The cytoskeleton and cell motility. Blackie, Glasgow

Preston T. M., Baines I. C., King C. A. (1992) The gliding motility of the cellular slime mold *Labyrinthula* - a possible cytoskeletal motor. *Eur. J. Protist.* **28:** 353

Ricci N. (1989) Locomotion as a criterion to read the adaptive biology of Protozoa and their evolution toward metazoa. *Boll. Zool.* **56:** 245-263

Ricci N. (1990) The behaviour of ciliated protozoa. *Anim. Behav.* **40:** 1048-1069

Russell D. G., Sinden R. E. (1981) The role of the cytoskeleton in the motility of coccidian sporozoites. *J. Cell Sci.* **50:** 345-359

Russell D. G., Sinden R. E. (1982) Three-dimensional study of the intact cytoskeleton of coccidian sporozoites. *Int. J. Parasitol.* **12:** 221-226

Schliwa M., Shimizu T., Vale R. D., Euteneuer U. (1991) Nucleotide specificities of anterograde and retrograde organelle transport in *Reticulomyxa* are indistinguishable. *J. Cell Biol.* **112:** 1199-1203

Schrevel J., Caigneaux E., Gros D., Philippe M. (1983) The three cortical membranes of the gregarines. I. Ultrastructural organisation of *Gregarina blaberi*. *J. Cell Sci.* **61:** 151-174

Southwick F. S., Purich D. L. (1994) Dynamic remodeling of the actin cytoskeleton: Lessons learned from *Listeria* locomotion. *Bioessays* **16:** 885-891

Stewart M. J., Vanderberg J. P. (1988) Malaria sporozoites leave behind trails of circumsporozoite protein during gliding motility. *J. Protozool.* **35:** 389-393

Stewart M. J., Vanderberg J. P. (1991) Malaria sporozoites release circumsporozoite protein from their apical end and translocate it along their surface. *J. Protozool.* **38:** 411-421

Svoboda K., Schmidt C. F., Schnapp B. J., Block S. M. (1993) Direct observation of kinesin stepping by optical trapping interferometry. *Nature* **365:** 721-727

Walther Z., Vashishtha M., Hall J. L. (1994) The *Chlamydomonas* FLA10 gene encodes a novel kinesin-homologous protein. *J. Cell Biol.* **126:** 175-188

Wesseling J. G., Smits M. A., Schoenmakers J. G. (1988) Extremely diverged actin proteins in *Plasmodium falciparum*. *Mol. Biochem. Parasitol.* **30:** 143-153

Zigmond S. (1993) Recent quantitative studies of actin filament turnover during cell locomotion. *Cell. Motil. Cytoskel.* **25:** 309-316

Received on 26th July, 1995

Acta Protozoologica (1996) 35: 13 - 28

ACTA
PROTOZOOLOGICA

The Ultrastructure of the Somatic and Oral Cortex of the Karyorelictean Ciliate *Loxodes striatus*

Thomas KLINDWORTH and Christian F. BARDELE

Department of Zoology, University of Tübingen, Tübingen, Germany

Summary. The ultrastructure of the somatic and oral cortex of the karyorelictean ciliate *Loxodes striatus* was reinvestigated with the Fernández-Galiano silver carbonate impregnation technique, scanning electron microscopy and ultrathin sections. The laterally compressed ciliate has a densely ciliated right lateral side with 11 somatic kineties. The right dorsolateral kinety surrounds the posterior end of the cell. The left lateral side of the cell is sparsely ciliated showing only two separate longitudinal kineties, their two anterior ends meet near the anterior end of the cell and their posterior ends meet near the posterior end of the cell. These two kineties thus do not form a single circumcellular kinety as stated in the literature. The somatic dikinetids are shown to be slightly different compared to earlier data. The kinetodesmal fiber, T-shaped in cross-section, is one broad shovel-like structure with a keel. The buccal cavity is located at the anterior left end of the cell and has a tube-like vestibular extension of unknown function. The 4 longitudinal oral kineties are all composed of dikinetids with different kinetosome-associated fiber systems. From right to left there is a loxodid paroral of closely spaced dikinetids with the anterior kinetosome ciliated; an intravestibular kinety in which the posterior kinetosome is ciliated (this kinety extends into the vestibular extension); 3-5 widely spaced anterior left buccal dikinetids in which the anterior kinetosome is ciliated. On the left margin of the buccal cavity lies a closely spaced file of dikinetids which owing to the orientation of the kinetosome-associated fiber systems, quite surprisingly, is an inverted somatic kinety. The kinetids of this kinety have the anterior kinetosome ciliated and the posterior kinetosome has a kinetodesmal fiber each. Because of the kinetodesmal fibers in this kinety it is no true buccal kinety, instead the term left pseudobuccal kinety is suggested. It is assumed that this inverted kinety, probably originating from the somatic kinety K_1, has secondarily taken over the function of an adoral ciliature, because the primary adoral ciliature, the intravestibular kinety, during evolution, has sunken down into the oral cavity. Detailed schematic drawings of the somatic dikinetid and the 4 oral dikinetids with their kinetosome-associated fiber systems are presented. This study is a prerequisite to a light and scanning electron microscopical investigation on stomatogenesis in the genus *Loxodes* (see accompanying paper), undertaken with the authors' aim to reconstruct ciliate evolution *via* ciliate morphogenesis.

Key words: Ciliophora, Karyorelictea, kinetid pattern, *Loxodes striatus*, oral ciliature, somatic cortex, ultrastructure.

INTRODUCTION

Current ideas on the phylogenetic relationships among ciliates are dominated by molecular data which show that heterotrichs together with the karyorelictean ciliate *Loxodes* form the earliest branch on the ciliate tree (Baroin-Tourancheau et al. 1992, Fleury et al. 1992). These studies have supported earlier suggestions, raised long before molecular RNA data became available, on a phylogenetic link between the Heterotrichea and the Karyorelictea, then based on the overall similarity in the structural organization of the somatic cortex of *Loxodes* and *Spirostomum* (de Puytorac and Njiné 1970), and *Trachelorapbis* and *Blepharisma* (Gerassimova and Seravin 1976, Raikov et al. 1976), respectively. Oral structures, on the other

Address for correspondence: Ch. F. Bardele, Universität Tübingen, Zoologisches Institut, Auf der Morgenstelle 28, D-72076 Tübingen, Germany; Fax: + 49-7071-294634; E-mail: christian.bardele@uni-tuebingen.de

hand, show a bewildering diversity in karyorelicteans, while classical heterotrichs like *Blepharisma*, *Spirostomum* and *Stentor* show a rather uniform oral ciliature.

The majority of the karyorelictean ciliates are marine interstitial ciliates, only the genus *Loxodes* is found in microaerophilic fresh water habitats. Karyorelictean ciliates are characterised by the inability of their paradiploid (nearly diploid) macronuclei to divide during asexual reproduction (Raikov 1985). A remark made by Grell (1962) that ciliates with never-dividing macronuclei might be regarded as "karyologische Relikte" stimulated Corliss to introduce formally an order Karyorelictida Corliss, 1974, comprising at that time the Trachelocercidae, Loxodidae and Geleiidae at family level. Later on de Puytorac et al. (1984) added *Protocruzia* to the karyorelicteans notwithstanding the principle differences of nuclear behaviour in *Protocruzia* and the classical karyorelicteans. This "clustering" of karyorelictean ciliates is also presented in the most recent volume of the "Traité de Zoologie" (de Puytorac et al. 1994), though the authors are well aware that the question whether the karyorelicteans form a monophyletic taxon or a polyphyletic assemblage is not yet settled.

Because of the poor development of the pellicular alveoli and the absence of parasomal sacs, both well developed in higher ciliates, Small (1984) regarded the classical karyorelicteans not only as karyorelicts but also as corticorelicts.

Our interest in *Loxodes* is based on the research concept to reconstruct ciliate phylogeny through comparative studies of ciliate morphogenesis (Bardele 1987, 1989, 1991). The idea was to check whether karyorelictean ciliates show perhaps an ancient mode of stomatogenesis and thus form stomatogenic relicts. Some time ago when holotrichous prostome ciliates like *Holophrya* were regarded as the most primitive ciliates their holotelokinetal mode of stomatogenesis, involving all somatic kineties, was also regarded as primitive. Eisler (1992), based on theoretical considerations on the origin of the somatic ciliature from oral ciliature, has proposed that the buccokinetal mode of stomatogenesis might be the most primitive. And indeed, there are preliminary reports on a buccokinetal mode of stomatogenesis in *Loxodes magnus* (Tuffrau 1963, Njiné 1970) which urgently deserved reinvestigation with modern techniques. When we started to work on the ultrastructural aspects of stomatogenesis in *L. striatus* we soon realised that the information about the oral ciliature (de Puytorac and Njiné 1970) was incomplete, and required reinvestigation first.

In addition to some corrections concerning the somatic kinetid pattern we describe 4 different oral dikinetids, characterized by different arrangement of the kinetosome-associated fiber systems. There is no doubt that the comparative analysis of somatic kinetid pattern has been a very successful approach to ascribe almost all ciliates to one of the major ciliate classes, primarily on account of their different somatic kinetid patterns (Seravin and Gerassimova 1978; Lynn 1981; Lynn and Small 1981, 1988; Small and Lynn 1981, 1985). Lynn (1991) and several other ciliatologists have extended this approach to the buccal kinetid patterns realising there is a much greater diversity in oral kinetid patterns not only at class level but down to genus level. Nonetheless, we hope that our "stock-taking" of oral dikinetid patterns in *Loxodes* will help in the discussion of monophyly of these ciliates once equivalent ultrastructural data become available of other karyorelictean genera.

MATERIALS AND METHODS

Our strain of *Loxodes striatus*, identified according to the description of Kahl (1932/35) and Dragesco and Dragesco-Kernéis (1986), came from the Brühlweiher, a small shaded pond in Schönbuch forest near Tübingen. Cultures were grown in test-tubes, 15 cm in height, using the method described by Finlay and Fenchel (1986). The ciliates were fed twice a week with *Euglena gracilis*. According to their preference for low oxygen tension the ciliates accumulate one to several cm below the surface of the water column, from where they could easily be collected in large density. Among all the silver staining procedures tried the pyridinated silver carbonate method of Fernández-Galiano (1976) using the modification recommended by Augustin et al. (1984) gave the best results. In order to yield superior resolution on the infraciliature cells were fixed for 20 s in osmium vapour and postfixed for 3 min in 1% formaldehyde. Further steps of the staining procedure had to be completed within 45-60 s.

For scanning electron microscopy of the very delicate cells the Parducz fixative (1952) was used in a 1 : 100 relation of cells to fixative for 15 min at room temperature. Following partial dehydration up to 70% ethanol the cells were mounted on polylysine-coated cover slips, 12 mm in diameter, critical point dried, sputter-coated with gold-palladium and observed in a Cambridge Stereoscan 250 MK2.

For transmission electron microscopy cells were fixed on ice using the Shigenaka et al. (1973) procedure. Bloc-stained cells (Locke et al. 1971) were embedded in Epon 812 (Luft 1961). Bands of serial sections were mounted on Formvar-coated 1-slot copper grids, stained with uranyl acetate (Reynolds 1963) and viewed in a Siemens Elmiskope 102.

To facilitate the comparison of light microscopical, scanning, and thin section micrographs all micrographs shown in this paper were mounted as seen from outside the cell.

RESULTS

Light microscopy of cell shape and somatic ciliature

Loxodes striatus (Engelmann, 1862) Penard, 1917, is a laterally compressed leaf-like ciliate. A medium-sized living and non-squashed cell of our strain of *L. striatus* measured 180 µm in length and 50 µm in "breadth" in lateral view. As judged from non-fed fixed cells it is approximately 15 µm thick (For detailed morphometric data of *L. striatus* and *L. magnus* see Foissner and Rieder 1983). *Loxodes* has a small anterior beak pointing to the right when seen from the right lateral side (Fig. 1). Immediately underneath the beak, thus subapically, there is the oral cavity, often called vestibulum, which shows a funnel-like extension bowed toward the posterior dorsal direction. The length of the oral cavity is 30-40 µm, its depth is 10-20 µm and the vestibular extension may reach 20 µm in length. At least since Penard (1917) the oral apparatus of *Loxodes* has been compared in plastic illustration with the lateral view of a sickle, with the vestibular extension representing the grip handle of the sickle. The three-dimensional form of the oral cavity can also be compared with a canoe, sickle shaped in longitudinal section and V-shaped in cross section, but with the distinctiveness that the right lateral wall of the canoe, that is the one facing to the left lateral side of the cell, is higher than the left lateral wall of the canoe which faces the right lateral side of the cell. In this picture the vestibular extension could be compared with an anchor-chain. Back to scientific terminology, the extension of the vestibulum is often called pharynx or tube pharyngien, terms we would like to avoid for reasons given below. The wall of the oral cavity and its funnel-like extension is underlain by numerous yellow-brown granules.

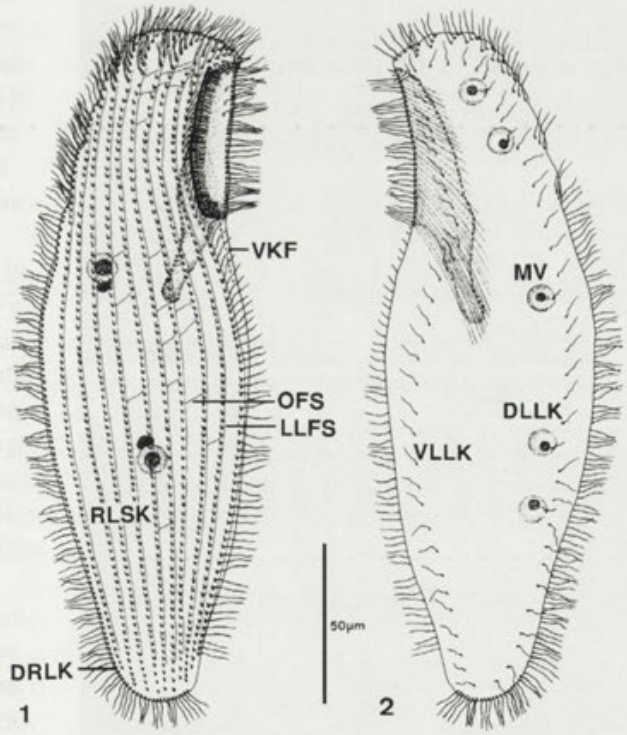

Fig. 1. Schematic drawing from a silver-stained specimen of *Loxodes striatus* showing the right lateral side of the cell with 11 right lateral somatic kineties (RLSK). The rightmost one, called dorsal right lateral kinety (DRLK), surrounds the posterior end of the RLSKs. There is a left longitudinal fibrillar system (LLFS) running parallel to the later kineties. Occasionally, oblique fibrillar strands (OFS) are seen between adjacent kineties. The wall of the buccal cavity is heavily pigmented and shows a tube-like extension pointing in posterior dorsal direction. Immediately behind the buccal cavity there is a non-ciliated ventral kinetofragment (VKF). The two sets of nuclei show one somatic macronucleus and one generative micronucleus each. For detailed labelling of the oral ciliature see Fig. 17

Using silver-stained cells like the one shown in Fig. 3 we have mapped the entire cortex of the cells. On the right lateral and slightly convex side the vast majority of the cells have 11 longitudinal somatic kineties composed of dikinetids, exclusively. The anterior ends of these right lateral somatic kineties (RLSKs) reach over to the left lateral side of the cell (Fig. 2). Since the RLSKs lie in longitudinal furrows the anterior end of the cell looks carved. It is useful to have them consecutively numbered: K_1 is the first kinety right of the oral cavity, further down this kinety is close to the ventral line of the cell. The rightmost of the RLSKs (usually K_{11}), called dorsal right lateral kinety (DRLK) here, shows a special feature. As reported first by Foissner and Rieder (1983) under the designation "lateral kinety" (and documented here more clearly, Figs. 6, 7) the posterior part of this kinety surrounds the posterior ends of most of the other right lateral somatic kineties.

Additionally, there are two argentophilic fiber systems in the right lateral cortex of *Loxodes*: a longitudinal filament to the left of most somatic kineties (only lacking in the anterior part of K_1 and the dorsal right lateral kinety) and less regularly seen, oblique filaments between adjacent kineties (Figs. 3, 16, 17). For reasons given in the ultrastructural chapter we use the term left lateral fibrillar strands (LLFS) for the first and oblique fibrillar strands (OFS) for the second filament. Both filaments form a kind of network. These fibrillar strands were first seen by Foissner and Rieder (1983) in silvercarbonate impregnations. As will be explained in the Discussion these authors described the fibrillar strands under the misleading name "postciliäre Fibrillen" or postciliary fibrils.

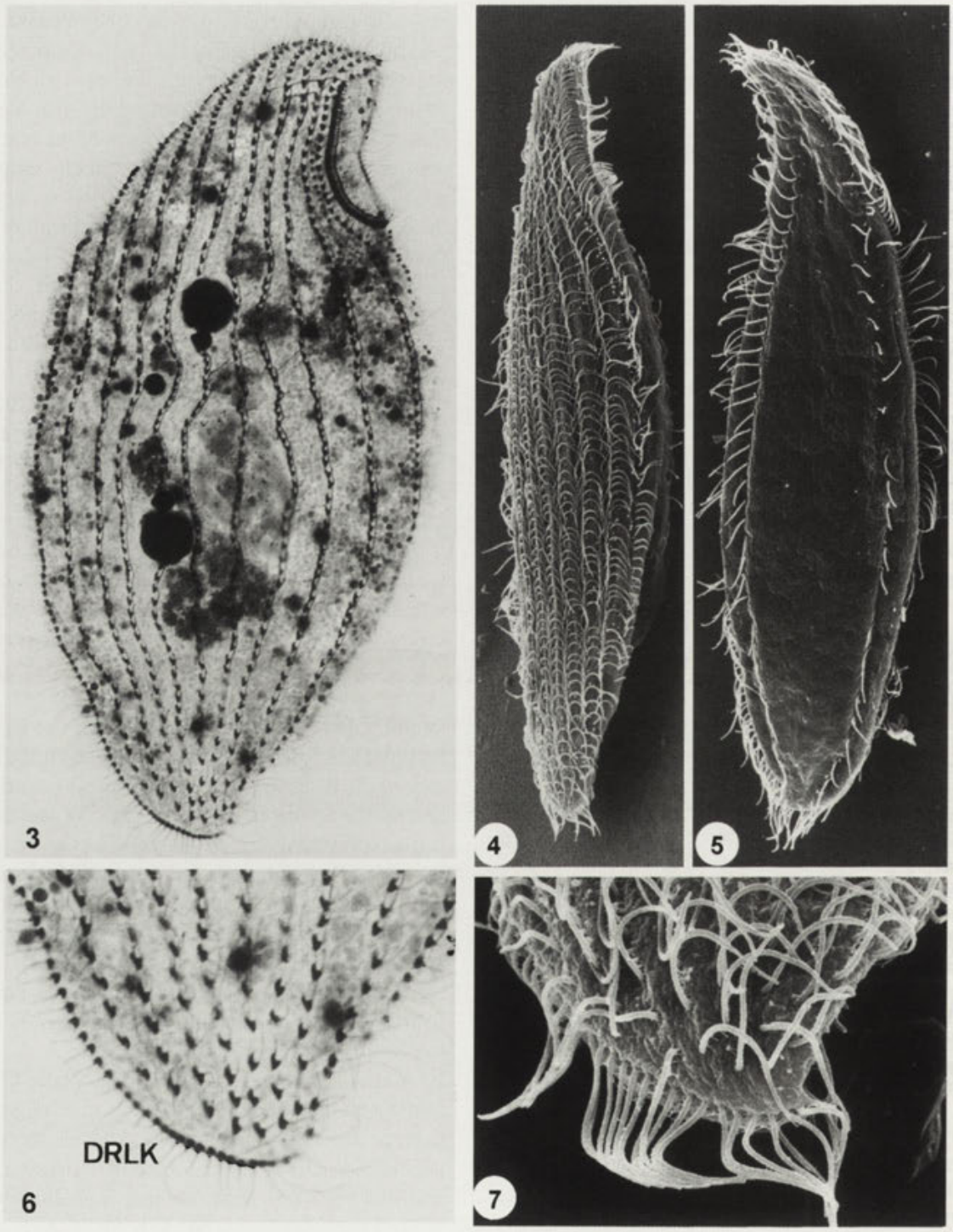

Fig. 3. Silver-impregnated specimens showing the left lateral side of the cell. Fernández-Galiano technique, cell artificially broadened through squeezing (x 1000). Fig. 4. Scanning electron micrograph of *Loxodes striatus* showing the right lateral side of the cell which is directed towards the substratum in crawling cells (x 1000). Fig. 5. SEM of the sparsely ciliated left lateral side of the cell (x 1000). Fig. 6. Enlargement of Fig. 3 to show the posterior part of the dorsal right lateral kinety (DRLK) (x 1700). Fig. 7. Corresponding SEM of the posterior end of the cell with the prominent DRLK (x 3000)

In the vast majority of the somatic dikinetids on the right lateral side of the cell both kinetosomes bear a cilium, but there are notable exceptions. Thus, in K_1 and DRLK for their entire length only the anterior kinetosome is ciliated, this holds also for the anterior ends of all the other right lateral kineties. Somatic cilia measure 10 μm in length. Finally, there is a longitudinal file of non-ciliated dikinetids on the left border of the

right side of the cell immediately behind the oral cavity (Figs. 16, 17). This structure which we call ventral kinetofragment (VKF) becomes of interest during stomatogenesis (see accompanying paper).

The left lateral side of the cell is only sparsely ciliated (Figs. 2, 5). It shows two marginal kineties, which we call ventral left lateral kinety (VLLK) and dorsal left lateral kinety (DLLK). In *L. striatus* the anterior and posterior ends of these two kineties meet each other near the anterior and the posterior pole of the cell. There is some disagreement in the literature with respect to the polarity of these two kineties in relation to the overall polarity of the cell. As will be documented by an ultrathin section it is the anterior end of both kineties which meet near the anterior end of the cell. The same holds for the posterior ends of the two kineties which come very close to each other near the posterior end of the cell (Fig. 2). Both kineties are composed of dikinetids, but they are more widely spaced than in the somatic kineties on the right lateral side of the cell. As noticed by Foissner and Rieder (1983) those dikinetids of the DLLK associated with the Müller vesicles lie at a slightly deeper focal plane. In schematic drawings like Fig. 2 they are shown shifted to the middle of the cell.

We have no new information on the Müller vesicles, which are thought to function as gravity receptors (Fenchel 1986, Finlay and Fenchel 1986) containing barium sulphate granules (Rieder et al. 1982). Other interesting peculiarities of *Loxodes*, likewise already in the literature, are the lack of a contractile vacuole (untypical for a fresh water ciliate), the absence of a permanent cytoproct, and, differing from most other ciliates, *Loxodes* has prominent Golgis (de Puytorac and Njiné 1970).

Free-swimming cells perform a counter-clockwise helical path. The left lateral and slightly concave side of the cell is oriented towards the axis of the helix, while the right lateral side points towards the outside. When crawling on the bottom of the culture dish it is the heavily ciliated right lateral side which is in contact with the substratum.

Light microscopy of oral ciliature

Though there are already quite a number of studies dealing with the rather complex oral ciliature of *Loxodes* we have to make several important corrections. Moreover, there is some disagreement with the terminology used by the various authors. Since much of the pertinent work was done by French ciliatologists (Dragesco 1960, de Puytorac and Njiné 1970, Dragesco and Dragesco-Kernéis 1986) and now has entered the most recent authoritative oeuvre on ciliate systematics, the Traité de Zoologie, Vol. 2/2 (de Puytorac et al. 1994) the terms used in the Traité are given here too for comparison. (It should already be mentioned here that the introduction of some new terms became necessary due to the result of our electron microscopical investigation.)

On the right side of the vestibulum (on the upper rim of the left lateral wall of the canoe), there is a densely spaced double row of kinetosomes, with the outer row being ciliated. This structure has been called "double cinétie droite". For reasons obvious from our ultrastructural investigation it seems justified to call it paroral (PO) for short. It is the most conspicuous element of the oral ciliature in *L. striatus* and consists of 85-120 paired kinetosomes. Except for the three anteriormost pairs they lie very close together. Left to the inner row of paroral kinetosomes there is an argentophilic band. At ultrastructural level this band corresponds to a fibrillar strand. Even at light microscopical level fine filaments connect the inner kinetosomes to the fibrillar strand as can be seen in Fig. 16. Paroral cilia measure 7 µm in length. Collectively they form a rake-like structure often ceiling the right half of the oral cavity and then hiding the shorter cilia of the intravestibular kinety.

The next oral kinety to the left (when the oral cavity is flattened into a plane as shown in Fig. 22) is the so-called intravestibular kinety (IVK), a term introduced by Foissner and Rieder (1983). It runs in the keel of the canoe and extends into the vestibular extension. In the lower part of the vestibular extension this kinety has no cilia. As will be shown in the accompanying paper the term "cinétie stomatogène" introduced by Njiné (1970) is not appropriate. The intravestibular kinety consists of 30-50 kinetids. In flattened light microscopical preparations, in particular after Fernández-Galiano staining, the course of the intravestibular kinety can vary. One can find specimen where it runs parallel to the paroral, but it can also "pass" underneath the paroral and in lateral view of the cell it is then seen between the paroral and the first somatic kineties to the right (Fig. 16, arrow heads).

Further to the left (on the anterior part of the right lateral wall of the canoe and close to its rim) there is a short file of 3-5 (usually 4) widely spaced cilia. It has been called inner left buccal kinety or "cinétie buccale interne" and hitherto it was regarded as a partial duplication of the outer left buccal kinety by

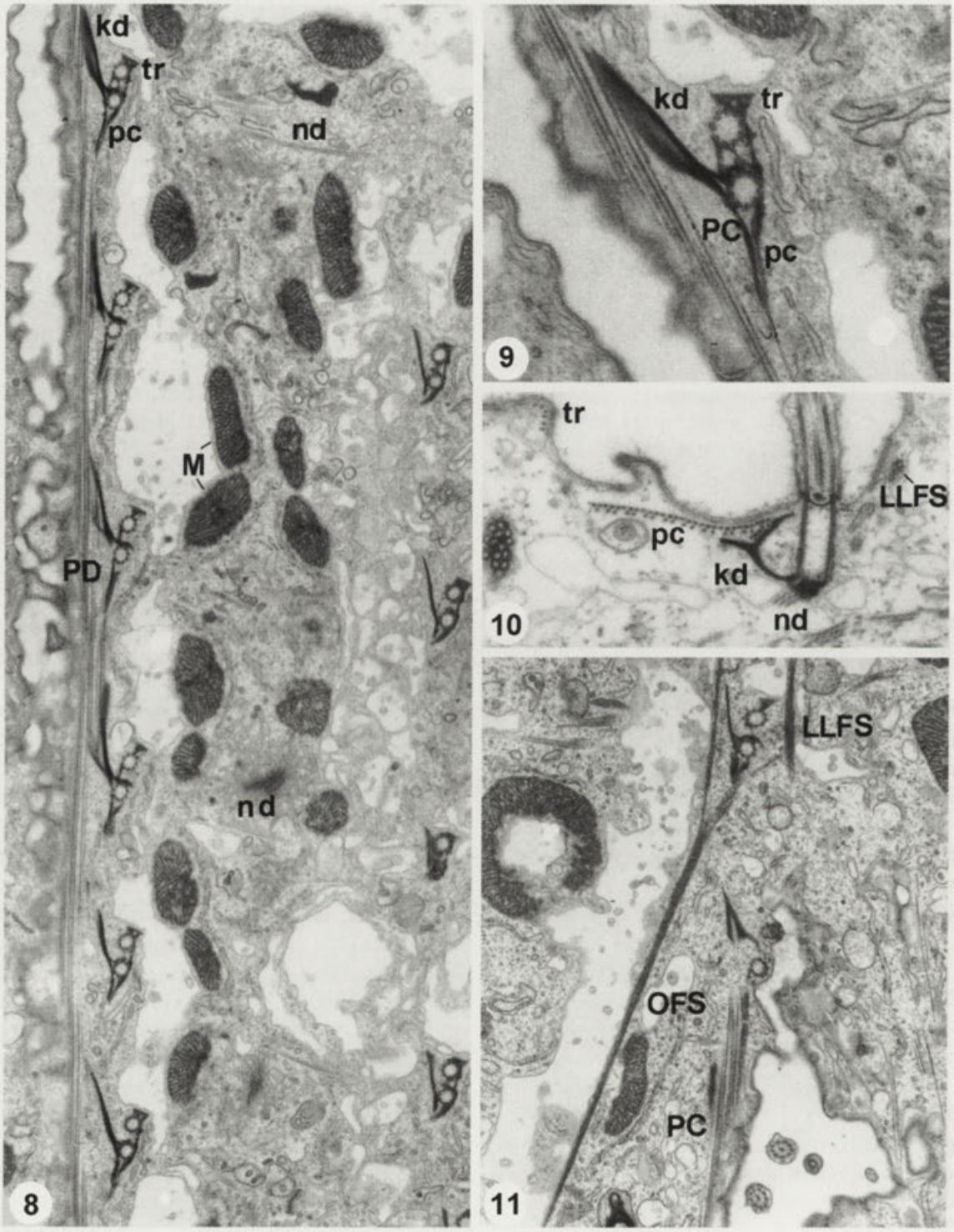

Figs. 8-11. Somatic cortex of *Loxodes striatus*. Fig. 8. General aspect as seen from outside the cell. At the left rim of the micrograph six dikinetids are shown at the level where they are accompanied by the postciliodesmos (PD) located on the right side of the dikinetids. M - mitochondria, kd - kinetodesmal fiber, nd - nematodesmata (x 15000). Fig. 9. A somatic dikinetid at higher magnification with a single kinetodesmal fiber (kd). Postciliary microtubules (pc) form the postciliodesmos (PC). Three desmoses (D) are seen between the anterior and the posterior kinetosome. The transverse microtubules (tr) in front of the anterior kinetosome are not resolved (x 15000). Fig. 10. Longitudinal section through the posterior kinetosome of a somatic dikinetid to show the broad Y-shaped form of the cross-cut kinetodesmal fiber. Postciliary (pc), transverse (tr), and nematodesmal (nd) microtubules as well as one of the left lateral fibrillar strands (LLFS) are marked (x 25000). Fig. 11. Occasionally, oblique fibrillar strands (OFS) are seen between somatic kineties. More regularly another fibrillar system running along the left longitudinal fibrillar system (LLFS) is seen in the somatic cortex which shows no direct connection to the dikinetids. Postciliary microtubules forming a postciliodesmos (PD) (x 15000)

the French ciliatologists. In the light of our electron microscopical results the latter statement can no longer be regarded as correct. The former inner left buccal kinety is a genuine buccal structure (contrary to the outer left buccal kinety). These four separate cilia (see Fig. 13 in Bardele and Klindworth 1996) have the same distance as somatic cilia and they do seem to form a functional unit compared with other oral kineties. It is difficult to suggest an appropriate name for them in particular as we know nothing about their function. Due to their position we call them anterior buccal cilia (ABC). They measure 10-12 µm in length and are said to be thicker than ordinary cilia and stiff (Dragesco and Njiné 1971).

On the left rim of the vestibulum, there is the left pseudobuccal kinety (LPK), formerly called outer left buccal kinety. Its cilia are 10 µm in length. The kinetosomes of this kinety give rise to prominent fibrillar structures identified as nematodesmata at electron microscopical level by de Puytorac and Njiné (1970), but may also be seen in phase contrast.

Ultrastructure of the somatic cortex

Since the ultrastructure of the somatic cortex of *L. striatus* has been already described in great detail by de Puytorac and Njiné (1970) our supplementary observations will be added to a short recapitulation of their findings. The plasma membrane of *Loxodes* covered with a faint glycocalyx is underlain by a discontinuous and rather inconspicuous layer of flat pellicular alveoli. No epiplasm and no parasomal sacs were observed in *Loxodes*. Over most of the length dikinetids in the RLSKs are 2-3 µm apart. The kinety axis and the dikinetid axis form an angle of 15° to the left (Fig. 8). Anterior and posterior kinetosome are connected by three fibrillar links or desmoses (Fig. 9). According to de Puytorac and Njiné (1970) the anterior kinetosome is associated with a ribbon of 6-8 transverse microtubules, arranged tangentially almost in front of the kinetosome. This transverse ribbon runs in anterior direction. The posterior kinetosome has a ribbon of 3-4 transverse microtubules. It has its point of origin near the upper left quarter of the kinetosome but

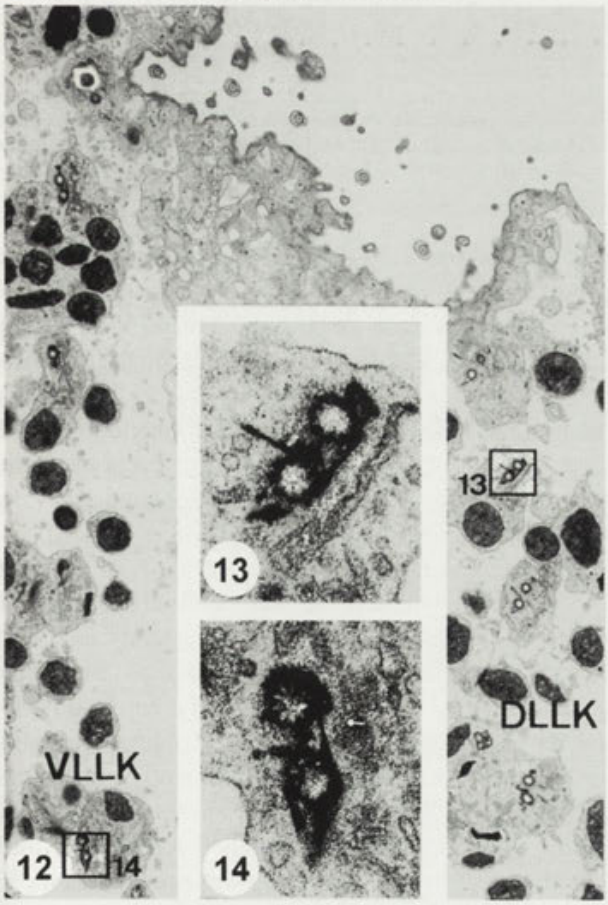

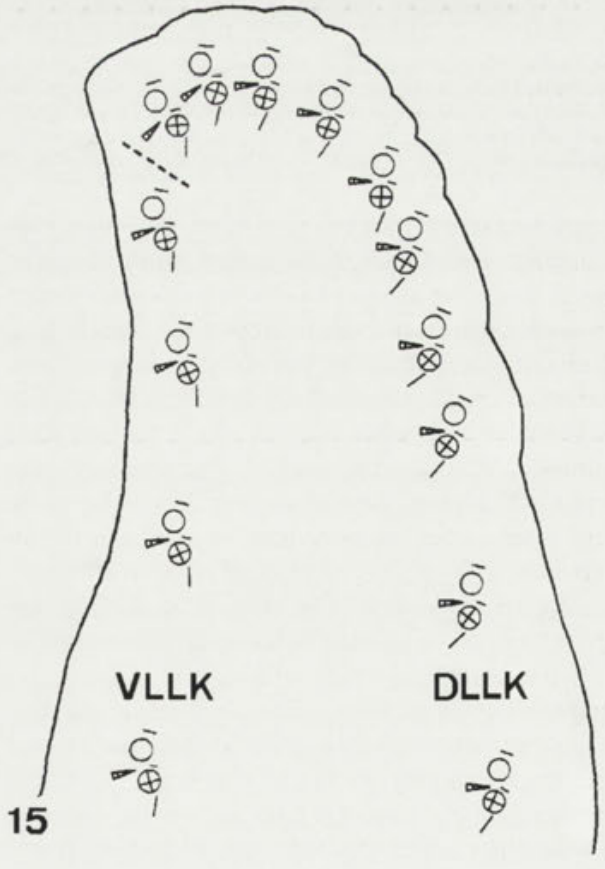

Fig. 12. Low power micrograph of the anterior end of the left lateral side of the cell to show the orientation of the dikinetids forming the ventral left lateral kinety (VLLK) and the dorsal left lateral kinety (DLLK) (x 6000). Figs. 13 and 14. Enlargements (x 32000) of the marked areas in Fig. 12. Fig. 15. Schematic drawing of the anterior left lateral side of the cell.○- kinetosome with cilium,⊗ - kinetosome without cilium

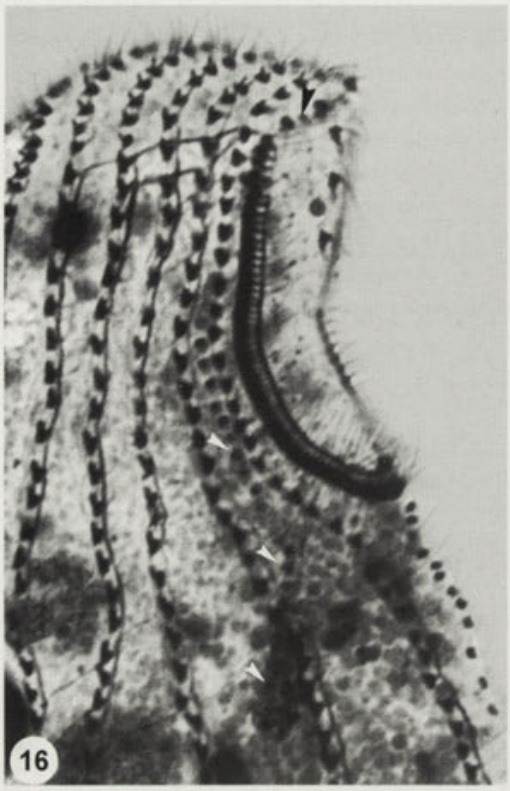

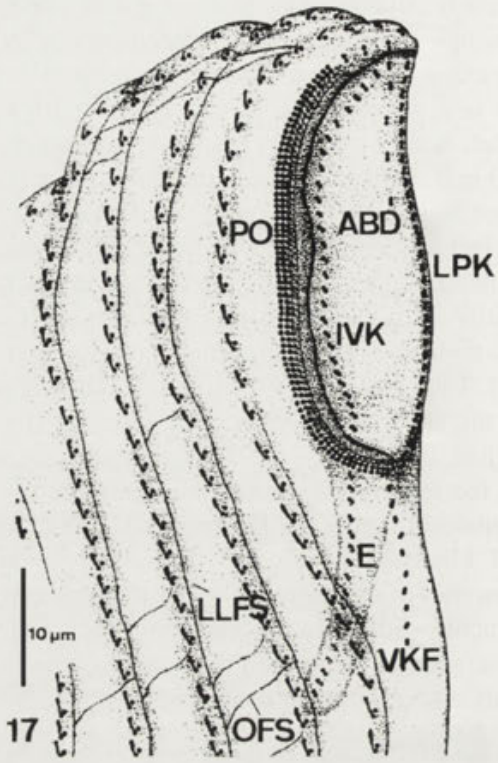

Fig. 16. Partial enlargement of Fig 3. to show details of the anterior right side of the cell and the subapical oral cavity. Some kinetosomes of the intravestibular kinety seen through the right lateral wall of the cell are marked with arrow-heads. For abbreviations see next figure (x 2000)
Fig. 17. Schematic drawing corresponding to Fig. 16. OFS - oblique fibrillar strands between adjacent somatic kineties, LLFS - left longitudinal fibrillar system accompanying somatic kineties, PO - paroral kinety, IVK - intravestibular kinety, ABD - anterior buccal dikinetids, LPK - left pseudobuccal kinety, VKF - ventral kinetofragment, E - extension of the vestibulum

then curves towards a posterior direction to cross over with the anterior transverse microtubules from the rear dikinetid. While the anterior kinetosome has no posterior microtubules, there is a divergent ribbon of 8-9 postciliary microtubules associated with the posterior kinetosomes. Postciliary microtubules of at least five dikinetids in a file lie adjacent to each other and thus form the so-called postciliodesma, the diagnostic character of the Postciliodesmatophora Gerassimova and Seravin, 1976. The proximal part of the postciliary microtubular ribbon is accompanied by a layer of electron dense material on both sides of the ribbon. The anterior as well as the posterior kinetosome give rise to a nematodesma made of some 15 microtubules arranged when seen in cross-section in a trapeze-shaped package. Curiously these nematodesmata do not dive down into the cytoplasm as oral nematodesmata usually do, but lie almost parallel to the cell surface (Fig. 8). Almost at right angle to the dikinetid from which they arose, they run towards the next kinety to the left. The texture of microfilaments which form the left lateral fibrillar strands (LLFS) and oblique fibrillar strands (OFS) shown in Fig. 11 is so dense that the diameter of the individual microfilament could not be determined.

From the posterior kinetosome a broad V- or Y-shaped kinetodesmal fiber starts with two roots on the kinetosome and runs in anterior direction and contacts the postciliary microtubule ribbon of the preceding dikinetid (Figs. 8-10). Cut tangentially, and depending on the level of sectioning as well as on the thickness of the section, one gets various aspects of the singular kinetodesmal fiber (Fig. 8).

Two fibrillar structures shown in Fig. 11 are of interest in comparison with silver-impregnated cells (Figs. 16, 17). The patterning of these osmiophilic strands seen in thin sections fits so well with the distribution of fine filaments in silver-stained cells that there can be hardly any doubt that they are identical structures. The oblique microfibrillar strands which are seen less frequently, run from the right side of a dikinetid in posterior direction to the next kinety were they join the so-called left lateral fibrillar strands, the distribution of which was specified in the light microscopical chapter. Part of a LLFS is seen in Fig. 11.

Dikinetids on the left lateral side of the cell differ to some extent from those of the right lateral side. Only

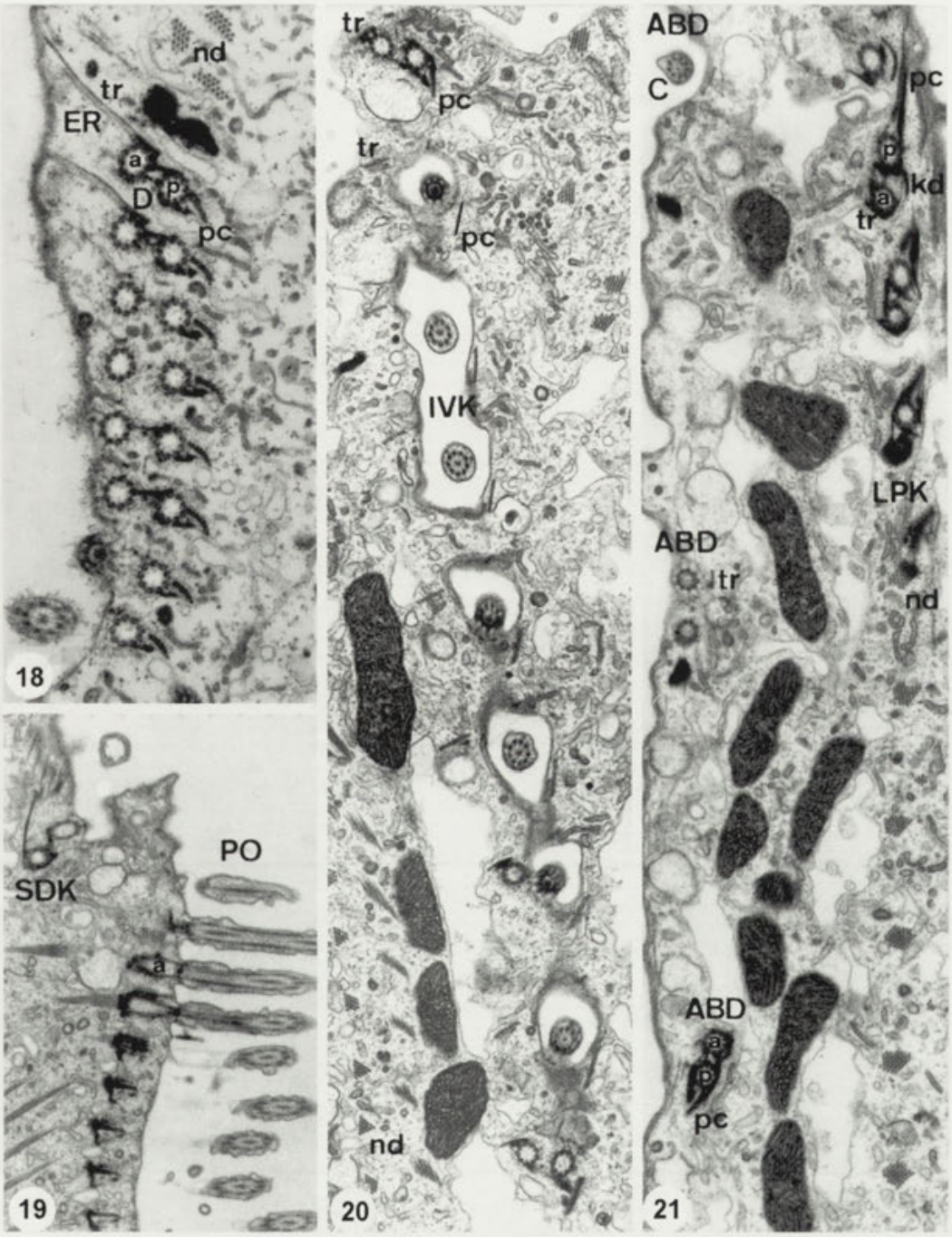

Figs. 18-21. Oral ciliature of *L. striatus*. Fig. 18. Paroral made of dikinetids oriented perpendicularly to its longitudinal axis. At a particular level anterior (a) and posterior (p) kinetosome of each dikinetid are connected by two desmoses (small arrows). The anterior (or outer) kinetosome is ciliated, its transverse microtubules (tr) are accompanied by a thin cisterna of endoplasmic reticulum (ER). The posterior (or inner) kinetosome has postciliary microtubules (pc) oriented towards the right dorsal wall of the vestibulum. Both kinetosomes give rise to a separate bundle of nematodesmal microtubules (nd) (x 31000). Fig. 19. Longitudinal section of paroral cilia. The nematodesmata of the anterior kinetosome (a) of the paroral dikinetids run parallel to the axis of the longitudinal axis of the respective kinetosomes, while the nematodesmata of the posterior kinetosomes (not in the level of section) run obliquely (see next figure). SDK - somatic dikinetid (x 17500). Fig. 20. The kinetids of the intravestibular kinety are also oriented perpendicularly to the longitudinal axis of the vestibulum. They are spaced at wider distance from each other compared with the paroral dikinetids. In the intravestibular dikinetids it is the posterior kinetosome which is ciliated. At the site of their origin the postciliary microtubules (pc) are oriented parallel to the longitudinal axis of the vestibulum. Transverse microtubules are labelled tr. Note the triangular cross-section of the nematodesmata of the anterior kinetosome of the paroral dikinetids and the obliquely cut nematodesmata of the posterior kinetosome in the lower left corner (x 21500). Fig. 21. Three anterior buccal dikinetids (ABD)) with the dikinetid axis oriented towards the anterior pole of the cell and a couple of inverted dikinetids of the left pseudobuccal kinety (LPK). Though not obvious from this micrograph it is only the anterior kinetosome which carries a cilium (C) and a nematodesma (nd), particularly prominent in the left pseudobuccal kinety (x 20000)

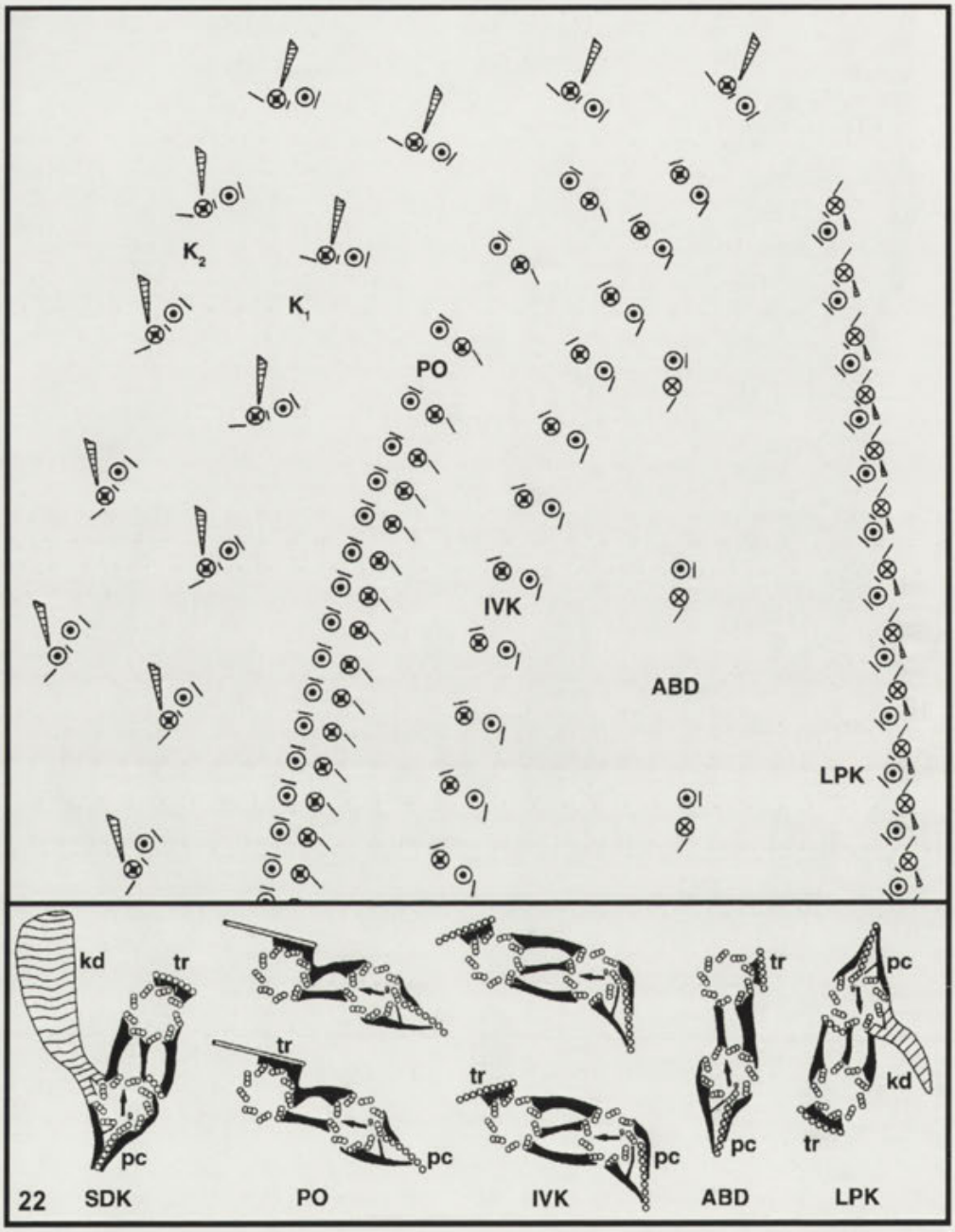

Fig. 22. The upper part of this schematic drawing shows the orientation of the oral dikinetids in the oral cavity and in two of the rightmost somatic kineties (for abbreviations see lower part). In the lower part of this drawing the five types of dikinetids are shown at higher magnification. From left to right a somatic dikinetid (SDK), two paroral dikinetids (PO), two intravestibular dikinetids (IVK), an anterior buccal dikinetid (ABD), and a dikinetid of the left pseudobuccal kinety (LPK). The dikinetid axis is obvious and the axis of the posterior kinetosome (arrow within the kinetosome) is also known from its association with triplet No. 9, the orientation of none of the anterior kinetosomes could be determined. ◯ - kinetosome with cilium, ⊗ - kinetosome without cilium, ⊙ - kinetosome with cilium and nematodesma, ⊗ - non-ciliated kinetosome with nematodesma

the anterior kinetosome is ciliated. The kinetodesmal fiber is much shorter and points to the right. With respect to the transverse and postciliary microtubules their arrangement of the point of origin is the same as in the dikinetid of the right lateral side. There are 3-6 and 3-4 transverse microtubules associated with the anterior and posterior kinetosome, respectively. The 4-6 postciliary microtubules do not overlap to form postciliodesma. Both kinetosomes have small bundles of 8-10 nematodesmal microtubules. We have seen no distinct fibrillar strands on the left lateral side of the cell.

The low power micrograph of the anterior part of the left lateral side in Fig. 12 together with the enlargements of the marked areas (Figs. 13, 14), admittedly of low

quality, is shown only to document the polarity of the ventral and dorsal left lateral kinety. As judged from the postciliary and transverse microtubules associated with the dikinetids the anterior pole of both kineties is directed towards the anterior pole of the cell. The significance of this finding will be dealt with in the discussion.

Ultrastructure of the oral cortex

The right oral kinety shows, as we will argue in the discussion almost all ultrastructural features of a typical paroral. The dikinetids are arranged at right angle to the longitudinal axis of the paroral. The lateral distance between adjacent paroral dikinetids measures 0.3 μm, only the three anteriormost dikinetids are 0.8 μm apart. The two kinetosomes of each paroral dikinetid are connected with two desmoses (Fig. 18). The anterior kinetosome is ciliated, while the posterior is barren. The anterior kinetosome has a tangential ribbon of transverse microtubules on the left lateral side with respect to the dikinetid axis. Some seven microtubules arranged radially with respect to the posterior kinetosome are identified as postciliary microtubules. This interpretation is supported by the existence of a fibrillar link connecting these tubules with the kinetosome (Fig. 18). Furthermore, these postciliary microtubules allow to determine the orientation axis of the kinetosome (The orientation axis of a kinetosome is the axis which passes through triplet No. 9 and between triplet No. 4 and 5). There are no postciliary microtubules associated with the anterior kinetosome which means that the orientation of this kinetosome cannot be determined. A kinetodesmal fiber is lacking in these paroral dikinetids. The anterior kinetosome is associated with a ribbon of seven microtubules, labelled tr in Fig. 18. At its point of origin this microtubular ribbon is attached laterally to the anterior kinetosome. This is a quite unusual situation for transverse microtubules. Moreover, this ribbon which is accompanied by flat cisternae of endoplasmic reticulum is oriented in slightly anterior direction towards the first somatic kinety. Finally, both paroral kinetosomes have stout nematodesmata, which consist of 15-20 microtubules. As seen in Fig. 18 the cross-section of the nematodesmata of the two paroral kinetosomes is different. The posterior nematodesma is trapeze-shaped in cross section with the longitudinal axis of the trapeze parallel to the orientation axis of the posterior kinetosome. The anterior nematodesma in cross-section has the longitudinal axis of the trapeze parallel to the paroral. As shown in Fig. 19 the orientation of the longitudinal axis of the two nematodesmata of each dikinetid is different. While the anterior nematodesma is in straight line with the anterior kinetosome and cilium, the posterior nematodesma is bent backwards. As a result these two sets of nematodesmata cross over each other at a certain level and may thus strengthen the right lateral wall of the buccal cavity. At a more distant level they may form part of a flattened cytopharyngeal basket (see Discussion).

On a couple of occasions, about 1 μm from the posterior end of the paroral we have seen the non-ciliated kinetosomes of the ventral kinetofragment. Though not shown here, we can specify that these kinetosomes are organized in dikinetids with transverse microtubules at the anterior and postciliary microtubules at the posterior kinetosome. We have seen no kinetodesmal fiber in these dikinetids but our current investigation on the role of the dikinetids in stomatogenesis will hopefully answer this question.

In the intravestibular kinety (Fig. 20) the dikinetids are about 1 μm apart and show almost the same orientation as those of the paroral. Differing from all other dikinetids it is the posterior kinetosome which is ciliated, while the anterior one is barren. Deep down in the extension of the vestibulum both kinetosomes are barren. The two kinetosomes are connected by three desmoses. The orientation of both the transverse and the postciliary microtubular ribbon is different from the paroral kinetids. The posterior kinetosome has a postciliary ribbon of nine microtubules. These microtubules are connected with a fibrillar link to triplet No. 7 of the posterior kinetosome (Grain 1969, 1984). Close to the kinetosome the cross-section of this ribbon is oriented parallel to the kinety axis. For the inspection of numerous micrographs we know that during their further course these postciliary microtubules run towards the posterior left of the buccal cavity. The anterior kinetosome bears nine transverse microtubules. Starting from a tangential position they run towards the anterior right, or in short, towards the paroral. Both kinetosomes have nematodesmata, and neither one has a kinetodesmal fiber. Rather than describing every little detail we would like to draw the reader's attention to Fig. 22 where a synoptic view of the various types of dikinetids is given. This also facilitates the under-

standing of the following structures, the adoral kinety and the left pseudobuccal kinety, documented in Fig. 21.

Thin sections have revealed that each anterior buccal cilia originates from the anterior kinetosome of a dikinetid, which we call anterior buccal dikinetid. The dikinetid axis is parallel to the longitudinal axis of the cell. As seen in Fig. 21, the two kinetosomes are connected by two desmoses, there is no kinetodesmal fiber associated with this type of dikinetid. Again, only the posterior kinetosome has a microtubular ribbon which at the site of origin is oriented almost parallel to the dikinetid axis. There is a tangential ribbon of five transverse microtubules to the left of the anterior kinetosome. The posterior kinetosome has a postciliary ribbon of 6-7 microtubules which run in posterior direction. Only the anterior kinetosome has a strong nematodesma made of 30-35 microtubules, running underneath the oral cavity and in dorsal direction.

The ultrastructural aspect of the left pseudobuccal kinety is a real surprise. Its dikinetids show an inverse orientation. Purposely, Fig. 21 was chosen to document this fact in relation to another positively identified structure as e. g. in this case the dikinetids of the widely spaced adoral kinety. The left pseudobuccal kinety consists of 30-40 dikinetids spaced at a distance of 0.2-0.5 µm. Except for the inverse orientation the dikinetid pattern in the left pseudobuccal kinety is very similar to the somatic dikinetids, but noteworthy differences do exist. The kinetodesmal fiber is smaller than in somatic dikinetids (and in this particular case runs towards the posterior end of the cell). The postciliary microtubules of adjacent dikinetids, now running towards the anterior pole of the cell, overlap and form a broad postciliodesma on the outermost left side of the vestibulum. Moreover, the posterior kinetosome has a few (3 or 4) transverse microtubules as indicated in Fig. 22. Along the entire length of the left pseudobuccal kinety it is the anterior kinetosome which is ciliated. The anterior kinetosome carries a thick nematodesma which runs underneath the wall of the buccal cavity and at right angle to the longitudinal axis of the left pseudobuccal kinety. These nematodesmata are so prominent that they can be seen in living specimen with phase contrast microscopy.

The plasma membrane of the entire vestibulum including the vestibular extension is underlain by flat pellicular alveoli and numerous pigment granules. Unfortunately, in the EM-preparation from which Figs. 18-21 were taken, the content of the pigment granules has been dissolved largely. Nonetheless, some of the remnants of the pigment granules have been labelled in Figs. 20 and 21.

DISCUSSION

Somatic cortex

Though de Puytorac and Njiné (1970) have given a very detailed description of the somatic cortex of *Loxodes* we want to propose two corrections. First, we came to the conclusion that *Loxodes* has only *one* kinetodesmal fiber, and second, the so-called retrodesmal fiber is no independent structure which would deserve a special name.

As mentioned already, in tangential sections of the cell surface several factors will influence the picture one gets of adjacent dikinetids. The right lateral side of *Loxodes* is slightly convex, thus even an ideal tangential section of the cell surface will show adjacent dikinetids at slightly different level (e. g. left kinety in Fig. 8). Small irregularities, like indentations or bulges in the cell surface will jeopardise a correct interpretation of locally restricted areas. Only a three-dimensional reconstruction from serial sections will circumvent this problem. As shown in cross section through a kinetodesmal fiber (Fig. 10) it is quite clear that it depends on the level of the section which aspect of the shovel-shaped fiber one gets. Cut close to its upper rim one gets two almost parallel strands, suggesting that there are two kinetodesmal fibers as shown in the drawing by de Puytorac and Njiné (1970, their Fig. 11). We think that two-dimensional drawings of kinetid patterns have their shortcomings in particular if they are done so elaborately as for *Loxodes*. They exaggerate a supposed distance between the different ciliate groups and may thus have a falsifying influence on phylogenetic considerations. *Remanella granulosa*, another member of the Loxodidae, has also only a single kinetodesmal fiber (Raikov 1994).

With respect to the discrepancy about the identification of the electron dense material which accompanies the postciliary microtubule ribbon we have to refer to the original description of the somatic dikinetid pattern of *Loxodes* by de Puytorac and Njiné (1970) and their Fig. 11, also reproduced on p. 25 of Traité de Zoologie 2/2 by de Puytorac et al. (1994). While the material on the left side of the microtubular ribbon is plainly (and

we think appropriately) labelled "E" for electron dense material, the material on the right, for no obvious reason, is called "fibre rétrodesmale". We think this term should be abandoned completely. It has to be stressed or repeated in other words, that in *Loxodes* and many heterotrichs the postciliary microtubules are accompanied by electrondense material on both sides of the microtubular band.

There is doubt that the left lateral fibrillar system and the oblique fibrillar system stained with silver carbonate for light microscopical demonstration both in Fig. 16 of this paper and in Fig. 6 in the paper by Foissner and Rieder (1983) are identical with the bundles of microfibrils seen in thin sections, e. g. in Fig. 11. Both fibrillar systems form a net-like structure as shown schematically in Fig. 17. Unfortunately, Foissner and Rieder (1983) used the term "postciliäre Fibrillen" in their German text and "postciliary fibrils" in the English abstract. Their terms are prone to misunderstandings, even among experts, because postciliary fibrils is often used as synonym for postciliary ribbons or postciliary microtubular ribbons which all mean the well known set of kinetosome-associated postciliary microtubules. The postciliary microtubules originate from the right posterior sector of the kinetosome and usually do not stain with silver carbonate. In *Loxodes* it is instead the left lateral fibrillar system (LLFS) and the oblique fibrillar system (OFS) which stain with silver carbonate. These fibrillar systems, in particular the left lateral one, should be clearly distinguished from the postciliodesmata located on the right of the somatic kineties, the name-giving character of the Postciliodesmatophora. Beyond the nomenclatural problem it would be interesting to know how far the left lateral fibrillar system is distributed among karyorelictine ciliates.

The polarity of the two kineties on the left lateral side of the cell (see Fig. 15) is of interest with respect to a suggestive but incorrect interpretation by Dragesco and Dragesco-Kernéis (1986, p. 204) of a schematic drawing for *Loxodes magnus* by Foissner and Rieder (1983, their Fig. 2d). Based on this drawing which shows the anterior kinetosome in the dikinetids of the DLLK and the posterior kinetosome in the dikinetids of the VLLK being ciliated the French authors were led to the conclusion that these two abutting kineties are just one circular kinety. In reality there are two distinct kineties (VLLK and DLLK) with the same orientation according to their dikinetids. If there would be only one circular kinety the kinetodesmal fibers should all point towards the centre of the left lateral side of the cell which is definitively not the case in *L. striatus*. If the interpretation of Dragesco and Dragesco-Kernéis (1986) would have been correct then the ventral left lateral kinety would have had the same inverted polarity as the left pseudobuccal kinety, a likely source for intermingling these two kineties. But a closer inspection of the distances between adjacent dikinetids in *L. striatus* immediately shows that the dikinetids in the left pseudobuccal kinety are arranged more closely to each other than in the ventral left lateral kinety.

We can however imagine other *Loxodes* species where the dorsal left lateral kinety moves over to the ventral rim of the left lateral side of the cell for a certain distance. In this case the hatched line in Fig 15 (where the two independent kineties meet) would lie more posterior. *Loxodes vorax* might be a possible candidate (Small and Lynn 1985).

Oral apparatus and oral ciliature

There is some controversy about the actual site of food intake in *Loxodes*. Penard (1922) and Canella (1970) claimed to have observed that a slit all along the entire length of the oral cavity close to the blunt part of the sickle opens during food intake. De Puytorac and Njiné (1970) give the impression that they regard the tube pharyngien as actual site of food intake which they have not observed itself. Upon criticism of their results by Canella (1970) they admit that larger prey will probably not become ingested through the small opening of the vestibular extension. But they do not want to exclude the possibility that small prey like little flagellates might be ingested through the tube pharyngien. In this case the upper end of the vestibular extension would have to be regarded as a permanently open cytostome followed by the tube pharyngien at the end of which food vacuoles should bud off. No such process has ever been observed and the fact that a kinety would extend beyond the cytostome down into the cytopharynx would be a totally unusual situation. In short, the function of the vestibular extension remains unknown and the term tube pharyngien (in connection with the description of the oral apparatus of *Loxodes*) should be abandoned.

The spatial situation in the oral cavity as judged from SEM cryofracture preparations makes very likely that the cytostomial slit opens in the right lateral wall of the oral cavity, that is to say between the paroral and the intravestibular kinety. The dikinetids of both the paroral and the intravestibular kinety have the dikinetids oriented more or less perpendicular to the longitudinal axis of these respective oral structures with the conse-

quence that a putative cytopharynx would be bordered by postciliary microtubules from the paroral and the transverse microtubules from the intravestibular kinety. Sections through deeper regions of the oral cavity have not allowed us to follow these microtubular ribbons for a great length with the intention to identify a cytopharyngeal area with certainty. More suggestive is the arrangement of the nematodesmata arising from the posterior kinetosome of the paroral dikinetids and the anterior kinetosome of the dikinetids forming the intravestibular kinety. Together these nematodesmata may form a kind of loose cytopharyngeal basket. The cytoplasm between the nematodesmata contains numerous small membrane-bound vesicles which could represent a so-called phagoplasm (de Puytorac and Njiné 1970). We have of course fixed *L. striatus* during feeding but we have never caught it in the very moment when an *Euglena* passed the oral area between the paroral and the intravestibular kinety.

At least theoretically there is an alternative, in which case the oral slit would have to open between the intravestibular kinety and the left pseudobuccal kinety. In this case the intravestibular kinety would play the role of a second paroral while the left pseudobuccal kinety would function as an adoral ciliature. Postciliary microtubules of the intravestibular kinety which curve upwards in the left lateral wall of the oral cavity and transverse microtubules of the left pseudobuccal kinety would have to border a cytopharyngeal zone. We have found no evidence for this alternative.

In higher ciliates which have a well organized layer of pellicular alveoli it is fairly easy to detect the actual cytostome as an area where the cell is covered by the plasma membrane only. This approach is not very helpful in *Loxodes*. The poorly developed pellicular alveoli do not form a continuous layer underneath the plasma membrane. Furthermore, in the oral cavity as well as in the vestibular extension there are numerous pigment granules located between the pellicular alveoli. Quite a number of these granules become discharged during the fixation procedure and leave behind irregularly shaped membrane patches in the oral plasma membrane lacking the underlying pellicular alveoli.

The oral ciliature of *Loxodes* has been a controversial topic, too. None of the previous authors dealing with the oral ciliature of Loxodes (Dragesco 1960, Njiné 1970, de Puytorac and Njiné 1970, Foissner and Rieder 1983, Dragesco and Dragesco-Kernéis 1986) identified correctly the kinety on the left side of the oral cavity. The entire oral ciliature of *Loxodes* consists of dikinetids. Though this ciliate has a highly developed paroral ciliature very similar to the paroral ciliature in higher ventrostomous ciliates it has no adoral polykinetids that is to say no adoral organelles like membranelles seen in so many higher ventrostomous ciliates. We will now discuss several specific aspects of the oral kinety in the same sequence as they were described in the Results.

Paroral

It may be questioned whether the paroral of *Loxodes* is homologous to the paroral in highly evolved ventrostomous ciliates. In both paroral structures the dikinetid axis and the orientation axis of the posterior kinetosome are oriented perpendicular to the longitudinal axis of the paroral. Compared to a tetrahymenine paroral the kinetosome of the paroral in *Loxodes* shows no zigzag arrangement. Moreover, the transverse microtubules of the anterior kinetosome show an arrangement not reported from other ciliates to our knowledge. Under these circumstances it seems appropriate to follow Lynn's recommendation (Lynn 1988) and to speak of a "loxodid paroral" in order to indicate some genus-specific peculiarities. Because the anterior kinetosome of the paroral dikinetids has no postciliary microtubules, the orientation axis of the anterior kinetosome is not known in either case. Despite the many differences in the adoral ciliature both in karyorelictean and higher ciliates, the loxodid and e. g. the tetrahymenine parorals could well be homologous structures. Some sort of a primary paroral could have arisen in a common ancestor of both the early ciliates (heterotrichs and karyorelicteans) on the one hand and higher ciliates on the other hand. Such a hypothetical ventrostome ciliate with a paroral ciliature but yet lacking an adoral ciliature was discussed in a scenario on ciliate evolution presented by Eisler (1992).

With respect to oral nematodesmata one may question whether the orientation of a particular cross-sectional shape of a nematodesma can be of help in determining the orientation axis of its kinetosome when postciliary microtubules are lacking. There are a few examples of paroral dikinetids where the orientation axis of both kinetosomes is known (see Eisler 1992, for the different ways in which kinetosomes can be oriented in paroral dikinetids). Such cases of known orientation should be checked carefully again to answer the question whether cross-sectional patterns of nematodesmata could help to determine the kinetosome orientation axis. In short, the dikinetid pattern is very close to a stichodyade.

Intravestibular kinety

Contrary to the statement of de Puytorac and Njiné (1970) the dikinetids of the intravestibular kinety do not

have an orientation similar to the somatic dikinetids, but they are oriented in the same way as the dikinetids of the paroral (Fig. 22). So theoretically we could even speak of a second paroral if the oral slit would have been on the left side of the intravestibular kinety. As already said, we have found no evidence for such a possibility. If a paroral is accompanied by additional kineties they are generally located on the right side of the paroral as e. g. the ophryokineties in frontonid ciliates and not on the left side of the paroral. There is only one case reported in literature, concerning the colpodid ciliate *Cyrtolophosis*, where a row of barren kinetosomes lies between the paroral and the adoral organelles (Didier et al. 1980). The ontogenetic origin of these kinetosomes as well as their function is unknown. With respect to the site where the oral slit opens during feeding the intravestibular kinety has to be regarded as an adoral ciliature. The location of this kinety deep down in the oral cavity and the short length of its cilia lead to question whether it is efficiently involved in food gathering.

Anterior buccal cilia

The number of anterior buccal cilia is usually fairly small, it varies between 3-5 in *L. striatus* and 10-12 in *L. magnus* for the better known *Loxodes* species. But it has to be mentioned that Dragesco and Njiné (1971) have described a giant *Loxodes* species, *L. rex*, which reaches up to 1200 µm in length and has over 60 anterior buccal cilia. In *L. striatus* the dikinetidal basis of these cilia looks rather similar to the paroral dikinetids except for the fact that the orientation of the transverse microtubules of the anterior kinetosome is different. Moreover, each kinetosome of the paroral carries a nematodesma while in the anterior left buccal dikinetids only the posterior kinetosome has a nematodesma. There are two desmoses in both dikinetids and only the anterior kinetosome is ciliated. The anterior buccal cilia are the longest of all buccal cilia. Due to their small number and the large distance from each other they may not play a major role in food capturing. The notion that these cilia are thick and stiff suggests a sensory function. But so far, we have been unable to identify them positively in freeze-fracture replicas in search for special arrays of transmembrane particles in the ciliary membrane which could clarify their function (Bardele 1981).

As far as the origin of these anterior buccal cilia is concerned it seems that their close neighbourhood to the left pseudobuccal kinety has deluded into thinking of an ontogenetic connection between these two structures (Njiné 1970, de Puytorac and Njiné 1970). In fact Pätsch (1974) had already observed that in the anterior buccal dikinetids (the former inner buccal kinety) the anterior kinetosome is ciliated while in the outer buccal kinety it ought to be the posterior one. Now we know about the inverse orientation of the pseudobuccal dikinetids, and thus it is the anterior kinetosome in both dikinetids which carries the cilium.

Left pseudobuccal kinety

It may be questioned whether this kinety got the right name. It is localised at the left border of the buccal cavity and its nematodesmata are one of the most prominent cytoskeletal structures of the oral area. Nematodesmata are by no means restricted to oral kinetids, instead they are often seen in somatic kinetids located close to the oral apparatus as it is e. g. the case here in *L. striatus* where the anterior dikinetids (more than ten in a row) of K_1 through K_3 have nematodesmata. Most important, the dikinetids of the left pseudobuccal kinety do have a kinetodesmal fiber not seen in other types of true oral ciliature. We do not yet have a satisfying explanation for the inverse orientation of this kinety. We can only speculate that during evolutionary history of *Loxodes* a part of a right somatic kinety (probably of K_1) moved over to the left side of the oral cavity to form a secondary adoral ciliature perhaps in compensation for a sinking of the intravestibular kinety down into the bottom of the oral cavity. Thus the inverse orientation of the left pseudobuccal kinety is probably the result of the phylogenetic process and at the same time a good apomorphous character of the Loxodidae.

Acknowledgements. We thank Mr. Horst Schoppmann for excellent work at the scanning electron microscope. This investigation was supported by a grant from the Deutsche Forschungsgemeinschaft (Ba 309/11-2).

REFERENCES

Augustin H., Foissner W., Adam H. (1984) An improved pyridinated silver carbonate method which needs few specimens and yields permanent slides of impregnated ciliates (Protozoa, Ciliophora). *Mikroskopie* **41:** 134-137

Bardele C. F. (1981) Functional and phylogenetic aspects of the ciliary membrane: a comparative freeze-fracture study. *BioSystems* **14:** 403-421

Bardele C. F. (1987) Auf neuen Wegen zu alten Zielen - moderne Ansätze zur Verwandtschaftsanalyse der Ciliaten. *Verh. Dtsch. Zool. Ges.* **80:** 59-75

Bardele C. F. (1989) From ciliate ontogeny to ciliate phylogeny: a program. *Boll. Zool.* **56:** 235-243

Bardele C. F. (1991) The implications of morphogenetic and molecular studies on our current understanding of ciliate phylogeny. Abstr., 7th European Conference on Cell and Molecular Biology of Ciliates, Toledo, Spain, 27

Bardele C. F., Klindworth T. (1996) Stomatogenesis in the karyorelictean ciliate *Loxodes striatus*: a light and scanning microscopical study. *Acta. Protozool.* **35:** 29-40

Baroin-Tourancheau A., Delgado P., Perasso R., Adoutte A. (1992) A broad molecular phylogeny of ciliates: Identification of major evolutionary trends and radiations within the phylum. *Proc. Natl. Acad. Sci. USA* **89:** 9764-9768

Canella M. F. (1970) Sur les organelles ciliaires de l'appareil buccal des hyménostomes et autres ciliés. *Ann. Univ. Ferrara (N.S. Sect. III, 3, Suppl)* 1-235

Corliss J. O. (1974) Remarks on the composition of the large ciliate class Kinetofragmophora de Puytorac et al., 1974, and recognition of several new taxa therein, with emphasis on the primitive order Primociliatida n. ord.. *J. Protozool.* **21:** 207-220

Didier P., Puytorac P. de, Wilbert N., Detcheva R. B. (1980) A propos d'observations sur l'ultrastructure du cilié *Cyrtolophosis mucicola* Stokes, 1885. *J. Protozool.* **27:** 72-79

Dragesco J. (1960) Ciliés mésopsammiques littoraux. Systématique, morphologie, écologie. *Trav. Stat. Biol. Roscoff (N.S.)* **12:** 1-356

Dragesco J., Dragesco-Kernéis A. (1986) Ciliés libres de l' Afrique intertropicale. Collection Faune Tropicale XXVI, éditions de l' Orstom, Paris

Dragesco J., Njiné T. (1971) Compléments à la connaissance des ciliés libres du Cameroun. *Ann. Fac. Sci. Cameroun* **7-8:** 97-140

Eisler K. (1992) Somatic kineties or paroral membrane: which came first in ciliate evolution? *BioSystems* **26:** 239-254

Engelmann T. W. (1862): Zur Naturgeschichte der Infusionsthiere. *Z. wiss. Zool.* **11:** 347-393

Fenchel T. (1986) The structure and function of Müller vesicles in loxodid ciliates. *J. Protozool.* **33:** 69-76

Fernández-Galiano D. (1976) Silver impregnation of ciliated protozoa: a procedure yielding good results with the pyridinated silver carbonate method. *Trans. Am. Micros. Soc.* **95:** 557-560

Finlay B. J., Fenchel T. (1986) Physiological ecology of the ciliated protozoon *Loxodes*. *Rep. Freshwat. biol. Ass.* **54:** 73-96

Fleury A., Delgado P., Iftode F., Adoutte A. (1992) A molecular phylogeny of ciliates: What does it tell us about the evolution of the cytoskeleton and of developmental strategies? *Develop. Genetics* **13:** 247-254

Foissner W., Rieder N. (1983) Licht- und rasterelektronenmikroskopische Untersuchungen über die Infraciliatur von *Loxodes striatus* (Engelmann, 1862) und *Loxodes magnus* Stokes, 1887 (Protozoa: Ciliophora). *Zool. Anz.* **210:** 3-13

Gerassimova Z. P., Seravin L. N. (1976) [Ectoplasmatic fibrillar system of infusoria and its role for the understanding of their phylogeny]. *Zool. Zh.* **55:** 645-656 (in Russin with English summary)

Grain J. (1969) Le cinétosome et ses dérivés chez les ciliés. *Ann. Biol.* **8:** 20-97

Grain J. (1984) Cinétosome, cil, systèmes fibrillaires en relation avec le cinétosome. In: Traité de Zoologie, (Ed. P.-P. Grassé) Masson, Paris, New York, **2:** 35-179

Grell K. G. (1962) Morphologie und Fortpflanzung der Protozoen (einschließlich Entwicklungsphysiologie und Genetik). *Fortschr. Zool.* **14:** 1-85

Kahl A. (1932/1935) Urtiere oder Protozoa. In: Wimpertiere oder Ciliata (Infusoria). *Die Tierwelt Deutschlands* (Hrsg. F. Dahl) Fischer, Jena

Locke M., Krishnan N., McMahon J. T. (1971): A routine method for obtaining high contrast without staining sections. *J. Cell. Biol.* **50:** 540-544

Luft J. H. (1961) Improvements in epoxy resin embedding methods. *J. Biophys. Biochem. Cytol.* **9:** 409-414

Lynn D. H. (1981) The organization and evolution of microtubular organelles in ciliated protozoa. *Biol. Rev.* **56:** 243-292

Lynn D. H. (1988) Cytoterminology of cortical components of ciliates: somatic and oral kinetids. *BioSystems* **21:** 299-307

Lynn D. H. (1991) The implications of recent descriptions of kinetid structure to the systematics of the ciliated protists. *Protoplasma* **164:** 123-142

Lynn D. H., Small E. B. (1981) Protist kinetids: structural conservatism, kinetid structure, and ancestral states. *BioSystems* **14:** 377-385

Lynn D. H., Small E. B. (1988) An update on the systematics of the phylum Ciliophora Doflein, 1901: the implications of kinetid diversity. *BioSystems* **21:** 317-322

Njiné T. (1970) Structure et morphogenèse buccales chez le cilié holotriche *Loxodes magnus* Stokes, 1887. *C. R. Acad. Sc. Paris* **270:** 519-522

Pätsch B. (1974) Die Aufwuchsciliaten des Naturlehrparks Haus Wildenrath. *Arb. Inst. Landwirtsch. Zool. Bienenkd.* **1:** 1-82

Parducz B. (1952) Eine neue Schnellfärbemethode im Dienste der Protistenforschung und des Unterrichts. *Ann. Hist. Nat. Mus. Nation. Hung. (N.S.)* **2:** 5-12 (in Ungarian with German summary)

Penard E. (1917) Le genre *Loxodes*. *Rev. Suisse Zool.* **25:** 453-489

Penard E. (1922) Etudes sur les Infusoires d'Eau douce. Georg & Cie, Genève

Puytorac P. de (ed.) (1994) Infusoires Ciliés. Traité de Zoologie. - Anatomie, Systématique, Biologie. Tome II, Fasc. 2, Masson, Paris.

Puytorac P. de, Njiné, T. (1970) Sur l' ultrastructure des *Loxodes* (ciliés holotriches). *Protistologica* **6:** 427-444

Puytorac P. de, Grain, J., Legendre, P., Devaux, J. (1984) Essai d' application de l'analyse phénétique à la classification du phylum des Ciliophora. *J. Protozool.* **31:** 496-507

Raikov I. B. (1985) Primitive never-dividing macronuclei of some lower ciliates. *Int. Rev. Cytol.* **95:** 267-325

Raikov I. B. (1994) Somatic cortical and endoplasmic fine structure of *Remanella granulosa* Kahl (Ciliophora, Karyorelictida). *Arch. Protistenkd.* **144:** 7-16

Raikov I. B., Gerassimova-Matvejeva Z. P., Puytorac P. de (1976) Cytoplasmic fine structure of the marine psammobiotic ciliate *Tracheloraphis dogieli* Raikov. I. Somatic infraciliature and cortical organelles. *Acta Protozool.* **14:** 17-42

Reynolds E. S. (1963) The use of lead citrate at high pH as an electron-opaque stain in electron microscopy. *J. Cell. Biol.* **17:** 208-212

Rieder N., Ott H. A., Pfundstein P., Schoch R. (1982) X-ray microanalysis of the mineral contents of some protozoa. *J. Protozool.* **29:** 15-18

Seravin L. N., Gerassimova Z. P. (1978) A new macrosystem of ciliates. *Acta Protozool.* **17:** 399-418

Shigenaka V., Watanabe K., Kaneda M. (1973) Effects of glutaraldehyde and osmium tetroxide on hypotrichous ciliates, and determination of the most satisfactory fixation methods for electron microscopy. *J. Protozool.* **20:** 414-420

Small E. B. (1984) An essay on the evolution of ciliophoran oral cytoarchitecture based on descent from within a karyorelictean ancestry. *Origins of Life* **13:** 217-228

Small E. B., Lynn D. H. (1981) A new macrosystem for the phylum Ciliophora Doflein, 1901. *BioSystems* **14:** 387-401

Small E. B., Lynn D. H. (1985) Phylum Ciliophora Doflein, 1901. In: An illustrated guide to the Protozoa, (Eds. J. J. Lee, S. H. Hutner and E. C. Bovee). Society of Protozoologists, Lawrence, Kansas, 393-575

Tuffrau M. (1963) Les structures infraciliaires et la stomatogenèse chez les *Loxodes*. 1st Int. Congr. Protozoology, Prague, Aug. 1961, Progress in Protozoology, 278-280

Received on 14th April, 1995; accepted on 5th July, 1995

Acta Protozoologica (1996) 35: 29 - 40

ACTA
PROTOZOOLOGICA

Stomatogenesis in the Karyorelictean Ciliate *Loxodes striatus*: a Light and Scanning Microscopical Study

Christian F. BARDELE and Thomas KLINDWORTH

Department of Zoology, University of Tübingen, Germany

Summary. Light microscopic and SEM studies have shown that the karyorelictean ciliate *Loxodes striatus* has a buccokinetal stomatogenesis. In the interphase cell the subapical oral cavity is equipped with four oral kineties of different organization. In addition, the oral cavity has a tube-like prolongation, called vestibular extension. On the right side the oral cavity is bordered by a paroral kinety and on the left side it is bordered by an inverted left pseudobuccal kinety. In between these most prominent oral kineties there lies an intravestibular kinety parallel to the entire length of the paroral and then continuing down into the vestibular extension. In the upper part of the oral cavity between the intravestibular kinety and the left pseudobuccal kinety there is a short file of four widely spaced buccal dikinetids, which give origin to four anterior buccal cilia. Posterior to the oral cavity close to the actual ventral line of the cell there is a ventral kinetofragment of 8-10 barren dikinetids.

Key words: buccokinetal stomatogenesis, ciliate evolution, Ciliophora, Karyorelictea, *Loxodes striatus*, morphogenesis, scanning electron microscopy.

INTRODUCTION

Karyorelictean ciliates are of considerable interest in the discussion on the origin of ciliates in general. Most of their representatives occur in the marine mesopsammon, thought to be an important cradle of lower invertebrate phyla (Swedmark 1964, Ax 1966). As a characteristic feature of the karyorelictean ciliates their paradiploid (nearly diploid) somatic macronuclei are unable to divide and need to be differentiated from dividing micronuclei during every round of cell division (Raikov 1982, 1985). The name of this group of ciliates arose from the once popular hypothesis that their nuclear behaviour might represent an important step in the evolution of nuclear dimorphism seen in all higher ciliates (Corliss 1974, 1975, 1979). Alternatively, we would like to argue that their nuclear behaviour represents an autapomorphous character of the karyorelictean ciliates, and, at the same time, is a dead end road as far as macronuclear evolution is concerned. It has also been suggested that the karyorelicteans represent corticorelicts (Small 1984) and we are inclined to regard their mode of stomatogenesis a very primitive one, thus regarding them as stomatogenic relicts. Our laboratory has shown that comparative studies of ciliate stomatogenesis are of considerable value in studying ciliate interrelationship (Huttenlauch and Bardele 1986; Bardele 1987, 1989; Eisler 1989; Hiller 1991, 1993; Hofmann-Münz 1991).

Address for correspondence: Ch. F. Bardele, Universität Tübingen, Zoologisches Institut, Auf der Morgenstelle 28, D - 72076Tübingen, Germany; Fax: +49-7071-294634; E-mail: christian.bardele@uni-tuebingen.de

Starting from theoretical considerations on the possible origin of somatic ciliature from a paroral Eisler (1992) drew attention to the possibly primitive character of buccokinetal stomatogenesis. This initiated our interest in the stomatogenesis of *Loxodes*, since earlier light microscopical studies of Njiné (1970) had indeed shown a buccokinetal mode of stomatogenesis in this ciliate. We soon learned that prior to a study on stomatogenesis a reinvestigation of the oral structures of the interphase cell of *Loxodes* was necessary, which has revealed several unexpected findings, e. g. an inverted left pseudobuccal kinety (Klindworth and Bardele 1996). Based on light microscopical observation of silver-impregnated cells and scanning electron microscopy we give a detailed description of stomatogenesis in *Loxodes striatus*, which in several important points deviated from the description by Njiné (1970). The present study is a prerequisite of an analysis using thin sections to elucidate finer details of stomatogenesis in *Loxodes* currently underway in our laboratory. We hope these studies are also of interest for those researchers who use ribosomal RNA sequence data to unravel ciliate interrelationship (Lynn and Sogin 1988, Greenwood et al. 1991, Schlegel 1991), in particular since molecular studies have shown that heterotrichs together with *Loxodes* form the earliest branch on the ciliate tree (Baroin-Tourancheau et al. 1992, Fleury et al. 1992).

MATERIALS AND METHODS

The origin of our strain of *Loxodes striatus* as well as the method of cultivation have been described in a previous paper (Klindworth and Bardele 1996). When cultivated in test tubules the majority of ciliates swims free close to the anoxic boundary. From there they were collected in large density and transferred to a Petri dish. After settling for a while several individuals crawled close to the bottom with their intensely ciliated right lateral side of the cell oriented towards the substratum. Partial synchronization of the cell cycle was reached by several starvation and feeding cycles, and cells in division were selected by hand using a micropipette. Early dividers which are difficult to recognise were found in bulk samples which contained a good number of mid-divisional stages.

For light microscopy the pyridinated silver carbonate method of Fernández-Galiano (1976) using the modification recommended by Augustin et al. (1984) was used. In order to yield superior resolution of the infraciliature the cells were fixed for 20 s in osmium vapor and post-fixed for 3 min in 1% formaldehyde. Further steps of the staining procedure had to be completed within 45-60 s.

For scanning electron microscopy of dividing cells, which are particularly fragile during this stage of their life cycle, the Parducz fixative (1952) was used in a 1:100 relation of cells to fixative for 15 min at room temperature. Following partial dehydration up to 70% ethanol the cells were mounted on round polylysine-coated cover slips, 12 mm in diameter, critical point dried, sputter-coated with gold-palladium and observed in a Cambridge Stereoscan 250 MK2.

RESULTS

Loxodes striatus is a laterally depressed cell with a subapical buccal cavity (Fig. 1). The cell measures approximately 180 µm in length and 50 µm in breadth in lateral view. The right lateral side has 11 somatic kineties made of dikinetids with both kinetosomes ciliated in most cases. The left lateral side of the cell is only sparsely ciliated showing two marginal kineties close to the rim of the cell.

The buccal cavity has a tube-like extension (also called vestibular extension) pointing in posterior direction. Since details of the oral ciliature have been described in a previous paper (Klindworth and Bardele 1996) only the major components are listed here (see Fig. 2 for overview). On the right margin of the buccal cavity lies a paroral kinety (PO) made of a closely spaced row of dikinetids. The three anteriormost dikinetids are spaced more widely (Fig. 2). Parallel to the paroral there is an argentophilic band. An intravestibular kinety (IVK) made of dikinetids runs in the keel-shaped bottom of the

Fig. 1. Silver-impregnated specimen of *Loxodes striatus* slowing the right lateral side of the cell with 11 somatic kineties and the oral apparatus (OA) in the upper right corner. The nuclei are organized in two groups, each consisting of a paradiploid macronucleus(MA) and a diploid micronucleus (MI). Fernández-Galiano silver impregnation (x 1000). From Klindworth and Bardele 1996

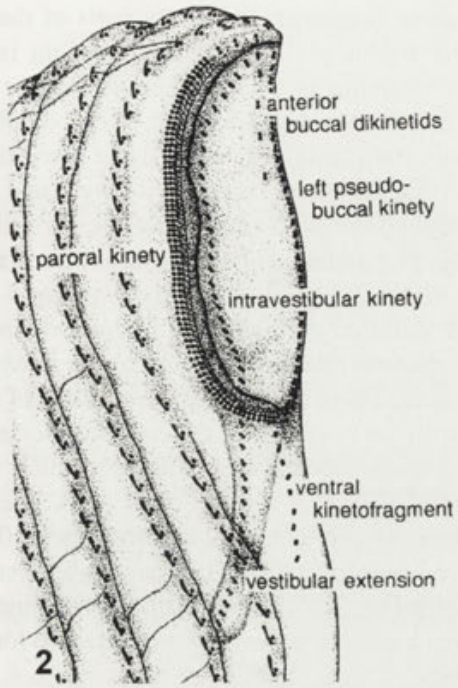

Fig. 2. Schematic drawing of the anterior end of *Loxodes striatus* to illustrate the oral ciliature. From Klindworth and Bardele 1996, modified

buccal cavity ending in the vestibular extension. In the anterior left wall of the buccal cavity there is a file of four dikinetids, which bear a long cilium each. Collectively, these cilia are called anterior buccal cilia. Finally, on the left margin of the buccal cavity lies a closely spaced row of dikinetids which owing to the kinetosome-associated fiber systems represents an inverted somatic kinety. It is called left pseudobuccal kinety (LPK). Posterior to the oral cavity there is a ventral kinetofragment composed of barren 8-10 dikinetids.

Prior to a detailed description of the morphogenetic process a short summary of the nuclear events during cell division is given. In connection with Fig. 15 it may allow an overview to what extent nuclear events go in parallel with the stomatogenic events. But the reader should take in mind that schematic drawings like Fig. 15 represent a simplification. Moreover, it splits up a continuous process into several separate snapshots usually not taken at regular intervals but determined by certain clearly recognisable changes. The reader is purposely informed that the nuclear and stomatogenic events are not as precisely synchronized as Fig. 15 might suggest.

The nuclei are organized in two groups which lie in the anterior and posterior half of the cell. Each group consists of a paradiploid macronucleus and a diploid micronucleus (Fig. 1). In the anterior group the micronucleus is lying immediately behind the macronucleus, while in the posterior group it is the other way round, thus the two micronuclei in interphase cells face each other. The micronuclei measure 2-3 µm in diameter. The macronuclei measure 6-9 µm in diameter and contain a distinctive nucleolus, 3 µm in diameter. Nuclear division in *L. striatus* (and other karyorelictean ciliates) has been studied in great detail by Raikov (1959) both with cytochemical and electron microscopical techniques (for comprehensive reviews see Raikov 1982, 1985). Naturally, the nuclear apparatus has to be duplicated during cell division. Unfortunately, the changes of the dividing nuclei do not occur in synchrony with particular stages of morphogenesis, so they cannot help to specify the different stages of this process. Nevertheless, the major steps of nuclear division and nuclear differentiation are summarised in Fig. 15 to facilitate the understanding of the following description. Either one of the micronuclei starts to divide (In Fig. 15 a it is arbitrarily the one of the posterior group of nuclei). One of the resulting daughter nuclei stays in close contact with the macronucleus, while the other one moves over a short distance toward the middle of the cell and undergoes a second mitotic division (Fig. 15b). One of the products of this second division starts to differentiate into a macronucleus, it swells (Fig. 15c) and several small nucleoli emerge (Fig. 15d), they grow larger (Fig. 15e) and finally fuse into a composite central nucleolus (Fig. 15f). Now, every daughter cell has again the full complement of nuclei. At no time the slightest sign of macronuclear division was observed. The onset of the first micronuclear division is no reliable sign for the start of cell division since it may occur several hours before the start of kinetosome proliferation in the somatic cortex, or later.

Cell division in *Loxodes striatus* is homothetogenic, that is perpendicular to the kineties, at about the middle of the cell . While the anterior part of the dividing cell, the proter, receives the parental oral apparatus, which is only slightly reorganized, the posterior part of the dividing cell, the opisthe, has to build a completely new oral apparatus. Major steps of stomatogenesis as far as they could be observed in silver- stained cells and by scanning electron microscopy comprise the proliferation of kinetosomes, morphogenetic movements of kinetofragments, the sprouting of new cilia, detachment, resorption and replacement of the vestibular extension as well as topological changes in the oral cavity. To facilitate the description,

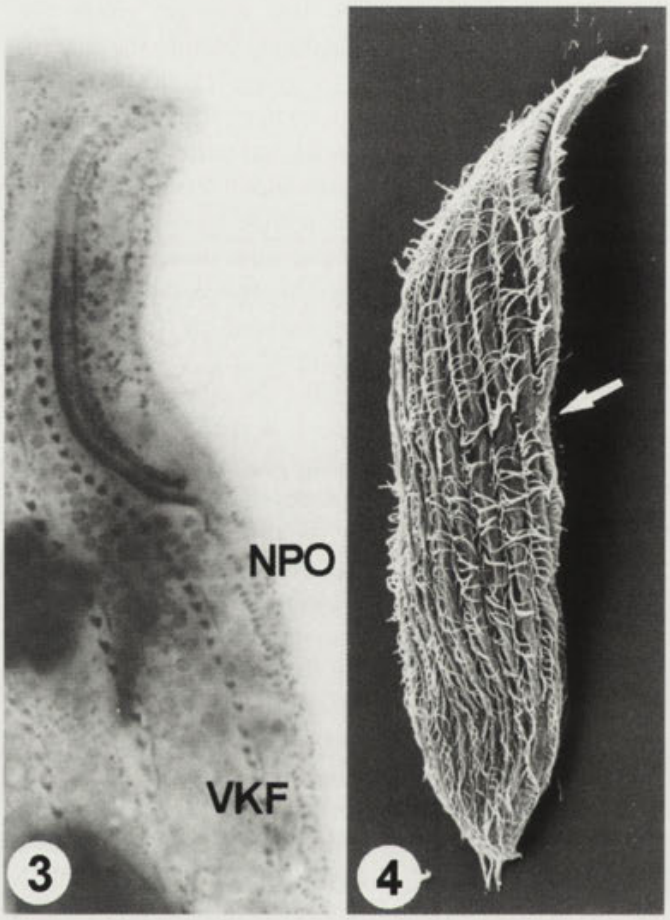

Figs. 3-4. Early stage 1. 3 - new kinetosomes (NPO) appear at the lower end of the paroral. The ventral kinetofragment (VKF) has migrated in posterior direction (x 1500). 4 - first sign of kinetosome proliferation in an oblique line (arrow) in the somatic cortex. Scanning electron micrograph (x 650)

morphogenesis in *L. striatus* has been divided in five stages.

Stage 1

The first sign of beginning cell division is the proliferation of kinetosomes in the somatic kineties in the middle of the cell at the site of the future cleavage furrow (Fig. 4, 15b). In early stage 1 the ventral kinetofragment which in interphase cells is seen as a file of about 10 dikinetids separated slightly from each other (Fig. 2) has become a continuous file of single kinetosomes which gradually moves backwards (Fig. 3) followed by new kinetosomes originating from the posterior end of the parental paroral. At late stage 1 the paroral of the future opisthe has grown longer. Often two (at stage 2 even three) slightly bent fragments form the anlagen of the new paroral (Fig. 5). As an indication that these fragments are really parts of the future paroral the argentophilic band at their right is taken, since this structure is a characteristic feature of the paroral in the interphase cell (for details see Klindworth and Bardele, 1996). At the same time the left pseudobuccal kinety has grown longer and clearly reaches beyond the posterior end of the paroral of the proter (Fig. 5). Its kinetosome proliferation towards the posterior end of the cell is easily explained by the inverted orientation of this kinety. In the corresponding scanning electron micrograph (Fig. 6) the new paroral is clearly seen. There is a distinctive gradient of sprouting cilia with the posterior cilia being the shortest. The new left pseudobuccal kinety, though much shorter than the new paroral, is also seen in Fig. 6. The barren kinetosomes of the ventral kinetofragment (Fig. 2) have moved posteriorly and thus cannot be seen in the part shown in Fig. 5. As judged from silver-stained cells, these barren kinetosomes rapidly proliferate to form new kinetosomes.

Stage 2

While the paroral and the left pseudobuccal kinety continue to grow in length the bottom of the vestibular cavity immediately in front of the connection to its posterior extension moves towards the surface. During this movement the tube-like extension is also elevated and shifted into a more perpendicular position with respect to the somatic kineties (Fig. 15c). Then the vestibular extension detaches from the parental oral cavity together with the posterior end of the intravestibular kinety, but stays in contact with the cell surface as judged from a temporary opening seen in SEM micrographs (Fig. 8, arrow). The newly built part of the paroral and the left pseudobuccal kinety separate from their parental anterior parts and move posteriorly. At this stage the paroral of the opisthe seems to be composed of three slightly bent parts (Fig. 15c). The scanning electron micrograph in Fig. 8 also shows three groups of paroral cilia.

Stage 3

The future cleavage furrow in the somatic cortex now shows up (Fig. 15d). Both the new paroral and the new left pseudobuccal kinety move further backwards together with the remainder of the parental vestibular extension which gradually becomes resorbed. For some while the barren kinetosomes of the intravestibular kinety are still seen in the ventral wall of the dissolving vestibular extension. The upper two parts of

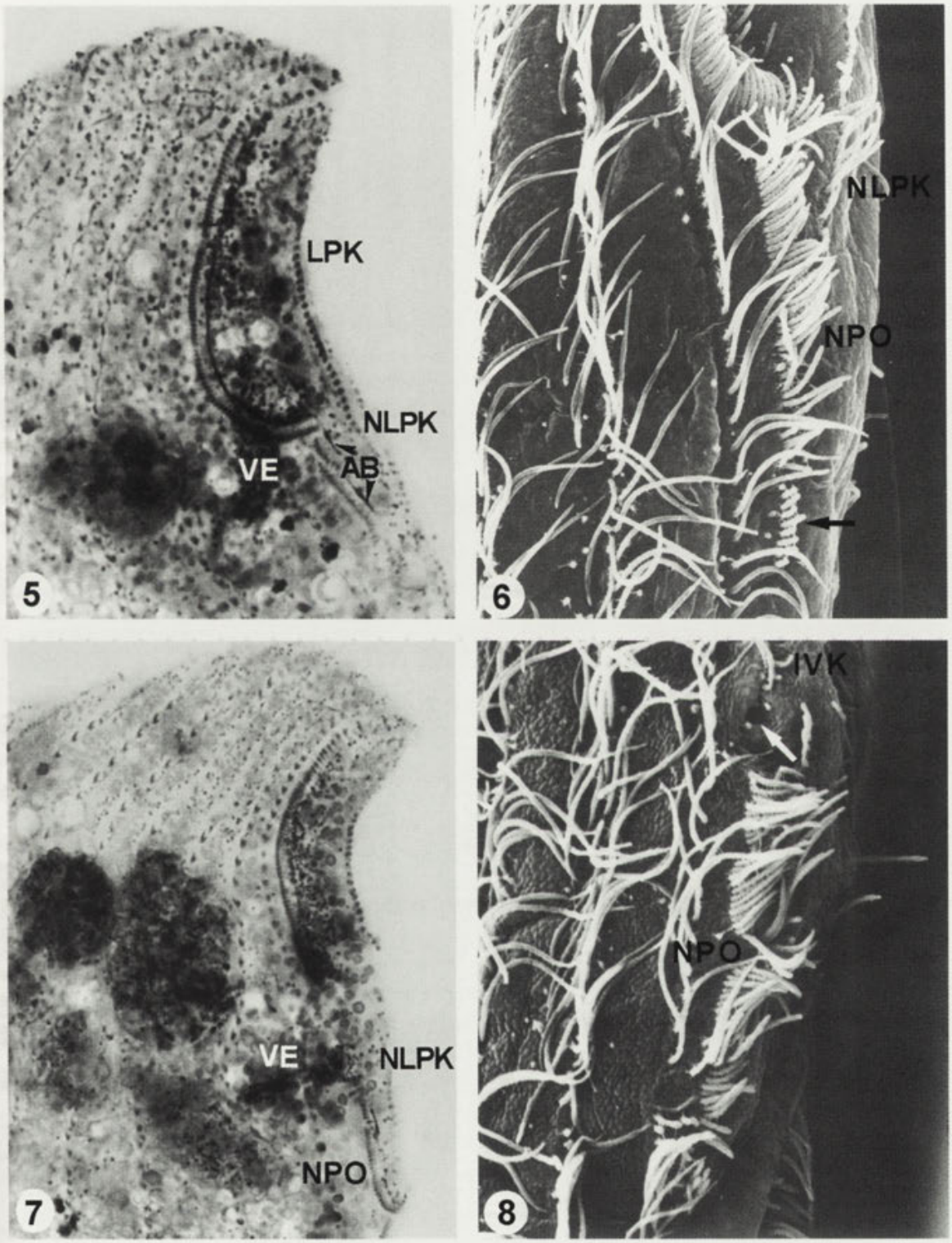

Figs. 5-6. late stage 1. 5 - in this rather early stage of stomatogenesis two parts of the new paroral are already seen, together with their argentophilc band (AB). The left pseudobuccal kinety (LPK) has grown beyond the posterior end of the parental oral cavity. The vestibular extension (VE) is still attached to the oral cavity (x 1500). 6 - scanning electron micrograph showing the new left pseudobuccal kinety (NLPK) and the new paroral (NPO) with graded growth of the cilia, the most posterior ones being the shortest (arrow) (x 6100). Figs. 7-8. Stage 2. 7 - the vestibular extension (VE) has become detached from the parental oral cavity. The new paroral (NPO) and the new left pseudobuccal kinety (NLPK) have separated from their anterior parts which stay in the proter (x 1400). 8 - the new paroral (NPO) is composed of three parts. In front of the most anterior part of the new paroral there is the opening of the detached vestibular extension to the cell surface (arrow) and in front of this opening a few small cilia (probably being resorbed) of the intravestibular kinety (IVK) are seen (x 3500)

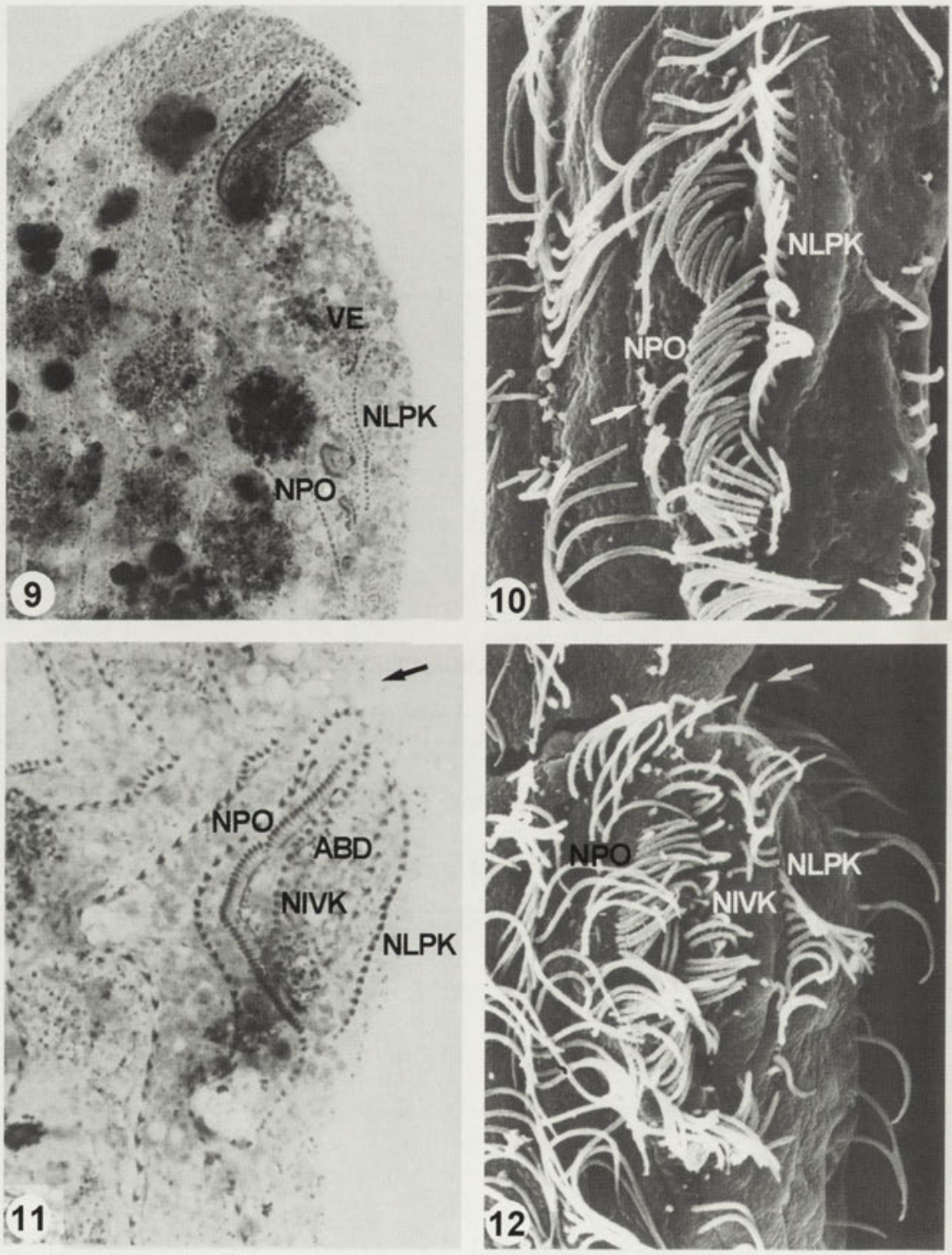

Figs. 9-10. Stage 3. 9 - the recently built new paroral (NPO) and the new left pseudobuccal kinety (NLPK) together with the detached posterior extension of the vestibulum (VE) have moved backwards (x 1000). 10 - scanning electron micrograph of the buccal area of the opisthe. The new left pseudobuccal kinety (NLPK) forms a straight line while the new paroral (NPO) consists of three bent parts. At this stage the newly forming oral apparatus is lying at the level where new somatic cilia grow from recently proliferated kinetosomes (arrows) (x 3400)
Figs. 11-12. Stage 4. 11 - the somatic kineties are split at the level of the future cleavage furrow (arrow). Posterior to the furrow the oral apparatus of the opisthe becomes organized between the new paroral (NPO) and the new left pseudobuccal kinety (NLPK), kinetosomes of the new intravestibular kinety (NIVK) and the anterior buccal dikinetids (ABD) are seen (x 1750). 12 - corresponding scanning electron micrograph. The arrow marks the cleavage furrow. The cavity between the new paroral (NPO) and the new left pseudobuccal kinety (NLPK) shows only a slight depression, so the intravestibular kinety (NIVK) is still at the same level as the paroral (x 2800)

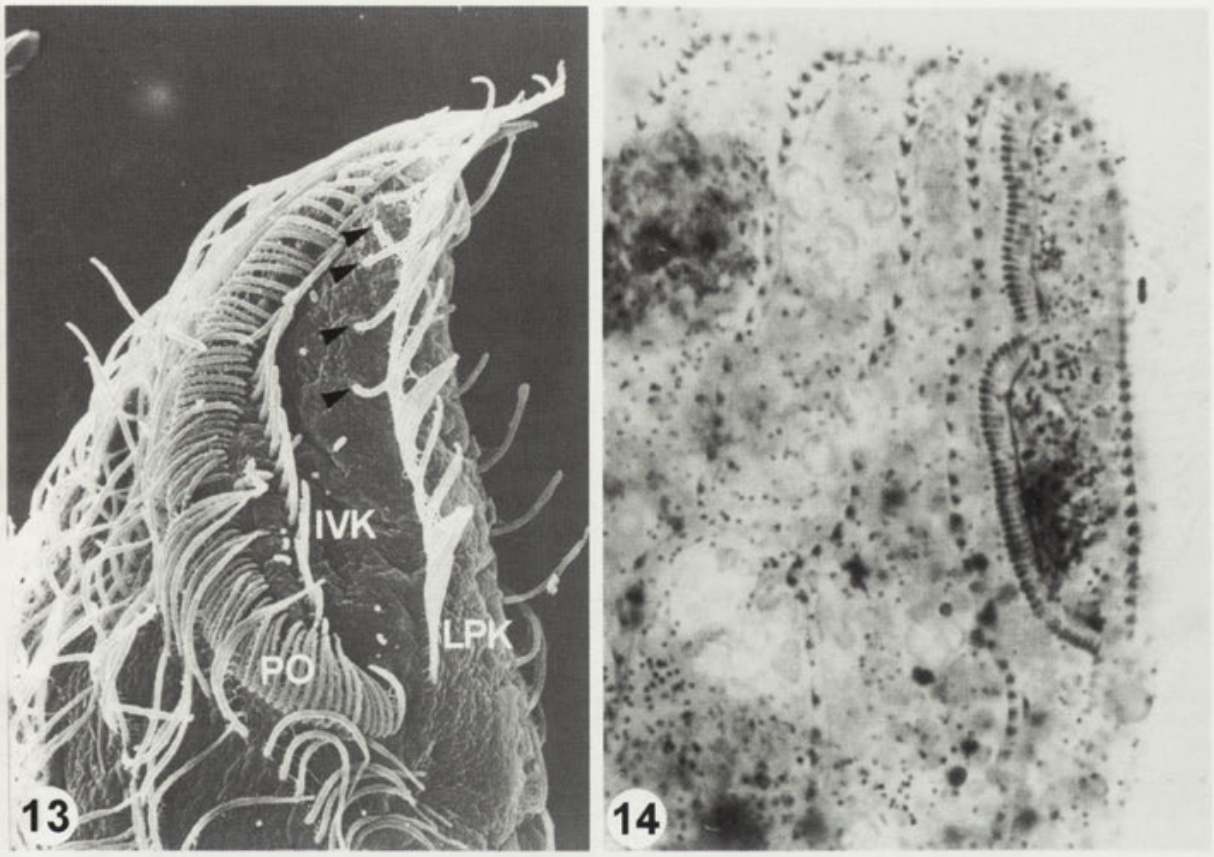

Fig. 13-14. Stage 5. 13 - SEM of a proter shortly after separation from the opisthe. The intravestibular kinety (IVK) is still lying close to the surface between the paroral (PO) and the left pseudobuccal kinety (LPK). The arrowheads mark the cilia of the anterior buccal dikinetids (x 3200). 14 - oral apparatus of an opisthe shortly after division. The paroral still consists of two parts and the vestibular extension has not yet formed (x 2000)

the paroral join and separate kinetosomes move in line with the posterior part, these kinetosomes will later become the dikinetids of the ventral kinetofragment of the opisthe. During the movement of the newly formed oral apparatus across the future fission furrow the left pseudobuccal kinety somewhat trails behind the other oral structures.

Stage 4

The contraction of the cleavage furrow proceeds and starts to the somatic kineties. The new paroral (still consisting of two parts) and the new left oral kinety of the future opisthe are now lying behind the cleavage furrow (Fig. 15 e). At the anterior end of the new paroral there are again three more widely spaced dikinetids which are a characteristic feature of the paroral in the interphase cell (Fig. 2). The space between the paroral and the left pseudobuccal kinety, which later will mark the lateral sides of the oral cavity, begins to widen. In this part of the oral field, still lying close to the surface of the cell, the widely spaced kinetosomes of the new intravestibular kinety and several kinetosomes of the future anterior buccal cilia appear suddenly (Fig. 11). Note that some important details about the origin of the latter two structures are lacking in our present documentation. The bottom of the oral cavity is still close to the cell surface which means that the new intravestibular kinety is lying at almost the same level as the paroral and the left pseudobuccal kinety. In the proter a new vestibular extension begins to differentiate.

Stage 5

The two daughter cells have split. Recently split cells are shorter in length than interphase cells and have a clumsy cell shape in lateral view (Fig. 15f). Further distinction whether a particular cell is a proter or an opisthe is to a certain extent possible because of the slightly different shape of the anterior end of the cell. In scanning micrographs the proter may soon have the pointed beak characteristic for the interphase cell, but a more reliable

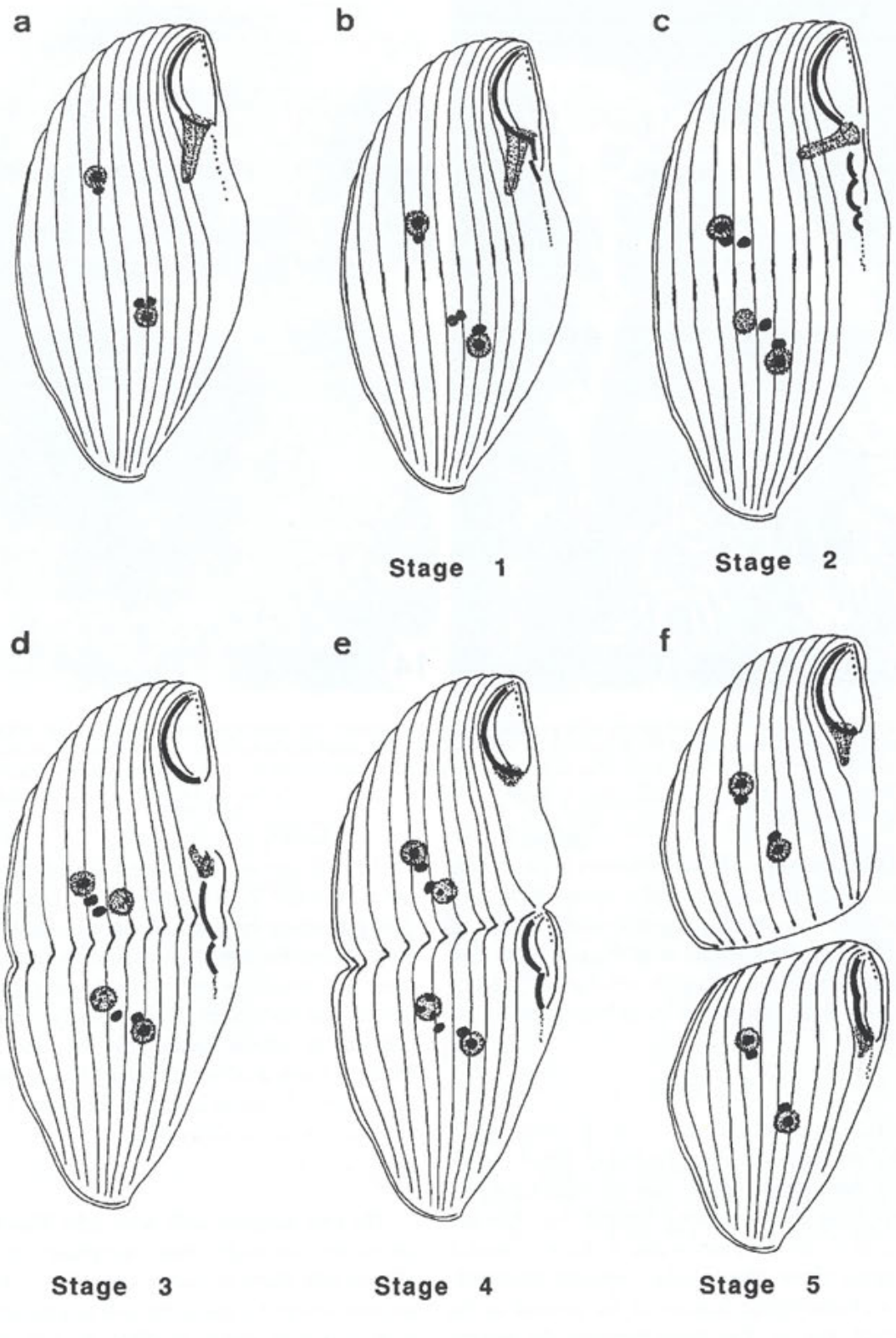

Fig. 15. Schematic drawing of nuclear events and morphogenesis in *Loxodes striatus*. The paroral is shown as a heavy line. Adjacent to the paroral is the intravestibular kinety, which dives down in the vestibular extension (dotted structure), the four anterior buccal dikinetids are seen to the right side of the left pseudobuccal kinety. For details of the buccal ciliature compare with Fig. 2

feature is the paroral which comes in one piece and the still elevated floor of the future oral cavity, all seen in Fig. 13. An opisthe is positively identified by the fact that its paroral still consists of two parts (Fig. 14). Oral reorganization in proter comprises further growth of the vestibular extension and the renewal of the posterior part of the intravestibular kinety, these events take place after the daughter cells have separated. A new ventral kinetofragment has to be rebuilt, too. Through further growth in length the daughter cells finally regain the cell shape which is typical for the interphase cells.

DISCUSSION

Our belief in studies on ciliate morphogenesis bears on an auxiliary criterion of phylogenetic research, the criterion of ontogenetic precedence (Hennig 1966) which under appropriate considerations of possible heterochronies may help to determine the direction of character transformation, among others e. g. also in the modes of stomatogenesis.

Stomatogenesis in *Loxodes striatus* is of the buccokinetal type (*sensu* Corliss 1973), the autonomous character of both the paroral and the left pseudobuccal kinety is clearly evident from this study. In recent times Njiné (1970) was the only investigator who studied stomatogenesis in the genus *Loxodes*. Using Protargol impregnation he studied *L. magnus* and likewise recognised a buccokinetal mode. In some very important details his observations disagree with ours. We cannot imagine that these differences are due to the fact that his and our study were done with two slightly different *Loxodes* species. Njiné (1970) took the intravestibular kinety as stomatogenic in *L. magnus*, which definitively is not true for *L. striatus*. Moreover, the labelling of his "cinétie buccale gauche" (CX) and his "double cinétie droite" (CY) in Fig. 2 of Njiné (1970) is reversed.

In addition to *L. striatus* we have also studied *L. magnus* in some detail, just for comparison. One of the major disadvantages of *L. magnus* is its size. Parallel to its large cell size the oral kineties and in particular the anlagen of the new kineties are longer and contain a higher number of kinetosomes than in *L. striatus*. Since the space near the posterior end of the oral cavity of the proter, where stomatogenesis takes place, is restricted, the new kineties in *L. magnus* get bent and tossed. This certainly makes a correct identification of the various anlagen more difficult. Although we have not yet any information on the origin of the kinetosomes of the anterior buccal cilia in the opisthe it is highly unlikely that the corresponding dikinetids originate from the left pseudobuccal kinety (or "cinétie buccale externe gauche") as Njiné (1970) has claimed. An origin from the inverted left buccal kinety would necessitate a turning of 180° for which we have found no indication. As far as the origin of the left pseudobuccal kinety is concerned we assume that it is derived from the somatic kinety K1. The possible reason for its migration to the left side of the buccal cavity (and thus its inverted orientation) might have been caused by the sinking of the primary adoral ciliature, the intravestibular kinety, down into the bottom of the buccal cavity.

Nowadays, admittedly, stomatogenesis shows no trace of the suggested migration process and we have to assume that it took place during the long evolutionary history of *Loxodes*.

The anlagen of both the new intravestibular kinety and the new anterior buccal dikinetids are seen first in the upper part of the new oral field in both species. But at least for the moment the origin of the kinetosomes in question remains unknown. One of the most puzzling problems is how the four different kinetid patterns found in the oral cavity (for details see Klindworth and Bardele 1996) get organized in close neighbourhood to each other. We hope to get some information on this topic in our TEM study currently in progress.

The ventral kinetofragment of *L. striatus* behaves similar to a scutica, it is positioned at the respective site and is certainly involved in stomatogenesis. The reorganization of the ventral kinetofragment in the proter seems to be a rather late event which we have not observed. It is reasonable to assume that it is derived from the paroral. We think it might be worthwhile to search for scutica-like structures in other ciliates, too. We can imagine that a reminder of highly reduced scutica-like structure resting near the surface in a postoral position could be involved in the parakinetal mode of stomatogenesis, or when located slightly deeper in the cytoplasm but still in close neighbourhood to the posterior end of the oral ciliature of the proter, it could be involved in apokinetal stomatogenesis. Thus the parakinetal and the apokinetal mode of stomatogenesis could have arisen from the buccokinetal mode. Up to the early seventies when hypotrichs and endodiniomorphs were regarded as highly derived ciliates their apokinetal mode of stomatogenesis was also thought to be derived. This may well be true, but perhaps in a more direct and shorter way than thought before.

The entire discussion also shows to what extent the contemporary view on morphogenesis was (and probab-

ly still is) influenced by the changing understanding of ciliate interrelationship. In connection with molecular data we may start to move on safer ground. But we should also keep in mind that any particular mode of stomatogenesis might have evolved more than once.

As mentioned already in the introduction, based on ribosomal RNA sequence data it is now fairly clear that heterotrichs are closely related to the karyorelicteans. Typical heterotrichs like *Blepharisma*, *Climacostomum*, *Spirostomum* and *Stentor* how a parakinetalstomatogenesis. Nonetheless, it might be worthwhile to check whether these ciliates show some indirect signs of buccokinetal stomatogenesis in the early stages, as for instance documented in *Nassula citrea* where the paroral ciliature produces somatic kinetofragments which in the subsequent division cycle serve as the anlagen of the paroral of the opisthe (Eisler and Bardele 1986).

This investigation has made no contribution to the still open question whether the inability of the karyorelictean macronuclei to divide is a plesiomorphous or an apomorphous character. We think the latter is correct (and consequently these ciliates may go by a false name). We would like to argue that their nuclear features make no good intermediate model for the evolution of dividing macronuclei in higher ciliates. Among other things it would be interesting to know whether there is any relationship between the rather restricted degree of oral regeneration of the oral structures in the proter and the ageing of macronuclei in *Loxodes*. In *L. striatus* it is obvious that the two macronuclei in each daughter cell differ in age. The longevity of the macronuclei of *Loxodes* (not specified which species) is said to be restricted to about seven cell generations (Raikov 1994). Raikov (1985) discusses the possibility of macronuclear replacement (through abnormalities in micronuclear divisions and extra macronuclear differentiation), but there is no hard evidence that these mechanisms of rejuvenescence really take place. Nature produces ciliates and all other organisms in access and usually there are self-regulatory mechanisms which keep a population within certain limits. The topic of macronuclear ageing should be followed up in context with the different age of the oral structures. In *L. striatus* with its two clusters of nuclei it is the anterior cluster of the proter with the old oral apparatus which gets one of the old macronuclei, while in the opisthe the old macronucleus is in the posterior cluster. We have not observed any major reorganization of the oral apparatus in the proter as far as the paroral and the left pseudobuccal kinety is concerned. Reorganization in the proter comprises the elevation and the later lowering of the floor of the oral cavity, the rebuilding of the vestibular extension in its part of the intravestibular kinety. We do not know which cells are thinned out in a clonal cylinder model as discussed by Frankel (1989), but it looks as if nuclear behaviour would enhance the probability of old proters (with non-renewed oral kineties) to die earlier relative to old opisthes in clonal sub-cylinders.

Loxodes shows a strange mosaic of primitive and highly evolved characters, as judged from our admittedly ignorant view. The buccokinetal mode of stomatogenesis is thought to be primitive (Eisler 1992), perhaps likewise primitive is the odd mitochondrial potential of nitrate respiration under low oxygen conditions (Finlay and Fenchel 1986, Finlay et al. 1986). *Loxodes* might be a biochemical relict from the times when *Paracoccus*-like bacteria changed into mitochondria (John and Whatley 1975). Perhaps the elaborate Golgi apparatus seen in *Loxodes* is a primitive or plesiomorphic character, too, inherited from the common ancestor of both the ciliates and the ciliates' sistergroup, the dinoflagellates. Recall that higher ciliates usually have very inconspicuous Golgi membranes. The Müller vesicles unanimously are interpreted as sensory organelles for geotaxis, definitively an apomorphous character of the Loxodidae. The inverted left pseudobuccal kinety has to be regarded as a derived feature. And we think their inability to divide their macronuclei is another derived character they share with all classical karyorelicteans.

What do we mean by the designation classical karyorelicteans? This leads necessarily to the discussion of the contents of the taxon Karyorelictea. Classical karyorelicteans (*sensu* Corliss 1979) comprise the Tracheloceridae, Loxodidae and Geleiidae. Based on a phenetic study of numerous morphological characters of the somatic and buccal cortex, stomatogenesis, nuclear features and mode of cell division de Puytorac et al. (1984) found *Protocruzia* in close neighbourhood to *Geleia*. Thus, for a certain period of time, *Geleia* and *Protocruzia* were classified as Protoheterotrichidae among the heterotrichs. Three years later (de Puytorac et al. 1987) the Protocruziidae were regarded as the fourth class of a subphylum Karyorelicta comprising also the classes Trachelocercea, Loxodea and Protoheterotrichea, a decision held in de Puytorac et al. (1994) where the four taxa are now lowered to subclass level.

Rather than discussing the dissatisfying question of taxon hierarchies, we would like to stress that the nuclear behaviour in classical karyorelicteans is so different

from nuclear phenomena seen in *Protocruzia*, that we can hardly agree with the placement of *Protocruzia* among the karyorelicteans. On the other hand one of us (Bardele 1987) has argued that *Protocruzia* might be the best model for the evolution of nuclear dimorphism in ciliates, while classical karyorelicteans with their never-dividing macronuclei were regarded as a dead end route. Though alternative views have been presented (Orias 1991), we can hardly imagine how nuclei which lost their ability to divide regained it at least two times in the heterotrichs and the higher ciliates, the latter comprising the hypotrichs and the rest of the ciliates. *Protocruzia* deviates in several important characters from the classical karyorelicteans. The somatic dikinetid pattern of *Protocruzia*, its oral ciliature and its parakinetal stomatogenesis justify its position among the heterotrichs (Grolière et al. 1980). Notably, adoral organelles have never been found among the classical karyorelicteans. If their never-dividing macronuclei is an apomorphy of this group we have to be prepared that the diversity of ciliature in karyorelicteans by convergence evolved along the same line as postulated for higher ciliates (Bardele 1989).

Beginning with ventrostomous forms (Geleiidae, Loxodidae) having some kind of (right) paroral and (left) adoral ciliature, well different in detail from the respective structures in higher ciliates, an apicalisation of oral structures might have occurred in raptorial forms (Trachelocercidae) leading to forms with non-functional apical remnants of an apical cytostome as in *Kentrophoros*. The prostome Trachelocercia (also called Protostomatida by Small and Lynn 1985) with e. g. *Tracheloraphis* show superficial similarities to the genuine Prostomatia (Dragesco and Dragesco-Kernéis 1986, Huttenlauch and Bardele 1987). *Kentrophoros*, grouped with the Loxodia in de Puytorac et al. (1994), but to our understanding better placed in the Trachelocercia, seems to have a non-functional oral apparatus due to an obligatory symbiosis with thiotrophic bacteria (Raikov 1972). We assume that this ciliate has reduced its oral structures secondarily. This also casts doubts on *Kentrophoros* as a model for the evolution of oral structures in ciliates in general as suggested by Small (1984). Nor do *Geleia* and *Avelia* (Nouzarède 1976) seem to be very early representatives of the karyorelicteans for they have paracytostomal monokinetids (Small 1984), a feature we regard as derived. The inverted pseudobuccal kinety of *Loxodes*, as said before, is likewise a derived character. Thus, *Loxodes* is no very favourable candidate for the early karyorelicteans either. So we are left with the somewhat disappointing, perhaps not really astonishing fact, that none of the extant karyorelictean makes a good model for the ancestral karyorelictean species. One is inclined to speak of an early radiation (a term so popular in molecular tree building) with respect to the formation of different types of oral ciliature in karyorelicteans. Admittedly, we have no idea of the adaptive reason of this oral radiation. The food which is preferred in nature by the various species and the actual feeding mechanism, is largely unknown for most of the karyorelicteans.

Finally, it is interesting to note that the overall similarity in the structural organization of the somatic cortex e. g. in *Loxodes* and *Spirostomum* (de Puytorac and Njiné 1970), and *Tracheloraphis* and *Blepharisma* (Gerassimova and Seravin 1976, Raikov et al. 1976) was discussed long before molecular RNA data gave further support for a phylogenetic link between the Heterotrichea and *Loxodes* (Baroin-Tourancheau et al. 1992, Fleury 1992). Unfortunately, up to this day, ribosomal RNA sequence data have been published of one karyorelictean species, only (*Loxodes striatus*, see Baroin-Tourancheau et al. 1992). The same unsatisfying situation holds for the morphogenetic data. Except for *Loxodes* we know almost nothing about stomatogenesis in other karyorelictean ciliates. Despite the bewildering diversity of oral structures of the karyorelicteans we keep it possible that some day through comparative morphogenetic studies a unifying pattern may be detected which clarifies the interrelationship within a hopefully monophyletic group of classical karyorelicteans.

Acknowledgements. We thank Mr. Horst Schoppmann for excellent work at the scanning electron microscope. This investigation was supported by a grant from the Deutsche Forschungsgemeinschaft (Ba 309/11-2)

REFERENCES

Augustin H., Foissner W., Adam H. (1984) An improved pyridinated silver carbonate method which needs few specimens and yields permanent slides of impregnated ciliates (Protozoa, Ciliophora). *Mikroskopie* **41:** 134-137

Ax P. (1966) Die Bedeutung der interstitiellen Sandfauna für allgemeine Probleme der Systematik, Ökologie und Biologie. *Veröff. Inst. Meeresforsch. Bremerhaven, Sonderbd.* **2:** 15-66

Bardele C. F. (1987) Auf neuen Wegen zu alten Zielen - moderne Ansätze zur Verwandtschaftsanalyse der Ciliaten. *Verh. Dtsch. Zool. Ges.* **80:** 59-75

Bardele C. F. (1989) From ciliate ontogeny to ciliate phylogeny: a program. *Boll. Zool.* **56:** 235-243

Baroin-Tourancheau A., Delgado P., Perasso R., Adoutte A. (1992) A broad molecular phylogeny of ciliates: Identification of major evolutionary trends and radiations within the phylum. *Proc. Natl. Acad. Sci. USA* **89:** 9764-9768

Corliss J. O. (1973) Evolutionary trends in the pattern of stomatogenesis in the ciliate protozoa. *J. Protozool.* **20:** (Suppl.) 506

Corliss J. O. (1974) Remarks on the composition of the large ciliate class Kinetofragmophora de Puytorac et al., 1974, and recognition of several new taxa therein, with emphasis on the primitive order Primociliatida n. ord.. *J. Protozool.* **21:** 207-220

Corliss J. O. (1975) Nuclear characteristics and phylogeny in the protistan phylum Ciliophora. *BioSystems* **7:** 338-349

Corliss J. O. (1979) The Ciliated Protozoa: Characterisation, Classification and Guide to the Literature. 2 nd. Pergamon Press, Oxford, New York

Dragesco J., Dragesco-Kernéis A. (1986) Ciliés libres de l' Afrique intertropicale. Collection Faune Tropicale XXVI, Éditions de l' Orstom, Paris

Eisler K. (1989) Electron microscopical observations on the ciliate *Furgasonia blochmanni* Fauré-Fremiet, 1967. Part II: morphogenesis and phylogenetic conclusions. *Europ. J. Protistol.* **24:** 181-199

Eisler K. (1992) Somatic kineties or paroral membrane: which came first in ciliate evolution? *BioSystems* **26:** 239-254

Eisler K., Bardele C. F. (1986) Cortical morphology and morphogenesis of the nassulid ciliates *Furgasonia blochmanni* Fauré-Fremiet, 1967 and *Nassula citrea* Kahl, 1930. *Protistologica* **22:** 461-476

Fernández-Galiano D. (1976) Silver impregnation of ciliated protozoa: a procedure yielding good results with the pyridinated silver carbonate method. *Trans. Am. Micros. Soc.* **95:** 557-560

Finlay B. J., Fenchel T. (1986) Physiological ecology of the ciliated protozoon *Loxodes. Rep. Freshwat. biol. Ass.* **54:** 73-96

Finlay B., Fenchel T., Gardener S. (1986) Oxygen perception and O_2 toxicity in the freshwater ciliated protozoon *Loxodes. J. Protozool.* **33:** 157-165

Fleury A., Delgado P., Iftode F., Adoutte A. (1992) A molecular phylogeny of ciliates: What does it tell us about the evolution of the cytoskeleton and of developmental strategies? *Develop. Genetics* **13:** 247-254

Frankel J. (1989) Pattern Formation - Ciliate Studies and Models. Oxford University Press, New York, Oxford

Gerassimova Z. P., Seravin L. N. (1976) Ectoplasmic fibrillar system of Infusoria and its role for the understanding of their phylogeny. *Zool. Zh.* **55:** 645-656 (in Russian with English summary)

Greenwood S. J., Schlegel M., Sogin M. L., Lynn D. H. (1991) Phylogenetic relationships of *Blepharisma americanum* and *Colpoda inflata* within the phylum Ciliophora inferred from complete small subunit rRNA gene sequences. *J. Protozool.* **38:** 1-6

Grolière C. A., Puytorac P. de, Detcheva R. (1980) A propos d'observations sur la stomatogenèse et l'ultrastructure du cilié *Protocruzia tuzeti* Villeneuve-Brachon, 1940. *Protistologica* **16:** 453-466

Hennig W. (1966) Phylogenetic Systematics. University of Illinois Press, Urbana

Hiller S. A. (1991) *Bursellopsis spaniopogon* (Ciliophora: Prostomatida). II. Stomatogenesis as revealed by light microscopy and scanning electron microscopy and some phylogenetic implications concerning prostome ciliates. *Europ. J. Protistol.* **28:** 102–119

Hiller S. A. (1993) Ultrastructure of *Prorodon* (Ciliophora, Prostomatida) I. Somatic cortex and some implications concerning kinetid evolution in prostomatid and colpodid ciliates. *J. Euk. Microbiol.* **40:** 467-486

Hofmann-Münz A. H. (1991) The oral apparatus of *Colpoda variabilis* Foissner, 1980 II. Ultrastructure of the oral ciliature, and its implications on ciliate phylogeny. *Europ. J. Protistol.* **26:** 288-302

Huttenlauch I., Bardele C. F. (1987) Light and electron microscopical observations on the stomatogenesis of the ciliate *Coleps amphacanthus* Ehrenberg, 1833. *J. Protozool.* **34:** 183–192

John P., Whatley F. R. (1975) *Paracoccus denitrificans* and the evolutionary origin of mitochondria. *Nature* **254:** 495-498

Klindworth T., Bardele C. F. (1996) The ultrastructure of the somatic and oral cortex of the karyorelictean ciliate *Loxodes striatus*. *Acta Protozool.***35:** 13-28

Lynn D. H., Sogin M. L. (1988) Assessment of phylogenetic relationships among ciliated protists using partial ribosomal RNA sequences derived from reverse transcripts. *BioSystems* **21:** 249-254

Njiné T. (1970) Structure et morphogenèse buccales chez le cilié holotriche *Loxodes magnus* Stokes, 1887. *C. R. Acad. Sc.* **270:** 519-522

Nouzarède M. (1976) Cytologie fonctionnelle et morphologie expérimentale de quelques protozoaires ciliés mésopsammiques géants de la famille des Geleiidae (Kahl). *Bull. Stat. Biol. Arcachon* **28(1,2):** 1-315

Orias E. (1991) Evolution of amitosis of the ciliate macronucleus: gain of the capacity to divide. *J. Protozool.* **38:** 217-221

Parducz B. (1952) Eine neue Schnellfärbemethode im Dienste der Protistenforschung und des Unterrichts. *Ann. Hist. Nat. Mus. Nation. Hung. (N.S.)* **2:** 5-12 (in Ungarian with German summary)

Puytorac P. de (Ed.) (1994) Infusoires Ciliés. Traité de Zoologie. - Anatomie, Systématique, Biologie. Tome II, Fasc. 2, Masson, Paris

Puytorac P. de, Njiné T. (1970): Sur l'ultrastructure des *Loxodes* (ciliés holotriches). *Protistologica* **6:** 427-444

Puytorac P. de, Grain J., Legendre P., Devaux J. (1984) Essai d' application de l' analyse phénétique à la classification du phylum des Ciliophora. *J. Protozool.* **31:** 496-507

Puytorac P. de, Grain J., Mignot J. P. (1987) Précis de Protistologie. Boubée, Paris

Raikov I. B. (1959) Der Formwechsel des Kernapparates einiger niederer Ciliaten. II. Die Gattung *Loxodes*. *Arch. Protistenkd.* **104:** 1-42

Raikov I. B. (1972) Ultrastructures cytoplasmiques de *Kentrophoros latum* Raikov, cilié holotriche psammophile: organisation corticale, endoplasme et trichocystes. *Ann. Stat. Biol. Besse-en-Chandesse* **6-7:** 21-51

Raikov I. B. (1982) The Protozoan Nucleus. Springer Verlag, Wien, New York

Raikov I. B. (1985) Primitive never- dividing macronuclei of some lower ciliates. *Int. Rev. Cytol.* **95:** 267-325

Raikov I. B. (1994) Somatic cortical and endoplasmic fine structure of *Remanella granulosa* Kahl (Ciliophora, Karyorelictida). *Arch. Protistenkd.* **144:** 7-1

Raikov I. B., Gerassimova-Matvejeva Z. P., Puytorac P. de (1976) Cytoplasmic fine structure of the marine psammobiotic ciliate *Trachelloraphis dogieli* Raikov. I. Somatic infraciliature and cortical organelles. *Acta Protozool.* **14:** 17-42

Schlegel M. (1991) Protist evolution and phylogeny as discerned from small subunit ribosomal RNA sequence comparisons. *Europ. J. Protistol.* **27:** 207-219

Small E. B. (1984) An essay on the evolution of ciliophoran oral cytoarchitecture based on descent from within a karyorelictean ancestry. *Origins of Life* **13:** 217-228

Small E. B., Lynn D. H. (1985) Phylum Ciliophora Doflein, 1901. In: An Illustrated Guide to the Protozoa, (Eds. J. J. Lee, S. H. Hutner and E. C. Bovee). Society of Protozoologists, Lawrence, Kansas, 393-575

Tuffrau M. (1963) Les structures infraciliaires et la stomatogenèse chez les *Loxodes*. 1st Int. Congr. Protozoology, Prague, Aug. 1961, Progress in Protozoology, 278-280

Swedmark B. (1964) The interstitial fauna of marine sand. *Biol. Rev.* **39:** 1-42

Received on 14th April, 1995; accepted on 5th July, 1995

ACTA
PROTOZOOLOGICA

Acta Protozoologica (1996) 35: 41- 48

An Ultrastructural Study of *Zschokkella leptatherinae* (Myxozoa: Myxosporea) from Atherinid Fish, *Leptatherina presbyteroides*

Xiao-qun SU

Department of Zoology, University of Tasmania, Hobart, Tasmania, Australia

Summary. The structure and development of *Zschokkella leptatherinae* from the hepatic ducts of *Leptatherina presbyteroides* (Richardson) were studied by transmission electron microscopy. Plasmodia are located in the lumen of hepatic ducts and they are not in close contact with the epithelial cells. The surface of the plasmodium is delimited by a single unit membrane. Numerous microvillous projections extend from the surface of the plasmodium. Pinocytic vesicles are situated beneath the cell membrane. The sporogenesis proceeds with the pansporoblast formation. The sporogonic cell undergoes a series of divisions until ten undifferentiated cells are present within the enveloping cell. Ten cells differentiate and divide into two sporoblasts; each has five cells including two capsulogenic cells, two valvogenic cells and one sporoplasm. Two spores are produced from one pansporoblast at the end of sporogenesis.

Key words: plasmodia, sporogenesis, transmission electron microscopy, *Zschokkella leptatherinae*.

INTRODUCTION

The studies on the ultrastructure of myxosporean parasites have been conducted on several species (e.g., Lom and Puytorac 1965, Current and Janovy 1977, Desser and Paterson 1978, Current 1979, Current et al. 1979, Pulsford and Matthews 1982, Desser et al. 1983, Lom and Dyková 1988, Sitjà-Bobadilla and Alvarez-Pellitero 1993b, El-Matbouli and Hoffmann 1994, Torres et al. 1994), however only four species of *Zschokkella*, i.e., *Z. nova* (Lom and Puytorac 1965), *Z. russelli* (Davies and Sienkowski 1988), *Z. icterica* (Diamant and Paperna 1992) and *Z. mugilis* (Sitjà-Bobadilla and Alvarez-Pellitero 1993a) have been described by transmission electron microscopy. *Zschokkella leptatherinae* was reported recently from the hepatic ducts and gall bladder of five atherinid fish species in Tasmania, Australia. The description of this parasite under the light microscope and the prevalence of infection in different fish species and different locations have been reported in a separate account (Su and White, in press). In the present paper, the ultrastructure of plasmodia and sporogenesis of *Zschokkella leptatherinae* occurring in the hepatic ducts of *Leptatherina presbyteroides* is reported.

MATERIALS AND METHODS

The samples of *Leptatherina presbyteroides* were collected with a seine net from seagrass meadows at Dru Point, North-West Bay, situated in South-eastern Tasmania, Australia, from January 1990 to June 1992. Fish were maintained in the laboratory in aerated tanks of sea water at 10°C. Ten fish with heavy infections of *Zschokkella leptatherinae* were used in the present study. Fresh infected liver tissue was fixed in 3% glutaraldehyde in 0.08 M cacodylate buffer (pH 7.2) for a minimum of 60 min at 4°C, followed by several washes for a total of 10 min in the same buffer. The specimens were postfixed in

Address for correspondence: X.-q. Su, 6/30 Eldridge St., Footscray, Victoria, Australia 3011

1% osmium tetroxide in 0.08 M cacodylate buffer for at least 60 min at room temperature. They were then washed several times in the buffer. The specimens were again post fixed in 4% uranyl acetate in water for 60 min and were then dehydrated in a graded ethanol series and embedded in spurr's resin. Semi-thin sections (0.5 μm) were cut with a glass knife and stained with toluidine blue. Ultrathin sections (0.05-0.1 μm) were cut with a diamond knife, mounted on formvar coated grids and stained with uranyl acetate and lead citrate. A Hitachi H300 electron microscope was used for observations and micrographs were taken with ILFORD EM technical film.

Terminology used in this study conforms to the previous publication by Lom and Dyková (1988).

RESULTS

Plasmodium

The polysporic plasmodia occupy a large space in the lumen of hepatic ducts of *Leptatherina presbyteroides* and they are not in close contact with the epithelial cells (Fig. 1). The surface of the plasmodium is delimited by a single unit membrane and numerous microvillous projections extend from it (Fig. 2). Beneath the surface membrane, there is a layer of finely granulated cytoplasm, containing agglomerations of what seem to be pinocytic vesicles although their formation at the cell surface could not be observed. Beneath this, there is a layer with abundant mitochondria. Golgi apparatus, scarce fragments of cisternae of rough endoplasmic reticulum and a numerous ribosome are also distributed in this area (Fig. 2). The inner cytoplasm contains the generative cells, vegetative nuclei, various stages of developing pansporoblasts and spores (Figs. 1, 3).

The generative cell is ellipsoid with a large nucleus and an eccentric, electron-dense nucleolus. In addition to a numerous free ribosome, mostly only a few mitochondria appear in the cytoplasm (Fig. 4).

Sporogenesis

The sporogenesis proceeds with the pansporoblast formation. The earliest recognisable stage is that two generative cells lie side by side (Fig. 5). Then one cell is enclosed in the other (Fig. 6). Later, one of them becomes an enveloping cell around the sporogonic cell. It is eventually reduced to the pansporoblastic membrane and persists even when spores reach an advanced stage of development. The sporogonic cell undergoes karyokinesis and cytokinesis to produce several undifferentiated cells. A pansporoblast with two, four and eight sporogonic progeny cells are shown in Figs. 7, 8 and 9 respectively. The sequence of final division, i.e. a pansporoblast with ten sporogonic progeny cells could not be traced in the present study.

The pansporoblast is disporic. Sporogonic progeny cells then differentiate and divide into two sporoblasts. Each has five cells including two capsulogenic cells, two valvogenic cells and one sporoplasm (Figs. 12, 13, 15).

The capsulogenic cell typically exhibits a capsular primordium, a large nucleus, mitochondria, ribosomes and rough endoplasmic reticulum (Fig. 10). Capsulogenesis follows the general pattern described for other myxosporea (Lom and Puytorac 1965). With further development, an external tubule extends from the capsular primordium. A bundle of microtubules is visible at the terminal region of the external tubule (Fig. 11) and the volume of capsular primordia increases considerably (Fig. 12). Several coils of the forming polar filaments are visible within the polar capsule and the external tubule is absent after they appear (Fig. 13). The polar capsule opening appears at a distance from the end of the spore and both openings occur on one side of the spore. This is consistent with observations by light microscopy. The maturation of the two polar capsules is asynchronous. Two polar capsules at different size and different developmental stage have been detected in one spore (Fig. 14).

Mature polar capsules are pyriform and each contains a dilated spirally-arranged filament (Figs. 15, 16). At the apex of the polar capsule, the electron-lucent walls are reflexed inwards and connect with the polar filaments. A cork-like stopper plugs the opening of the polar capsule into the discharge channel (Fig. 15).

The flattened valvogenic cells are situated on the side of the sporoplasm and capsulogenic cells. Each cell contains few mitochondria and numerous ribosomes (Figs. 10, 12, 13). Later on, the ends of two valvogenic cells join together to form a suture line which is flanked by electron-dense material (Figs. 13, 14). The valvogenic cells eventually form the spore walls which are composed of outer and inner layers. The valvogenic cells become narrower and the cytoplasm appears electron-dense with maturation. The nuclei and other organelles degenerate. Ten to twelve surface ridges can be seen on each spore valve (Fig. 16). The wall of a mature spore consists of an outer coat and underneath bilayered electron-dense band, which is formed in the cytoplasm of the val-

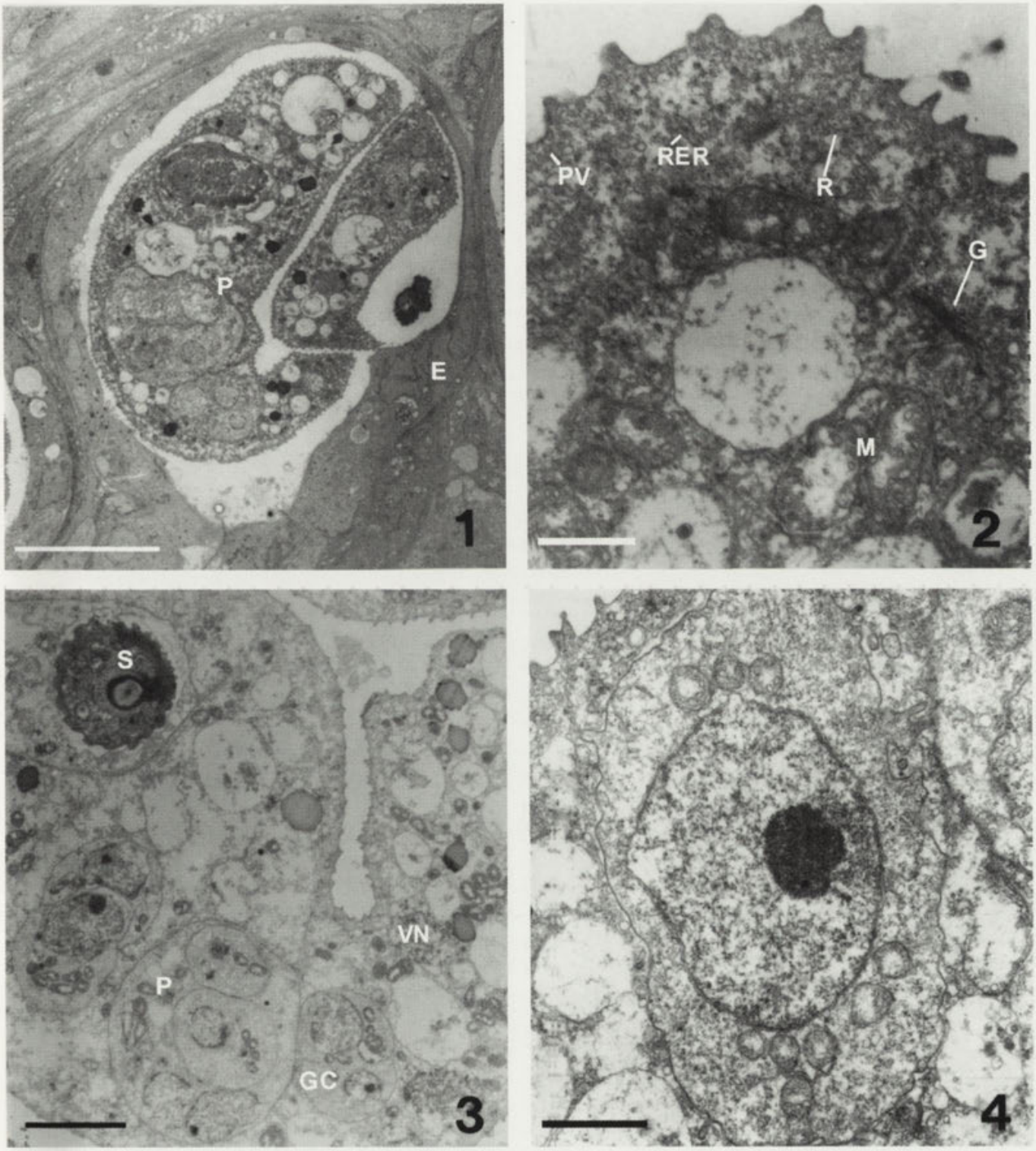

Fig. 1. *Zschokkella leptatherinae* plasmodia (P) within the hepatic ducts of host fish. E - hepatic epithelium. Fig. 2. A plasmodium with pinocytic vesicles (PV), mitochondria (M), Golgi apparatus (G), rough endoplasmic reticulum (RER) and ribosomes (R). Fig. 3. A plasmodium with generative cell (GC), vegetative nucleus (VN), developmental pansporoblasts (P) and spore (S). Fig. 4. A generative cell. Bar - 5 µm in Fig. 1, 1 µm in Figs. 2 and 4, 2.5 µm in Fig. 3

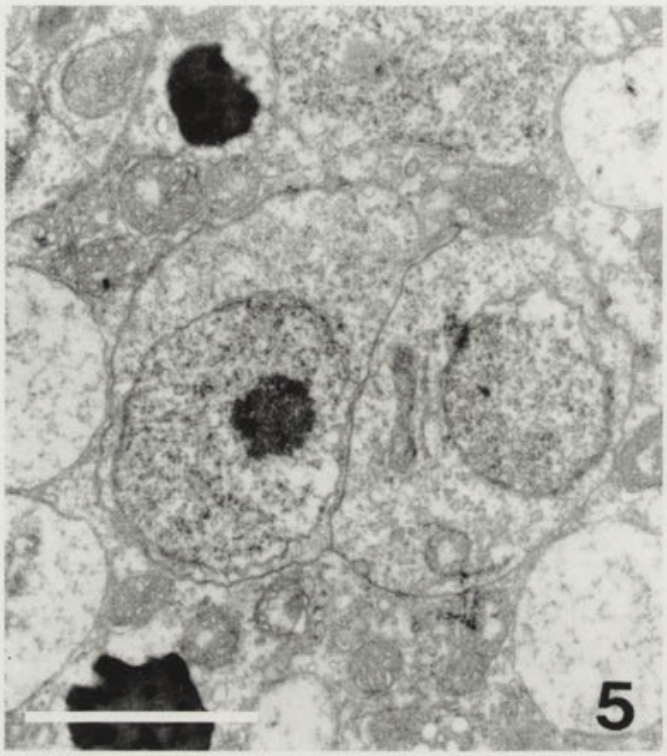

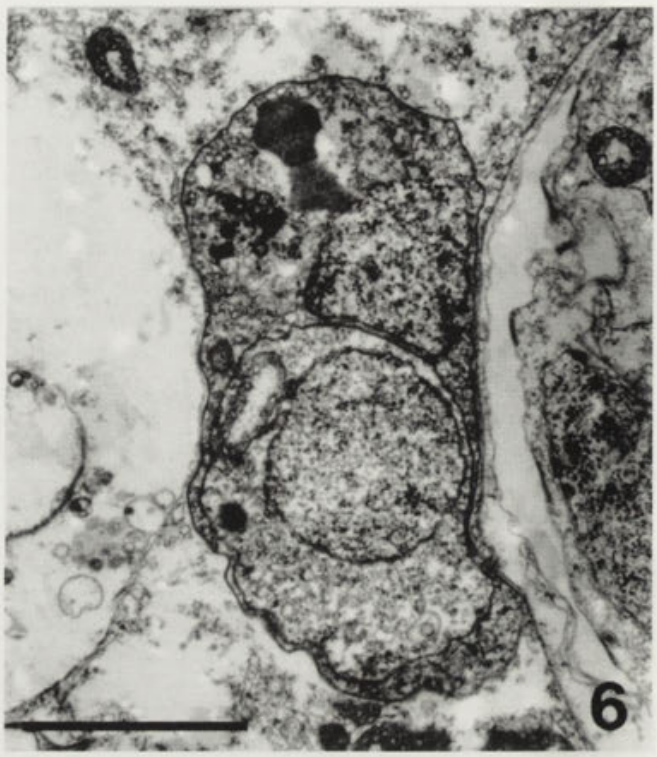

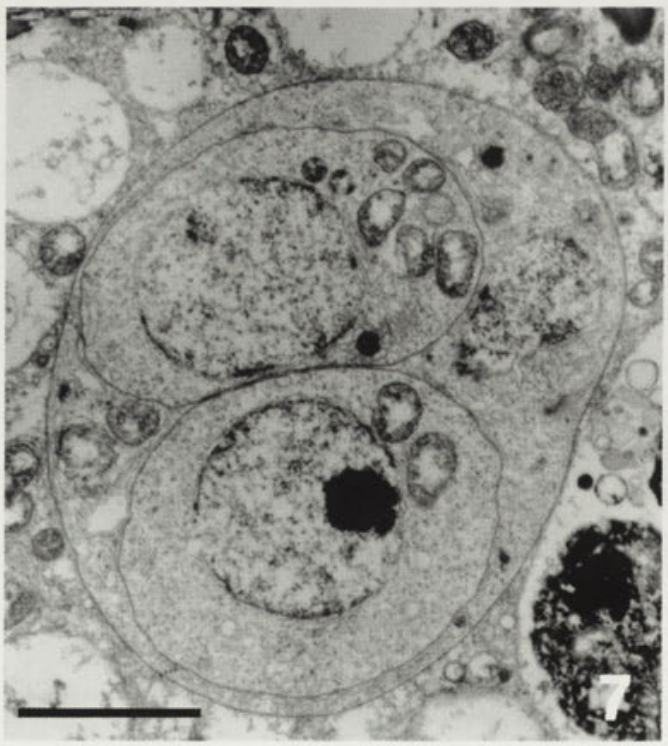

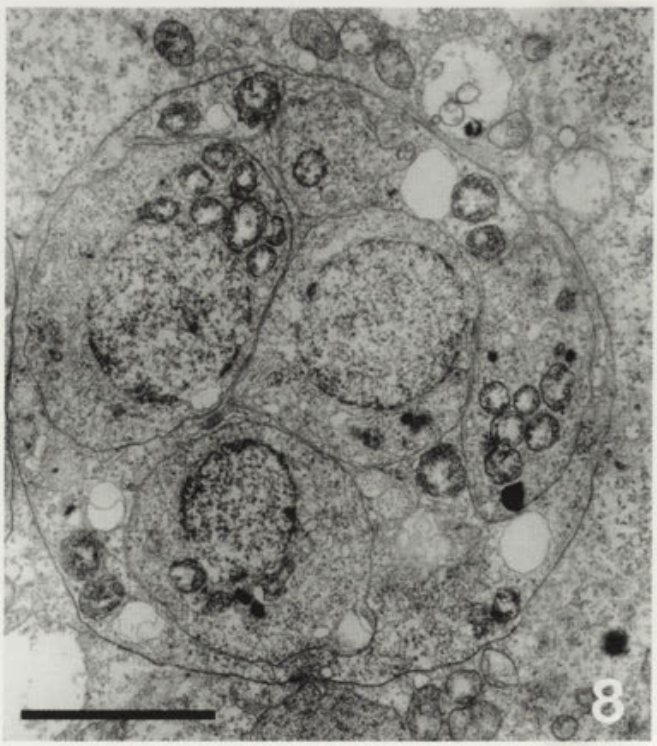

Fig. 5. *Zschokkella leptatherinae* two generative cells. Fig. 6. An early pansporoblast. Fig. 7. Two sporogonic progeny cells vere enclosed within an envelope cell. Fig. 8. Four sporogonic progeny cells were enclosed within an envelope cell. Bar - 2 μm

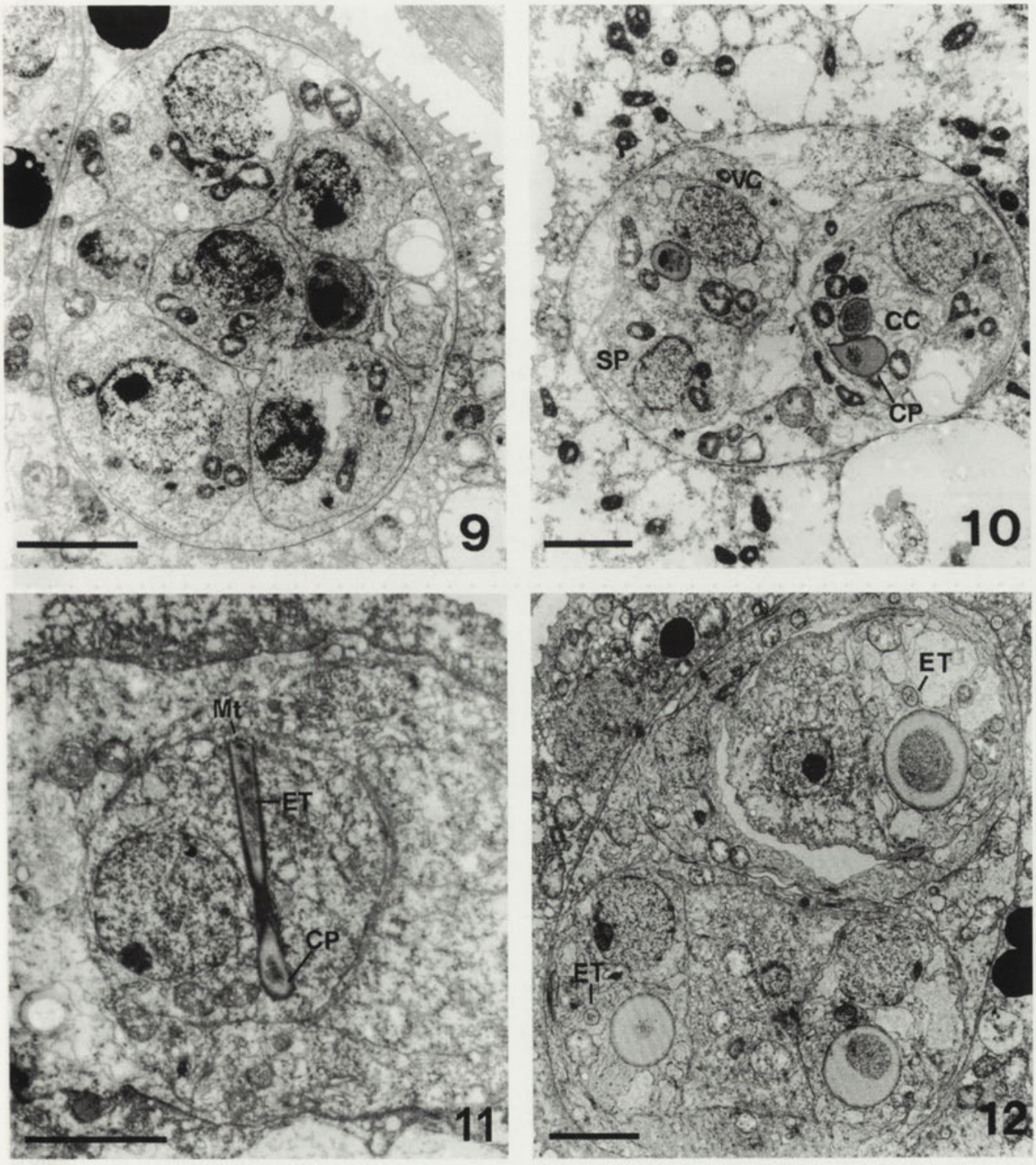

Fig. 9. *Zschokkella leptatherinae* eight sporogonic progeny cells were enclosed within an envelope cell. Fig. 10. Two sporoblasts within the pansporoblast. Note the capsulogenic cell (CC), capsular primordium (CP), valvogenic cell (VC) and sporoplasm (Sp). Fig. 11. A developmental capsulogenic cell within the pansporoblast. Note the external tubule (ET), capsular primordium (CP) and microtubules bundle (Mt). Fig. 12. Two sporoblasts surrounded by an envelope cell. Note transverse sections of external tubule (ET) within the capsulogenic cell. Bar - 2 μm

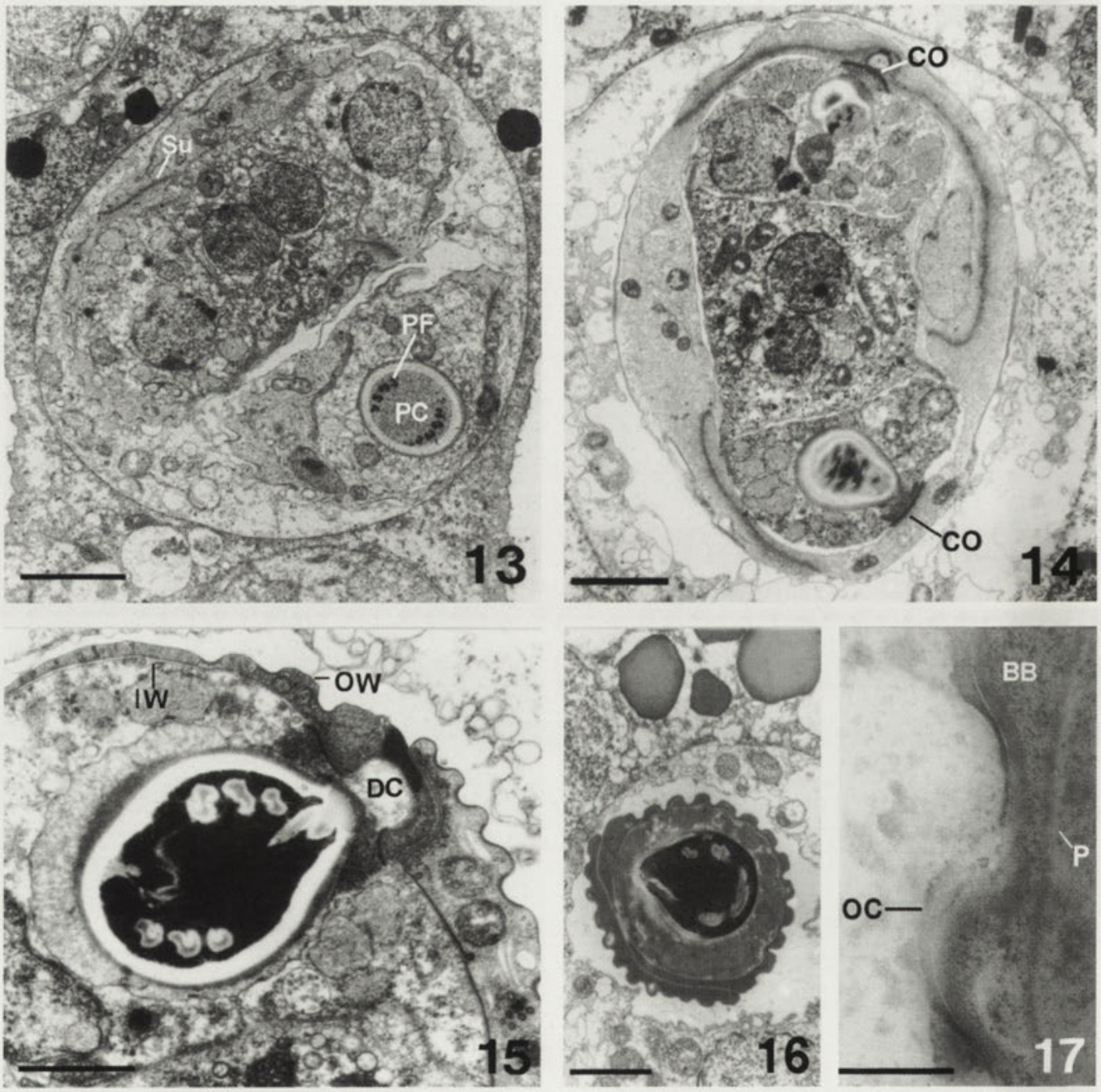

Fig. 13. *Zschokkella leptatherinae* two advanced sporoblasts. Note polar filament (PF), polar capsule (PC) and suture line of two valvogenic cells (Su). Fig. 14. A nearly mature spore within pansporoblast showing rudiment of polar capsule openings (CO). Fig. 15. A nearly mature spore. Note discharge channel (DC), outer valvular wall (OW) and inner valvular wall (IW). Fig. 16. A mature spore. Fig. 17. The wall of a mature spore showing outer coat (OC), bilayered electron-dense band (BB) and plasmalemma (P). Bar - 2.5 μm in Figs. 13 and 14, 1 μm in Figs. 15 and 16, 0.2 μm in Fig. 17

vogenic cells. The plasmalemma of the underlying cells is closely applied to the dense band (Fig. 17).

The earliest recognised uninucleate sporoplasm is located close to the capsulogenic cell in the sporoblast (Fig. 10). It then divides into a binucleate sporoplasm between the two capsulogenic cells and is surrounded by two valvogenic cells (Figs. 13, 14). The cytoplasm contains mitochondria, Golgi apparatus and ribosomes

(Figs. 12, 13). The spherical sporoplasmosomes are visible (Fig. 14).

DISCUSSION

In a previous ultrastructural study on myxosporea, Current et al. (1979) indicated that the ultrastructure of plasmodium may depend upon the location of the parasite within the host. Coelozoic plasmodia have a single outer unit membrane which forms numerous microvilli-like projections and extends into the host fluid. Histozoic plasmodia have one or two unit membranes which form pinocytic canals extending into the parasite ectoplasm. However, Paperna et al. (1987) detected the pinocytic system in the coelozoic plasmodium of *Myxidium giardi* and indicated that the coelozoic and histozoic plasmodia may differ in their fine structures of the pellicle of plasmodium instead of the appearance of pinocytic systems. Moreover, the pinocytic vesicles have also been found in several other myxosporean species (Lom and Puytorac 1965, Hulbert et al. 1977, Davies and Sienkowski 1988, Diamant and Paperna 1992, Sitjà-Bobadilla and Alvarez-Pellitero 1993a). The present study on *Zschokkella leptatherinae* reveals that a single unit membrane with a number of microvilli projections covers the plasmodium externally and beneath this membrane, there are agglomerations of pinocytic vesicles. Therefore, some doubt must be cast on the conclusion of location differences of myxosporean plasmodia suggested by Current et al. (1979).

Uspenskaya (1982) found that the surface structure of myxosporean vegetative stages is closely connected with the mode of their nutrition and different nutritional types often occur in various combinations in different species. For *Z. leptatherinae*, it is most likely that the external digestion of nutrients is followed by its active pinocytosis like what occurred in other coelozoic species. The arrangement of microvilli projections are presumably to increase the absorbing surface (Uspenskaya 1982).

Although the origin of the pansporoblast of *Z. leptatherinae* is not ascertained in the present study, the facts that no trace of division of generative cells has been observed and two generative cells are present frequently in pairs suggest that the pansporoblast is most likely formed by the association of two generative cells. One of them, the pericyte, envelops the other, the sporogonic cell divides to produce the ten cells necessary to produce two sporoblasts. This pattern of sporogenesis has been previously reported in two *Zschokkella* species, *Z. nova* and *Z. russelli* (Lom and Puytorac 1965, Davies and Sienkowski 1988) and several species of other genera, e.g. *Myxobolus* sp. (Desser and Paterson 1978); *Henneguya adiposa* (Current 1979); *Myxobolus funduli* (Current et al. 1979); *Myxobolus exiguus* (Pulsford and Matthews 1982) and *Thelohanellus mikolskii* Desser et al. (1983). However, in the study of *Myxidium zealandicum*, Hulbert et al. (1977) found that the binucleate sporocyst was formed by the mitotic division of a uninucleate germ (generative) cell. For *Z. mugilis*, the sporogenesis was supposed to start with the endogenous division of a primary cell (Sitjà-Bobadilla and Alvarez-Pellitero 1993a) and there are two different membranes surrounding each maturing spore inside the plasmodium. The authors explained this as that either each spore was produced in a different pansporoblast or there was no pansporoblast formation as in *Ceratomyxa shasta* (Yamamoto and Sanders 1979) and several species of *Sphaerospora* (Lom et al. 1982, 1985).

Sitjà-Bobadilla and Alvarez-Pellitero (1993a) indicated that it is difficult to establish patterns of sporogenesis, and this calls into question the validity of generalisations about myxosporean sporogonic cycles. The present observations on *Z. leptatherinae* confirms once more this conclusion.

The development of the polar capsule begins early in the sporogenesis. The origin of capsular primordium was reported by Desser and Paterson (1978), and Pulsford and Matthews (1982) as from the rough endoplasmic reticulum in immature capsulogenic cells. In other myxosporea, the Golgi apparatus seems also to be involved in the development of polar capsules (Desser et al. 1983, El-Matbouli et al. 1990). No trace of the origin of capsular primordium has been found in the present study. In *Z. leptatherinae*, the capsular primordia appear earlier than the external tubule and the latter is formed by the extension of the capsular primordium. This result is consistent with the report of *Z. nova* (Lom and Puytorac 1965), *Myxobolus exiguus* (Pulsford and Matthews 1982) and *Myxobolus* sp. (Desser and Paterson 1978). But in *Thelohanellus nikolskii*, Desser et al. (1983) found that the capsular primordia and the external tubule occur simultaneously in the sporoblast.

The pattern of formation of the polar filament is not clear in the present study. However, after the rudiment of the polar filament appears, the external tubule is absent. Also, as shown in Fig. 16, the walls of polar capsule are reflexed inwards and connect with the polar

filaments. These provide the evidence that the external tubule may be withdrawn into the capsular primordium and its components form the filament. This may be a very rapid process so no details have been revealed.

Acknowledgements. I am grateful to Dr. R.W.G. White for constructive criticism on an earlier version of the manuscript. Thanks are also due to Mr. R. Tennent and Mrs. I. Jacobs for their assistance with electron microscopy.

REFERENCES

Current W. L. (1979) *Henneguya adiposa* Minchew (Myxosporida) in the channel catfish: ultrastructure of the plasmodium wall and sporogenesis. *J. Protozool.* **26:** 209-217

Current W. L., Janovy J. Jr. (1977) Sporogenesis in *Henneguya exilis* infecting the channel catfish: an ultrastructural study. *Protistologica* **3:** 157-168

Current W. L., Janovy J. Jr., Knight S. A. (1979) *Myxosoma funduli* Kudo (Myxosporida) in *Fundulus kansae*: Ultrastructure of the plasmodium wall and of sporogenesis. *J. Protozool.* **26:** 574-583

Davies A. J., Sienkowski I. K. (1988) Further studies on *Zschokkella russelli* Tripathi (Myxozoa: Myxosporea) from *Ciliata mustela* L. (Teleostei: Gadidae), with emphasis on ultrastructural pathology and sporogenesis. *J. Fish. Dis.* **11:** 325-336

Desser S. S., Paterson W. B. (1978) Ultrastructural and cytochemical observations on sporogenesis of *Myxobolus* sp. (Myxosporida: Myxobolidae) from the common shiner *Notropis cornutus*. *J. Protozool.* **25:** 314-326

Desser S. S., Molnár K., Weller I. (1983) Ultrastructure of sporogenesis of *Thelohanellus nikolskii* Akhmerov, 1955 (Myxozoa: Myxosporea) from the common carp, *Cyprinus carpio*. *J. Parasitol.* **69:** 504-518

Diamant A., Paperna I. (1992) *Zschokkella icterica* sp. nov. (Myxozoa, Myxosporea), a pathogen of wild rabbitfish *Siganus iuridus* (Ruppell, 1829) from the Red Sea. *Europ. J. Protistol.* **28:** 71-78

El-Matbouli M., Hoffmann R. W. (1994) *Sinuolinea tetraodoni* n. sp., a myxosporean parasite of freshwater pufferfish *Tetraodon palembangensis* from Southeast Asia - light and electron microscope observations. *Dis. Aquat. Org.* **19:** 47-54

El-Matbouli M., Fischer-Scherl T., Hoffmann R. W. (1990) Light and electron microscopic studies on *Myxobolus cotti* El-Matbouli and Hoffmann, 1987 infecting the central nervous system of the bullhead (*Cottus gobio*). *Parasitol. Res.* **76:** 219-227

Hulbert W. C., Komourdjian M. P., Moon T. W., Fenwick, J. C. (1977) The fine structure of sporogenesis in *Myxidium zealandicum* (Protozoa: Myxosporidia). *Can. J. Zool.* **55:** 438-447

Lom J., Dyková I. (1988) Sporogenesis and spore structure in *Kudoa lunata* (Myxosporea, Multivalvulida). *Parasitol. Res.* **74:** 521-530

Lom J., Puytorac P. de (1965) Studies on the myxosporidian ultrastructure and polar capsule development. *Protistologica* **1:** 53-65

Lom J., Dyková I., Lhotková S. (1982) Fine structure of *Sphaerospora renicola* Dyková and Lom, 1982 a myxosporean from carp kidney and comments of the origin of pansporoblasts. *Protistologica* **18:** 489-502

Lom J., Körting W., Dyková I. (1985) Light and electron microscope redescription of *Sphaerospora tincae* Plehn, 1925 and *S. galinae* Evlanov, 1981 (Myxosporea) from the tench, *Tinca tinca* L. *Protistologica* **21:** 487-497

Paperna I., Hartley A. H., Gross R. H. M. (1987) Ultrastructural studies on the plasmodium of *Myxidium giardi* (Myxosporea) and its attachment to the epithelium of the urinary bladder. *Int. J. Parasitol.* **17:** 813-819

Pulsford A., Matthews R. A. (1982) An ultrastructural study of *Myxobolus exiguus* Thelohan, 1895 (Myxosporea) from grey mullet, *Crenimugil labrosus* (Risso). *J. Fish Dis.* **5:** 509-526

Sitjà-Bobadilla A., Alvarez-Pellitero P. (1993a) *Zschokkella mugilis* n. sp. (Myxosporea: Bivalvulida) from Mullets (Teleostei: Mugilidae) of Mediterranean Waters: light and electron microscopic description. *J. Euk. Microbiol.* **40:** 755-764

Sitjà-Bobadilla A., Alvarez-Pellitero P. (1993b) Light and electron microscopical description of *Ceratomyxa labracis* n. sp. and a redescription of *C. diplodae* (Myxosporea: Bivalvulida) from wild and cultured Mediterranean sea bass *Dicentrarchus labrax* (L.) (Teleostei: Serranidae). *Syst. Parasitol.* **26:** 215-223

Su X., White R. W. G. 1995 A new myxosporean *Zschokkella leptatherinae* n. sp. (Myxozoa: Myxidiidae) from the hepatic ducts and gall bladder of Australian marine fishes. *Syst. Parasitol.* **32:** 125-129

Torres A., Matos E., Azevedo C. (1994) Fine structure of *Henneguya amazonica* (Myxozoa) in ovarian follicles of *Hoplosternum littorale* (Teleostei) from the Amazon river. *Dis. Aquat. Org.* **19:** 169-172

Uspenskaya A. V. (1982) New data on the life cycle and biology of Myxosporidia. *Arch. Protistenk.* **126:** 309-338

Yamamoto T., Sanders J. E. (1979) Light and electron microscopic observations of sporogenesis in the myxosporidan, *Ceratomyxa shata* (Noble, 1950). *J. Fish Dis.* **2:** 411-428

Received on 29th November, 1994; accepted on 19th July, 1995

ACTA
PROTOZOOLOGICA

Acta Protozoologica (1996) 35: 49 - 59

Gregarines (Eugregarinorida: Apicomplexa) in Natural Populations of *Dociostaurus maroccanus, Calliptamus italicus* and other Orthoptera

Jerzy J. LIPA[1], Pedro HERNANDEZ-CRESPO[2,3] and Candido SANTIAGO-ALVAREZ[3]

[1]Department of Biological Control and Quarantine, Institute of Plant Protection, Poznań, Poland; [2]Institute of Virology and Environmental Microbiology, Oxford, UK; [3]Departamento de Ciencias y Recursos Agrícolas y Forestales, E.T.S.I.A.M., Universidad de Cordoba, Córdoba, Spain

Summary. *Gregarina acridiorum* Léger is redescribed based on material from *Calliptamus italicus* and *Dociostaurus maroccanus* collected in Spain and in *Locusta migratoria* in Uzbekistan. This gregarine has a wide range of hosts and is broadly distributed in Palearctic region. *Gregarina garnhami* Canning is considered to be a junior synonym of *G. acridiorum*. Intensity of parasitization in some host insects was very high which indicates a detrimental effect on gut functions. Gregarine infections have been also recorded in the natural populations of the acridids *Ailopus* sp., *Anacridium aegyptium*, and *Oedaleus decorus* and of the tettigoniid *Decticus albifrons* collected on Iberian Peninsula and Canary Islands.

Key words: *Ailopus* sp., *Anacridium aegyptium*, *Calliptamus italicus*, *Decticus albifrons*, *Dociostaurus maroccanus*, *Gregarina*, gregarines, insect parasites, *Locusta migratoria*, *Oedaleus decorus*, Orthoptera.

Abbreviations: LD - length of deutomerite, LP - length of protomerite, TL - total length of gamont or sporont, WD - width of deutomerite, WP - width of protomerite.

INTRODUCTION

During the collaborative research programme on biological control of locusts by means of entomopathogens a survey for parasites and pathogens in populations of locusts and grasshoppers species is being conducted in Spain since 1989 (Hernandez-Crespo 1993). Special attention in this research is given to the Moroccan locust, *Dociostaurus maroccanus* (Thnb.) whose outbreaks have been numerous in the Iberian Peninsula until beginning of this century (Cañizo 1939, Vazquez Lesmes and Santiago-Alvarez 1994). Results of studies on entomopathogenic fungi (Santiago-Alvarez 1991), mermithid parasites (Hernandez-Crespo and Santiago-Alvarez 1991) and entomopoxvirus infection (Lipa et al. 1994) from various orthopterans have been recently published and they present an interest for microbial control of these pests (Bidochka and Khachatourians 1991).

During 1992 survey a gregarine infection was recorded among adults of *D. maroccanus*. Surprisingly, this locust was not among locusts and grasshopers listed by Uvarov (1928), Canning (1956) and Geus (1969) as hosts for gregarines (Gregarinomorpha). However, an infection caused by *Gregarina* sp. in *D. maroccanus* was reported by Nurzhanov (1989), but without taxonomic identification of the species. When it become obvious to us that we recorded a new gregarine infection in *D. maroccanus* we

Address for correspondence: J. J. Lipa, Department of Biological Control and Quarantine, Institute of Plant Protection, ul. Miczurina 20, 60-318 Poznan, Poland; Fax: (4861) 676301; E-mail: jjlipa@vm.amu.edu.pl

undertook a specific research on this pathogen. In this paper we report on its morphological features and its occurrence among field host populations of *D. maroccanus* and *Calliptamus italicus* (L.) in Spain and also in a laboratory culture of *Locusta migratoria* (L.) from Uzbekistan. We also include here observations on gregarines recorded in five other orthopterans found during our studies.

MATERIALS AND METHODS

Specimens of different developmental instars of *D. maroccanus* and *C. italicus* were collected regularly (7-15 day intervals) by means of a sweeping net in the permanent breeding area in La Serena region (Badajoz province, Spain) from March 24 to July 8, 1992. Specimens of these two species as well as of other Orthoptera were also collected in the Valencia city, in Santa Marta (Albacete) and on islands El Hierro and Tenerife (Canary Islands Archipelago).

Specimens of *L. migratoria* were taken from the laboratory culture kept at the All-Russian Institute of Plant Protection at Sankt Petersburg but the stock of that locust originated from Uzbekistan.

Using the stereoscopic microscope nymphs and adult insects were dissected, in a Petri dish filled with paraffin and physiological solution (0.6-0.8% NaCl) or with water, by cut open along the dorsal side of the body in order to have the access to visual examination of their fat body, intestine and other tissues. Recorded gregarines were transferred with the gut contents and a small volume of physiological solution on a microscopic slide and then measured and photographed. Permanent slides of gamonts and sporonts fixed in methyl alcohol for 2 min were stained with 0.25% Giemsa water solution.

RESULTS

Morphology of gregarines in *Dociostaurus maroccanus* and *Calliptamus italicus*

Gamonts

The gamonts (trophozoites) are solitary with the pale appearance as compared with sporonts (Figs. 1, 2). The knoblike epimerite is transparent, and being from 7 to 9 µm long and 9 to 10.6 µm wide. After the epimerite is detached the scar on the top of protomerite remains well seen for some time but later becomes healed. The protomerite of gamont is oval or slightly conical and separated from the ovoidal deutomerite by very distinct constriction. Deutomerite is ovoidal with well seen ectocyte. Its endocyte is much less granular than of sporonts and thanks to that the gamonts easily change the shape of their bodies while moving (Fig. 2).

Sporonts

The sporonts are biassociative as only two sporonts made syzygies; associations of three sporonts or more were never observed. Small and large sporonts enter into the syzygial phase but their future size and shape greatly depends on the fact whether they are primites or satellites. In general, primites are shorter and ovoidal while satellites are longer and cylindrical or ellipsoidal (Figs. 3, 4). The largest observed syzygies were up 1006 µm long (Table 1).

Primites. Protomerite semicircular, wider than long with well seen ectocyte about 5-7 µm thick. The endocyte of protomerite is coarsely granular and not translucent. Deutomerites of the majority of primites are ovoidal and relatively wide, with the maximum width 467 µm. Their ectocyte is thinner than in protomerite. The endocyte is coarsely granular and less translucent than of protomerite. The end of primite's deutomerite is oval or slightly flattened.

Due to densely granular endocyte the nucleus is weakly seen or not seen at all. Only using the highly diluted solution of TAF, which clears the endocytic granules, it is possible to demonstrate the location of nuclei. The nuclei of the primite have the diameter from 46 to 56 µm and contains several small size karyosomes (Fig. 8).

Satellites. Protomerites of the satellites are much shorter and wider than protomerites of primite and have smaller ratios WP:LP (Table 1). In most cases the ectocyte of the satellite's protomerite is very thick (up to 11.4 µm) and forms a peculiar circular ridge (Fig. 5).

The apical part of the protomerite, surrounded by this circular ridge, is elevated up to the ridge edges or slightly less. This protomerite structure allows the satellite to attach firmly to the posterior end of the primite deutomerite at the caudo-frontal association. Attachment is so firm that syzygies are not broken when gut is dissected and the gregarines are released into the dissecting pan (Fig. 6). The deutomerite of the satellite is cylindrical or ellipsoidal and narrows toward the posterior end which is flattened. The ectocyte is well seen and the endocyte is coarsely granular. The nucleus is located in the centre of the satellite's deutomerite and has the diameter of 46 to 56 µm.

Gametocyst

Gametocysts were rather rarely observed with the diameter from 473 x 422 to 650 x 590 µm. The young gametocyst has a more translucent body while gametocyst at the advanced maturation process is opaque (Fig. 7).

Habitat

Young gamonts are developing within midgut epithelium or in the gastric intestinal caeca (ampules)

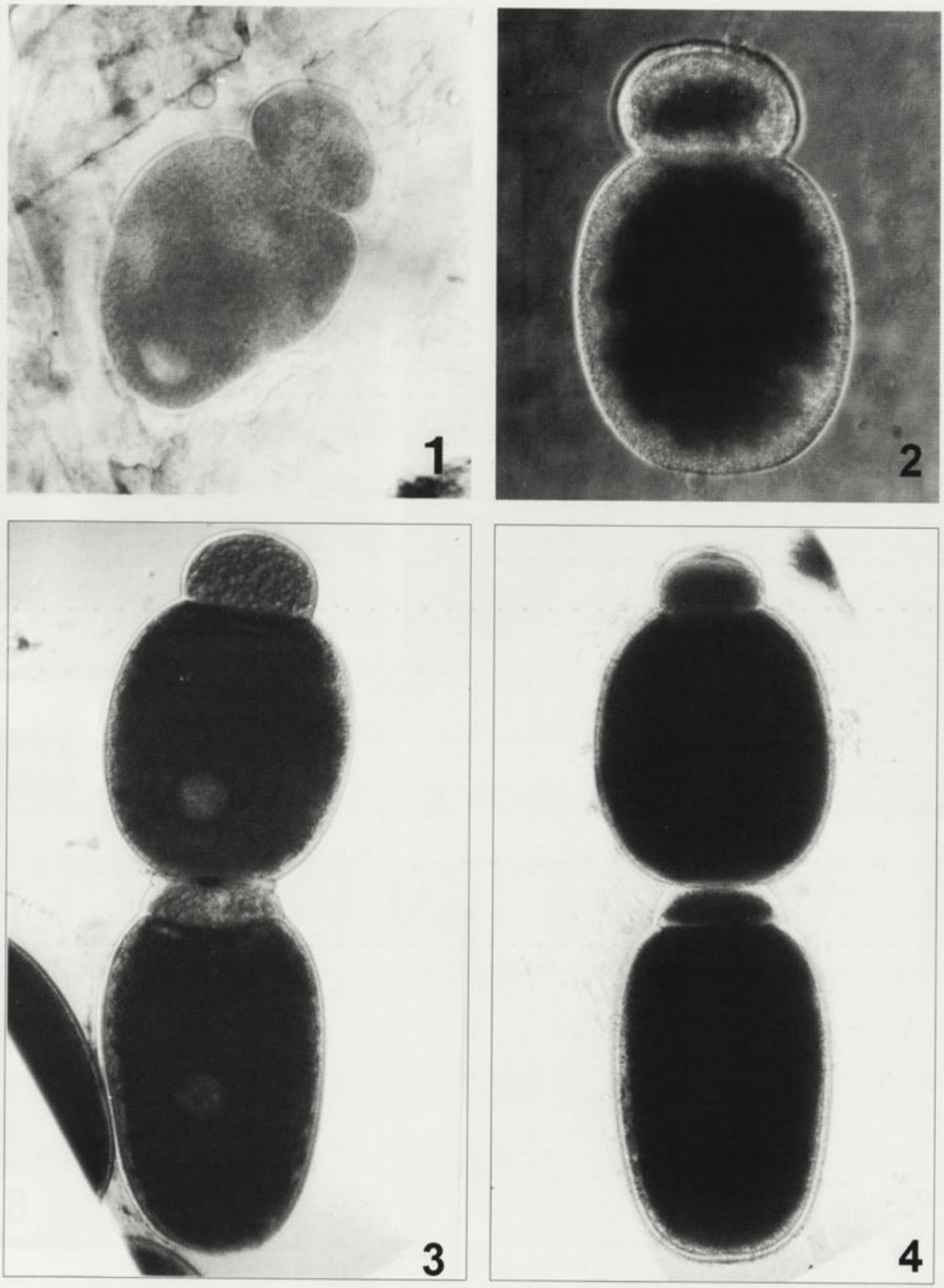

Figs. 1-4. *Gregarina acridiorum* from *Calliptamus italicus* and *Dociostaurus maroccanus*. 1 - gamont from *C. italicus* (x 500), 2 - gamont from *D. maroccanus* (x 400), 3 - sporonts in syzygy from *C. italicus* (x 200), 4 - sporonts in syzygy from *D. maroccanus* (x 200)

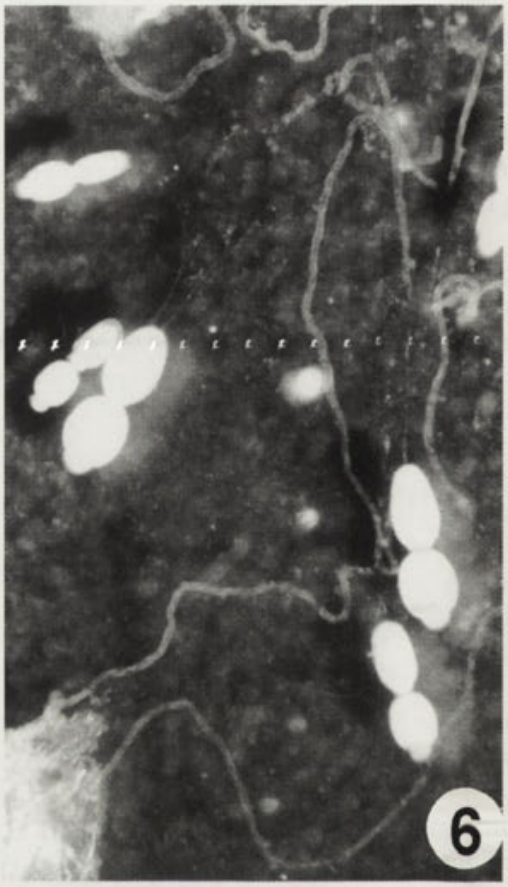

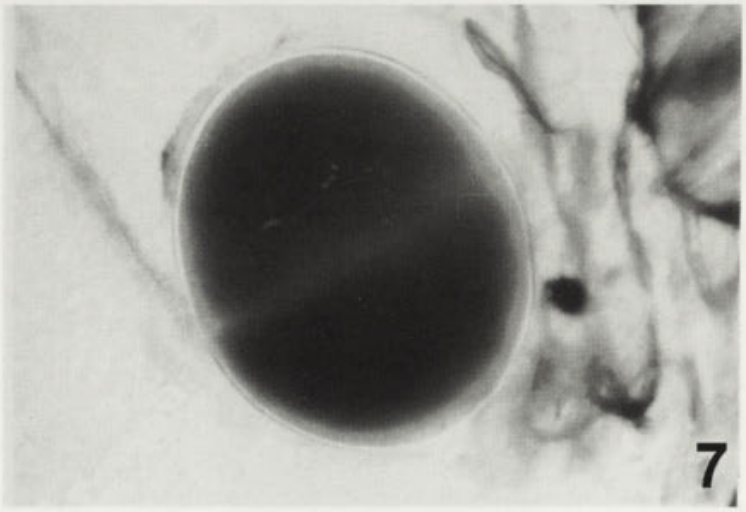

Figs. 5-8. *Gregarina acridiorum* from *Calliptamus italicus* and *Dociostaurus maroccanus*. 5 - ridge structure of the satellitess protomerite which secures the firm lock with primite and ridge on the top of the protomerite of sporonts from *C. talicus* (x 500), 6 - a group of sporonts in syzygies from *C. italicus* released from the gut of *D. maroccanus* into the dissecting fluid (x 40), 7 - an early gametocyst from *C. italicus* (x 100), 8 - nucleus of sporont from *C. italicus* with karyosomes (x 800)

Table 1. Comparison of sizes of gregarines from *D. maroccanus* and *C. italicus* with data given for *Gregarina acridiorum* by Geus (1967)

		TL	LP	LD	WP	WD	LP:TL	WP:WD	WP:LP
from *Dociostaurus maroccanus*									
Gamonts (n=9)	Range	183-328	51-85	128-246	71-125	94-101	1:2.9-4.0	1:1.2-1.6	1:0.7-0.9
	Mean	243.4± 54.9	70.5±13.4	172.8± 43.6	89.6± 17.6	125.5 ±31	1:3.4±0.4	1:1.4±0.1	1:0.8±0.1
Sporonts (n=16)									
Primites	Range	250-518	62-102	218-416	68-176	132-380	1:3.1-6.2	1:1.4-2.3	1:0.5-1.0
	Mean	351.5±107.7	79.5±13.6	271.9±97.4	119.6±36.0	216.2±81.3	1:4.4±0.9	1:1.8±0.3	1:0.7±0.1
Satellites	Range	232-587	44-72	175-524	62-224	120-352	1:4.1-10.9	1:1.2-2.1	1:0.3-0.8
	Mean	376.6±122.4	55.3±7.2	321.2±121.8	130.6±44.3	200.4±77.1	1:6.9±2.3	1:1.5±0.2	1:0.5±0.2
from *Calliptamus italicus*									
Gamonts (n=10)	Range	150-360	44-80	108-294	64-128	94-185	1:3.2-5.5	1:1.4-1.6	1:0.4-0.9
	Mean	259.8±57.6	63.7±10.4	196.1±52.4	96.7±19.0	142.9±29.6	1:4.1±0.8	1:4.1±0.8	1:0.7±0.1
Sporonts (n=22)									
Primites	Range	284-570	62-114	210-456	106-210	180-467	1:3.8-5.9	1:1.2-2.5	1:0.4-0.9
	Mean	427.1±77.1	89.3±13.2	337.7±67.7	152.3±27.7	281.8±72.3	1:4.8±0.6	1:1.8±73	1:0.6±0.1
Satellites	Range	301-576	40-47	243-518	110-205	171-342	1:5.2-12.4	1:1.3-1.8	1:0.2-0.5
	Mean	451.0±87	53.8±9.0	397.1±87.5	153.9±27.4	245.±55.4	1:8.6±2.3	1:1±0.1	1:0.4±0.1
Gregarina acridiorum									
Gamonts (n=6)	Range	405-622	80-118	325-504	90-130	108-157	1:4.9-5.3	1:1-1.4	1:0.8-0.9
	Mean	492.2±77.5	96.5±15	395.7±64.3	108.3±15.0	130.5±15.7	1:5.1±0.1	1:1.2± 0.1	1:0.9±0.1
Sporonts (n=5)									
Primites	Range	521-802	103-159	418-643	116-163	129-203	1:5.0-5.7	1:1.1-1.3	1:0.9-1.0
	Mean	695.6±121.0	131.6±23.6	564.0±98.6	141.4±20.2	169.4±33.3	1:5.3±0.3	1:1.±0.1	1:0.±0.0
Satellites	Range	103-789	98-147	405-642	122-175	137-208	1:5.1-5.9	1:1.1-1.2	1:0.8-0.9
	Mean	684.2±121.2	123.6±29.7	560.6±101.5	151.6±22.3	178.8±30.5	1:5.5±0.3	1:1.2± 0.1	1:0.8±0.1

but with the maturation they move to the gut lumen where they meet other gamonts and enter into the syzygies as sporonts. However, some gamonts evidently fail to move into the intestine lumen maturing within the caeca.

The intensity of parasitization in some adult locusts was extremely high and in some specimens the whole intestine was filled with hundreds of gamonts, sporonts in associations and gametocysts which are easily visible in the dissected insects through the midintestine wall (Fig. 9). Such great number of gregarines without doubt has the detrimental effect on food movement and its assimilation in the insect host gut.

It is generally thought that gregarines (Eugregarinorida) do not affect seriously the life processes of their hosts. However, Lipa (1967) and Brooks and Jackson (1990) demonstrated that some eugregarine species can greatly increase the host mortality due to serious damage of the gut epithelium and intestinal caeca. This effect interferes with the proper assimilation of the food by their hosts or make port of entry to the haemcoel for intestinal bacteria what results in the septicemia.

Parasitization level

The populations of *D. maroccanus* and *C. italicus* were regularly monitored in La Serena (Badajoz province) for the presence of pathogens beginning from March 24, 1992. Although over a thousand of nymphs were examined no gregarine infection was observed. The adult insects which appeared in May were also free from infection, but starting on June 19 eleven adults of *D. maroccanus* out of 110 and one *C. italicus* out of three examined were found infected. On July 8, one out of fourteen *D. maroccanus* adults and six out of sixteen *C. italicus* were found infected.

In addition, nine out of sixty one adults of *D. maroccanus* collected in La Laguneta (Tenerife Island) on July 15, 1992 and two out of eight collected in the same place on October 3, 1992 were found infected.

One infected *C. italicus* was found in Santa Marta (Albacete) out of three collected on July 4,1992.

Late occurrence of gregarine infection among populations of *D. maroccanus* and *C. italicus* registered by us is not surprising. Bush (1928) observed that grasshoppers in the spring were free from infection but later in the season practically every grasshopper was infected.

Gregarine in *Locusta migratoria*

An eugregarine was also found in two adults out of six examined from laboratory rearing of *Locusta migratoria* in Sankt Petersburg but the insects were originally collected in Uzbekistan Republic. Morphology of gamonts, type of syzygies and size parameters (Table 1) indicate that it can be considered as identical with the eugregarine observed in *D. maroccanus* and *C. italicus*.

Gregarines in other Orthoptera

During late summer of 1992 eugregarine infections were recorded in adults of the following orthopterans collected in the Iberian Peninsula (Albacete, Badajoz and Valencia) and in the Canary Islands (El Hierro and Tenerife):

Anacridium aegyptium L. (Orthoptera, Acrididae). One out of three collected at Valencia city on July 2, 1992 was infected with *Gregarina* sp. but lack of sufficient number of measurements make impossible to idetify this gregarine to species.

Oedaleus decorus (Germ.)(Orthoptera, Acrididae). One out of five collected at La Laguneta (Tenerife Island) on July 15, 1992 was infected with *Gregarina* sp. forming syzygies (Table 2). Only three syzygies were observed, possibly by young sporonts, with the maximum size of 356 μm. Therefore, although this eugregarine was similar to the eugregarine observed in *D. maroccanus*, we cannot make a firm conclusion that they are identical.

Ailopus sp. (Orthoptera; Acrididae). In one out of four collected at La Laguneta (Tenerife) on October 3, 1992 only solitary gamonts (sporonts) with the maximum size of 257 μm were present (Fig. 10) (Table 2) having the characteristic of *Leidyana* genus.

Decticus albifrons (F.) (Orthoptera, Tettigoniidae). In one collected at El Cascajo (El Hierro Island) three solitary gamonts were present having the maximum length up to 553 μm (Table 2). Although it resembled the eugregarine observed in *D. maroccanus* we cannot make a firm conclusion that they are identical, due to lack of sufficient data.

DISCUSSION

Eugregarines are common parasites of Orthoptera and several species have been described or recorded on various continents (Watson 1916a, b, 1922; Geus 1969; Levine 1988). However, for the taxonomic consideration we have taken into account only gregarine species recorded in orthopterans occurring in the Palearctic region from which originates our research material.

Table 2. Size of gregarines from *Ailopus* sp., *Decticus albifrons*, *Locusta migratoria* and *Oedaleus decorus*

		TL	LP	LD	WP	WD	LP:TL	WP:WD	WP:LP
Ailopus sp.									
Gamonts (n=6)	Range	143-257	29-60	114-200	51-81	68-123	1:3.8-4.9	1:1.3-1.6	1:0.6-0.9
	Mean	206.8±42.1	49.7±157.2	157.2±31.4	62.5±11.8	92.0±19.1	1:4.2±0.5	1:1.5±0.1	1:0.8±0.1
Decticus albifrons									
Gamonts (n=3)	Range	205-553	60-171	143-450	63-154	89-342	1:1.3-5.4	1:1.4-2.2	1:0.7-2.7
	Mean	228.7±194.6	111.3±56.0	250.0±173.3	93.3±52.5	177.0±143.0	1:3.4±2.0	1:1.7±0.4	1:1.4±1.1
Locusta migratoria									
Gamonts (n=5)	Range	79-468	22-82	57-383	35-126	46-246	1:3-5.7	1:1.3-2.0	1:0.6-0.9
	Mean	215.4±170.1	48.8±28.4	165.4±141.5	70.2±43.7	109.8±84.2	1:4.1±11.0	1:1.5±0.3	1:0.7±0.1
Sporonts (n=5)									
Primites	Range	201-410	55-82	146-338	137-526	115-219	1:3.7-6.3	1:1.3-1.9	1:0.5-0.8
	Mean	334.4±80.0	65.8±11.0	268.6±74.5	105.2±22.0	166.2±40.7	1:5.1±1.1	1:1.6±0.2	1:0.6±0.1
Satellites	Range	262-438	38-72	224-394	104-115	115-191	1:4.3-10.0	1:1.1-1.7	1:0.3-0.7
	Mean	348.2±70.9	48.4±13.5	299.8±74.3	107.2±4.9	146.6±28.3	1:7.6±2.2	1:1.4±0.2	1:0.5±0.1
Oedaleus decorus									
Gamonts (n=1)	Range	-	-	-	-	-	-	-	-
	Mean	118	52	136	84	116	1:2.3	1:1.4	1:0.6
Sporonts (n=3)									
Primites	Range	280-304	72-76	208-228	100-108	148-192	1:3.9-4.0	1:1.5-1.8	1:0.7-0.8
	Mean	293.3±12.2	74.7±2.3	218.7±10.1	102.±4.6	170.7±22.0	1:3.9±0.1	1:1.7±0.2	1:0.7±0.1
Satellites	Range	256-356	28-36	220-320	100-112	148-188	1:7.1-12.1	1:1.5-1.7	1:0.3-0.4
	Mean	317.3±53.7	33.3±4.6	284.0±55.6	105.3±6.1	165.3±20.5	1:9.7±2.5	1:1.6±01	1:0.3±0.1

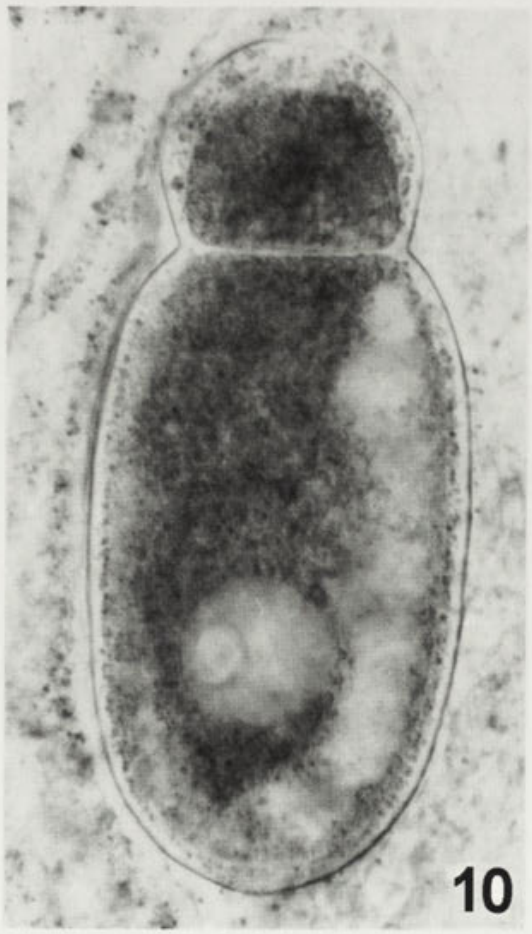

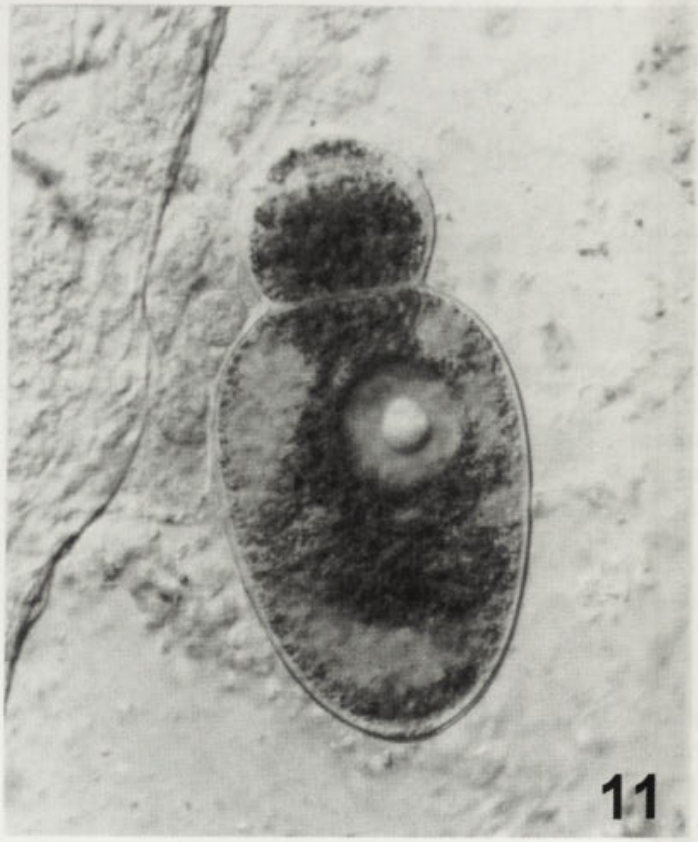

Fig. 9. Hundreds of syzygies of *Gregarina acridiorum* seen through the gut wall of *Calliptamus italicus* (x 40)

Figs. 10-11. *Leidyana* sp. from *Ailopus* sp. 10 - young gamont (x400), 11 - maturing gamont (x 400)

Table 3. Comparison of mean size of eugregarines from *D. maroccanus*, *C. italicus*, and *L. migratoria* with *Gregarina acridiorum* and *Gregarina garnhami*

	TL	LP	LD	WP	WD	LP:TL	WP:WD	WP:LP
Gamonts								
Dociostaurus maroccanus	243.4	70.5	172.8	89.6	125.5	3.4	1.4	0.8
Calliptamus italicus	259.8	63.7	196.1	96.7	142.9	4.1	1.5	0.7
Locusta migratoria	215.4	48.8	165.4	70.2	109.8	4.1	1.5	0.7
Gregarina acridiorum	492.2	96.5	395.7	108.3	130.5	5.1	1.2	0.9
Gregarina garnhami	n.a.	n.a.	n.a.	n.a.	n.a.	4.0	1.5	n.a.
Sporonts								
Primites								
Dociostaurus maroccanus	351.5	79.5	271.9	119.6	216.2	4.4	1.8	0.7
Calliptamus italicus	427.1	89.3	337.7	152.3	281.8	4.8	1.8	0.6
Locusta migratoria	334.4	65.8	268.6	105.2	166.2	5.1	1.6	0.6
Gregarina acridiorum	695.6	131.6	564.0	141.4	169.4	5.3	1.2	0.9
Gregarina garnhami	n.a.	n.a.	n.a.	n.a.	n.a.	4.0	1.4	0.6
Satellites								
Dociostaurus maroccanus	376.6	55.3	321.2	130.6	200.4	6.9	1.5	0.5
Calliptamus italicus	451.0	53.8	397.1	153.9	245.1	8.6	1.6	0.4
Locusta migratoria	348.2	48.4	299.8	107.2	146.6	7.6	1.4	0.5
Gregarina acridiorum	684.2	123.6	560.6	151.6	178.8	5.5	1.2	0.8
Gregarina garnhami	n.a.	n.a.	n.a.	n.a.	n.a.	5.5	1.4.	n.a.

n.a. - no data in original description

Type of epimerite, shape of gamonts and sporonts, type of syzygies, gametocysts and size features of the gregarines observed in *Callipatmus italicus*, *Dociostaurus maroccanus* and *Locusta migratoria* indicate that they represent the genus *Gregarina* Dufour.

Foerster (1938a, b), Semans (1943), Geus (1969) and Levine (1988) list a number of gregarines from Orthoptera from which only *Gregarina acridiorum* Léger (Léger 1893) and *Gregarina garnhami* Canning (Canning 1956) are taken into consideration of the taxonomic position of the recorded by us gregarines. It must be mentioned that none of these authors list *D. maroccanus* as host for any gregarine species, but *C. italicus* is mentioned by them as host for *G. acridiorum* and *Locusta migratoria* as host for *G. garnhami*. Also Corbel (1964) reported *L. migratoria* as an experimental host for *G. garnhami*. However, a gregarine infection caused by *Gregarina* sp. in *D. maroccanus* was observed by Nurzhanov (1988).

In Table 3 we compare size parameters of gregarines recorded in *C. italicus, D. maroccanus* and *L. migratoria* with size parameters of *G. acridiorum* given by Geus (1969). These data indicate that all three acridids studied by us were infected by the same gregarine species which we identify as *G. acridiorum*.

Unfortunately, similar comparison with *G. garnhami* is not possible as at its original description Canning (1956) has not provided any data on size of protomerites and deutomerites of gamonts and gave only maximum size of sporonts, size of cysts, and ratio TL:LP, WP:WD, LP:WP. However, even such scarce data, together with illustrations demonstrating the ridge structures securing the firm caudo-frontal associations, indicate that *G. garnhami* is identical with our material of *G. acridiorum*. This structure of the satellites protomerites was noticed and described by Canning (1956) but here we illustrate it by photographs. Such type of the attachement secures the metabolic communication between primite and satellite which is needed to coordinate movements while producing the gametocyst. This type of "lock" attachement, may indicate that vacuum suction may be involved as suggested by Canning (1956).

Our oppinion that *G. garnhami* is a synonym of *G. acridiorum* is based not only on morphology but also on size parameters. The maximum length of sporont of *G. garnhami* given by Canning is 554-643 µm and the diamater of cysts varied from 114 to 470 x 428 µm. In our material sporonts had up to 576 µm in length and cysts varied from 473 x 422 to 650 x 590 µm in diameter. It may be here mentioned that the maximum length of *G. acridiorum* given by Geus (1969) is 802 µm.

While describing *G. garnhami* Canning (1956) was not aware about existence in the literature of *G. acridiorum* which she confirmed later (Canning 1992). It is also surprising that *G. garnhami* was not included by Geus (1969) in his monograph. These facts created to us some difficulties in interpreting the taxonomic position of the involved gregarines but we consider that our studies and this discussion provided grounds to conclude that *Gregarina garnhami* Canning (1956) is not a valid species but is a synonym of *Gregarina acridiorum* Léger (1893).

Acknowledgements. J. J. Lipa would like to express his thanks to the Ministerio de Educación y Ciencia, Direccion General de Investigacion Cientifica y Tecnica for grant SAB-92-0115 and to Universidad de Cordoba, E.T.S.I.A.M., for providing the facilities to carry this research in 1992, during the 10-month sabbatical period. This research was partly supported by the European Community Project No. TS2*-0302-D (MB) [Biological Control of Locust by Entomopathogens] and it is part of P. Hernandez-Crespo Ph.D. Thesis supported by "Ministerio de Agricultura Pesca y Alimentación", grant BOE 25 April 1989 (Servicio de Investigaciones Agrarias, Badajoz).

REFERENCES

Bidochka M. J., Khachatourians G. G. (1991) Microbial and protozoan pathogens of grasshoppers and locusts as potential biocontrol agents. *Biocontrol Sci. Technol.* **1:** 243-259

Brooks W. M., Jackson J. J. (1990) Eugregarines: current status as pathogens in corn rootworms. *Vth International Colloquium on Invertebrate Pathology and Microbial Control, Adelaide (Australia)*, 512-514

Bush S. F. (1928) A study on the gregarines of the grasshoppers of Pietermaritzburg, Natal. *Ann. Nat. Mus.* **6:** 97-169

Cañizo J. (1939) Las plagas de langosta en España. *Bol. Pat. Veg. Ent. Agr.* **8:** 27-47

Canning E. U. (1956) A new eugregarine of locusts, *Gregarina garnhami* n. sp., parasitic in *Schistocerca gregaria* Forsk. *J. Protozool.* **3:** 50-62

Canning E. U. (1992) Personal letter dated 2nd December 1992

Corbel J. C. (1964) Infestations experimentales de *Locusta migratoria* L. (Insecte, Orthoptere) par *Gregarina garnhami* Canning (Sporozoaire, Gregarinomorphe): relations entre le cycle de l'hote et celui du parasite. *C. R. Acad. Sci. Paris* **259:** 207-210

Geus A. (1969) Sporentierchen, Sporozoa, Die Gregarinida der land- und süsswasserbewohnenden Arthropoden Mitteleuropas. In: *Die Tierwelt Deutschlands*. VEB Gustav Fischer, Jena **57:** 1-608

Foerster H. (1938a) Gregarinen in schlesiches Insekten. *Z. Parasitenk.* **10:** 157-209

Foerster H. (1938b) Beobachtungen über das Auftreten von Gregarinen in Insekten. *Z. Parasitenk.* **10:** 649-673

Hernandez-Crespo P. (1993) La Langosta Mediterranea, *Dociostaurus maroccanus* (Thunberg), sus Enemigos Naturales Autoctonos y el Posible Control de sus Plagas por Medio de Microorganismos Patogenos. Ph.D. Thesis, Universidad de Córdoba

Hernandez-Crespo P., Santiago-Alvarez C. (1991) On the occurrence of a mermithid on Spanish acridids. *IOBC/WPRS Bulletin* **14:** 208-211

Léger L. (1893) Sur une grégarine nouvelle des Acridiens d'Algerie. *C.R. Acad. Sci.* Paris **117:** 811-813

Levine N. (1988) The Protozoan Phylum Apicomplexa. CRC Press, Boca Raton, Vol. 1, 2

Lipa J. J. (1967) Studies on gregarines (*Gregarinomorpha*) of arthropods in Poland. *Acta Protozool.* **5:** 93-179

Lipa J. J., Hernandez-Crespo P., Gonzalez-Reyes J. A., Santiago-Alvarez C. (1994) A newly recorded *Entomopoxvirus* B in *Anacridium aegyptium* (Orthoptera: Acrididae). *Biocontrol Sci. Technol.* **4:** 343-345

Nurzhanov A. A. (1989) Entomopathogenic Microorganisms of Gregarious Locusts of Uzbekistan and Perspectives of their Use in Biological Protections of Plants. Ph.D. Thesis VASKHNIL and VIZR, Leningrad, (in Russian)

Santiago-Alvarez C. (1991) The knowledge of fungal entomopathogens in Spain. *IOBC/WPRS Bulletin* **14:** 208-211

Semans F. M. (1943) Protozoan parasites of the *Orthoptera*, with special reference to those of Ohio. IV. Classified list of the protozoan parasites of the *Orthoptera* of the World. Classes Mastigophora, Sarcodina, and Protozoa. *Ohio J. Sci.* **43:** 221-245

Uvarov B. P. (1928) *Locusts and Grasshoppers*. The Imperial Bureau of Entomology. London

Vazqez Lesmes, Santiago-Alvarez C. (1994) Las Plagas de Langosta en Cordoba. Monte de Piedad y Caja de Ahorras de Cordoba. Collection Mayor, Cordoba

Watson M. E. (1916a) Studies on gregarines I. *Ill. Biol. Monogr.* **2:** 1-258

Watson M. E. (1916b) Some new gregarine parasites from *Arthropoda. J. Parasitol.* **2:** 27-36

Watson-Kamm M. (1922) Studies on gregarines II. *Ill. Biol. Monogr.* **7:** 1-104

Received on 14th June, 1995; accepted 25th September, 1995

Acta Protozoologica (1996) 35: 61- 67

ACTA
PROTOZOOLOGICA

An Endosymbiotic Trichodinid, *Trichodina rhinobatae* sp. n. (Ciliophora: Peritrichia) Found in the Lesser Guitarfish, *Rhinobatos annulatus* Smith, 1841 (Rajiformes: Rhinobatidae) from the South African Coast

Jo G. VAN AS and Linda BASSON

Department of Zoology and Entomology, University of the Orange Free State, Bloemfontein, South Africa

Summary. During parasitological surveys on the West coast of South Africa a population of trichodinids (Ciliophora: Peritrichia) was found in the urogenital tract of a lesser guitarfish *Rhinobatos annulatus* Smith, 1841 (Rajiformes: Rhinobatidae). This trichodinid is described as a new species, *Trichodina rhinobatae* sp. n. using silver impregnation. Aspects of its morphology are illustrated by means of scanning electron microscopy. *T. rhinobatae* has denticles with broad blades, robust central parts and strongly developed rays. The overall body dimensions fall well below the range recorded for other species found as endosymbionts in the reproductive system of marine fish.

Key words: endosymbiont, guitarfish, morphology, South Africa, *Trichodina rhinobatae*.

INTRODUCTION

Members of the peritrich family Trichodinidae are best known as ectoparasites of fish with most of the species reported from freshwater environments. Representatives of three genera have been found as endosymbionts of freshwater fish. Of these two species of the genus *Vauchomia* Mueller, 1938 were recorded from the urinary system of pikes in North America by Mueller (1931, 1932, 1938) as well as by Lom and Haldar (1976). A number of *Paratrichodina* Lom, 1963 species were reported as endosymbionts of freshwater fish and described from Eastern Europe and the former USSR by Vojtek (1957), Lom (1963) and Lom and Haldar (1976).

Nine species of the genus *Trichodina* Ehrenberg, 1838, from both freshwater and marine environments, were also described as endosymbionts of fish from different parts of the world (Lom and Haldar 1976, Li and Desser 1985, Basson 1989, Basson et al. 1990). Of these four species were recorded from marine fish, whilst the rest were found associated with freshwater fish. Two species, i.e., *T. fariai* Da Cunha and Pinto, 1928 from Brazil and *T. luba* Basson, Van As and Fishelson, 1990 from South Africa, Hawaii and New Guinea were found in the intestine of marine fish by Da Cunha and Pinto (1928) and Basson et al. (1990) respectively. Two species, i.e., *T. oviducti* Poljansky, 1955 and *T. rajae* Evdokimova, Kuznetsova and Stein, 1969 were described from the urinary system of dif-

Address for correspondence: L. Basson, Department of Zoology and Entomology, University of the Orange Free State, P.O. Box 339, Bloemfontein, 9300, South Africa; Fax: (51) 488 711; E-mail: dlb@rs.uovs.ac.za

ferent skate species from South America (Evdokimova et al. 1969, Lom and Haldar 1976), Canada (Khan 1972, Lom and Haldar 1976) and the former USSR (Poljansky 1955).

During fish parasitological surveys along the West coast of southern Africa a single adult female of the lesser guitarfish, *Rhinobatos annulatus* Smith, 1841 (Rajiformes: Rajiformes) was collected from the mouth of the Olifants River and found to host trichodinids in the urogenital tract. This symbiont, clearly identified as a member of the genus *Trichodina* by its denticle morphology and adoral ciliary spiral, was found to be a new species that is described below.

MATERIALS AND METHODS

An adult female (one meter in length) of the lesser guitarfish *Rhinobatos annulatus* was collected by cast nets in the shallow upper reaches of the Olifants River mouth, taken to a field laboratory, anaesthetized with MS222 and examined for parasites. The only parasites found were trichodinids in the urogenital tract.

The urogenital tract was removed and dissected. Pieces of the tract were smeared over glass slides and these smears were left to dry. The air-dried smears were impregnated with silver nitrate to study details of the adhesive disc as suggested by Lom (1958). All measurements are presented in micrometres and follow the uniform specific characteristic system proposed by Lom (1958). Detailed descriptions of the denticles are presented according to the method proposed by Van As and Basson (1989) and follow the sequence as indicated in Van As and Basson (1992). All the measurements are presented in Table 1.

For scanning electron microscopy (SEM), material was collected and fixed in 10% buffered seawater formalin, washed in tap water, dehydrated in a series of ethanols and critical point dried. Sputter coating was done with gold and specimens were examined in a JEOL WINSEM at 5 kV.

In order to study the denticle morphology, the soft material of the trichodinids was removed by dissolving specimens in a nitric acid solution, whereafter specimens were prepared for SEM as described above. This solution by Luna (1968) is normally used for softening chitin and keratin and sometimes leads to minor damage of the soft body of the trichodinids with some cilia either partially or totally removed.

RESULTS

Trichodina rhinobatae sp. n.

Description

Type-host: Lesser guitarfish, *Rhinobatos annulatus* Smith, 1841 (Rajiformes: Rhinobatidae) female.

Locality: Olifants River mouth, West coast of southern Africa (31°22'S 18°18'E).

Type material: holotype, slide 94/01/17-05 (NMB P115), and paratype, slides 94/01/17-12 (NMB P116) and 95/01/17-16 (NMB P117), in the collection of the National Museum, Bloemfontein, South Africa.

Position in host: urogenital tract.

Etymology: this species was named after the generic name of the guitarfish.

Biometrical data is summarized in Table 1 together with comparative measurements of *T. oviducti* and *T. rajae* known from the urogenital tract of skates.

Trichodina rhinobatae is a medium sized trichodinid with a disc-shaped body of which the height is roughly half that of the body diameter, i.e. 20 µm (Fig. 1). The adoral ciliary wreath spirals close to the periphery of the body, entering the infundibulum at a point lower (aboral) to its origin (Fig. 1). The poli- and haplokineties originate in phase, with the inner polikinety consisting of three rows and the outer haplokinety of a single row situated on an elevated ridge (Fig. 2). The mouth of the infundibulum is large and tear-shaped. The polikinety enters directly when reaching the infundibulum whilst the haplokinety enters 180° later at the opposite side (Fig. 2). Kinetosomes from both poli- and haplokineties are ciliated throughout, also when entering the infundibulum (Fig. 1). Distinct ridges are visible supporting the infundibulum between the two entering kineties.

The pellicle of the body surface is smooth, without ornamentation. Between the ciliary girdle and adoral spiral distinct body indentations are visible (Fig. 1).

The aboral ciliary complex consists of two rings of cilia (Fig. 3). No marginal cilia are present. The outer ciliary ring, i.e. the compound wreath, consists of numerous rows (approximately six to eight) of increasing lengths with the longest row, situated adorally, almost five times the length of the shortest aborally-placed row. These cilia are not detached from one another for their whole length as normally found for most trichodinid species studied by means of SEM, but rather closely associated for half their length while the distal ends are unattached (Figs. 1, 3). The inner ciliary ring, i.e. the basal cilia, consists of a single row of short cilia separated from the outer cilia by a septum (Fig. 4).

The morphology of the denticle ring and the individual denticles is not always accurately represented by silver impregnated specimens. In our silver impregnated material, the specimens appear to have broad blades with some spaces between them and delicate rays of equal thickness throughout (Figs. 7-9), whilst the blades and rays were shown to be strongly developed and tight fitting in SEM micrographs (Figs. 5, 6).

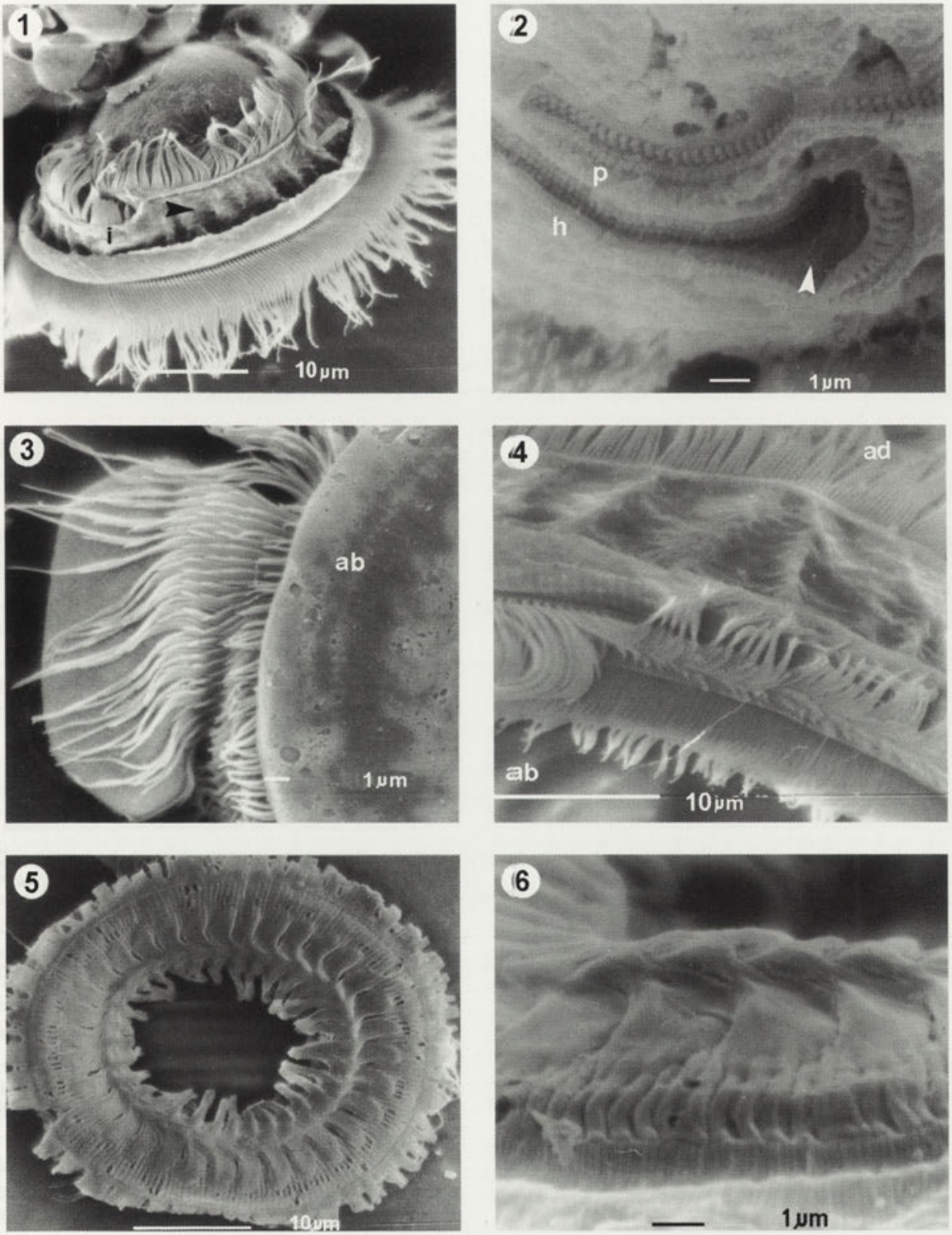

Figs. 1-6. Scanning electron micrographs of *Trichodina rhinobatae* sp. n. from the lesser guitarfish *Rhinobatos annulatus* Smith, 1841. 1 - adoral view of ciliophoran showing adoral spiral and aboral ciliary complex. Arrow indicates body indentations, i - opening of infundibulum; 2 - opening of infundibulum with cilia removed. Arrow indicates ridges supporting infundibulum, h - haplokinety, p - polikinety; 3-4 - aboral ciliary complex illustrating different lengths of cilia. ab - aboral side, ad - adoral side; 5 - aboral view of denticle ring as well as radial- and peripheral pins. Soft body material removed; 6 - tilted aboral view of denticles illustrating elevated central parts

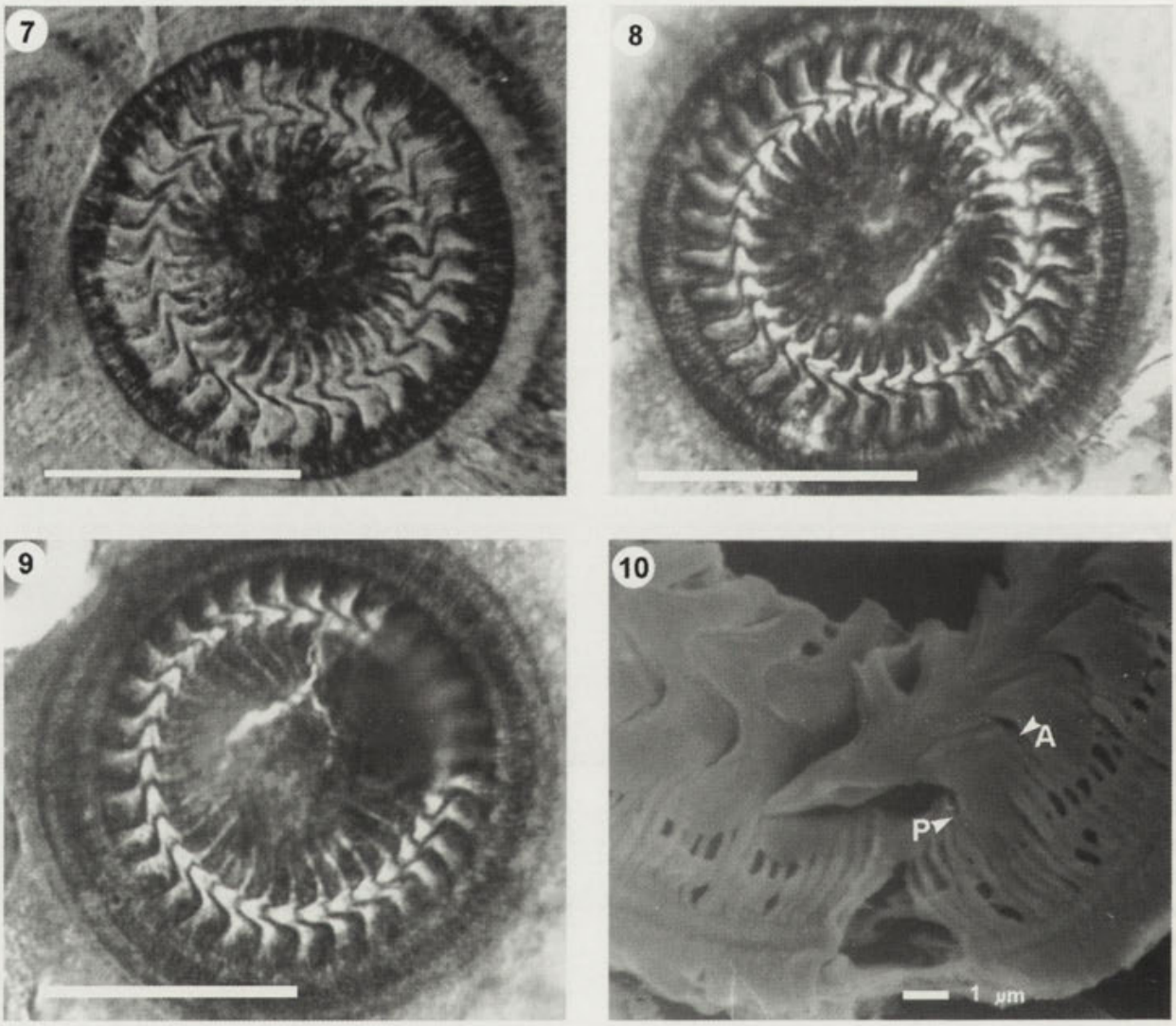

Figs. 7-10. Photomicrographs (7-9) and scanning electron micrograph (10) of *Trichodina rhinobatae* sp. n. from the lesser guitarfish *Rhinobatos annulatus* Smith, 1841. 7-9 - silver impregnated adhesive discs; 10 - aboral view of part of denticle ring showing robust conical part (cone). P - posterior side of denticle, A - anterior side of denticle. Bar - 20 µm (7-9)

The blade is broad and angular, filling most of the section between the y axes (Fig. 11). The distal blade surface is only slightly rounded. The tangent point is rounded, situated proximally to the distal blade surface. The anterior blade surface slopes down to form a V- shape with the y axis. The blade apex is prominent and rounded, extending to and sometimes just past the y+1 axis. The blade apophysis is prominent and in close articulation with the posterior projection of the preceding denticle. This is less visible in silver impregnated specimens than in those studied with the aid of the SEM. The blade connection in relation to blade is narrow. The posterior blade surface has a shallow curve with the deepest part at the proximal side of the blade. The central part is robust, fitting tightly into the preceding denticle. The central conical part (cone) is strongly developed, extending deep into the following denticle (Fig. 10). The shape of the sections above and below the x axis is similar. Prominent indentations in the proximal central sections correspond to strongly developed ray apophyses which are directed distally. This feature is clearly defined in silver impregnated specimens. Rays are strongly developed as seen in the SEM, but less visible is silver impregnated specimens. The point of the ray is rounded with the rays tapering only slightly towards their tips. The rays touch the y axes and are arranged parallel to these.

The ratio of the denticle distally from the x axis to the section proximally from the x axis is slightly less than one (0.9).

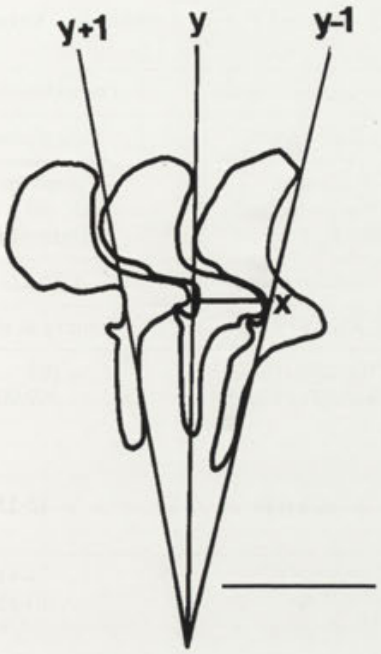

Fig. 11. Diagrammatic drawing of the denticles of *Trichodina rhinobatae* sp. n. from the lesser guitarfish *Rhinobatos annulatus* Smith, 1841. Bar - 5 µm

DISCUSSION

Of the nine endosymbiotic species of *Trichodina* described to date, four are found associated with marine fish. Both *T. luba* and *T. fariai* show unique intestinal localization in their host. According to Lom and Haldar (1976) the description of *T. fariai* is inadequate since it was described without silver impregnation. Further comparison with *T. rhinobatae* is therefore not possible. *T. luba* was described from the colon of the surgeonfish, *Acanthurus xanthopterus*, collected from the coast of South Africa, Hawaii and New Guinea. This species shows some resemblance in denticle morphology with *T. rhinobatae* in having robust denticles with broad blades and well-developed rays. The differences lie in the far more prominent ray apophysis as well as shorter rays in *T. rhinobatae*. The true denticle shape in *T. luba* is clearly illustrated in silver impregnated specimens. Furthermore, *T. luba* was found to be restricted to the colon, never being encountered in the urogenital tract of *A. xanthopterus*.

The only other two marine endosymbiotic species are *T. oviducti* and *T. rajae*, both described from the urogenital tact of different skate species. *T. oviducti* is to date one of the largest species of the genus *Trichodina* so far recorded with an adhesive disc diameter of up to 271 µm and a mean of 156 µm recorded by Khan (1972) from *Raja radiata* of Newfoundland. This is well outside the range of both *T. rhinobatae* and *T. rajae* (Table 1). Furthermore, both *T. oviducti* and *T. rajae* have many more denticles than the present species. Both these species also have slender elongated denticles compared to the robust stout denticles of *T. rhinobatae*.

One of the characteristics of *T. rhinobatae* is that in silver impregnated specimens the denticles appear somewhat delicate, whilst appearing strongly developed and tight fitting in SEM micrographs. One of the reasons for this phenomenon is that the strongly developed central parts protrude further in an aboral direction than the blades and rays and are, therefore, not on the same plane as can be observed using the SEM (Fig. 6). The fact that these structures are not on the same plane, causes focus problems in light microscopy. The denticle becomes thinner from the central part in both a distal and proximal direction. The posterior surface of the blade is also thicker than the anterior blade surface, therefore having a wedge-like shape. This also makes the interpretation of the denticle shape difficult based only on light microscopy.

Another feature illustrated by this species is clear body indentations visible in Fig. 1. These are most likely points of attachment for micro-fibrils, similar to those described by Van As and Basson (1993) for *Pallitrichodina rogenae* Van As and Basson, 1993 and *P. stephani* Van As and Basson, 1993.

The present material represents the first urogenital trichodinid in any fish from African waters and the only record so far from the guitarfish and also of the family Rhinobatidae.

Trichodina rhinobatae was found mostly inside the genital tract and to a lesser extent in the urinary system. Several developing embryos were also encountered inside the genital tract. Quite a number of trichodinids was found on the external gill filaments of these embryos. These proved to belong to the same species as those from the urogenital tract. Since no trichodinids were found on the body of the embryos, it could indicate that the body surface of the developing embryos is not preferred by *T. rhinobatae*. A theory is put forward that this endosymbiont would not leave the adult host by way of the young, but is rather associated with the genital tract of the adult host and therefore transmission could somehow be implicated in the reproductive behavior of these fish.

It is possible that both male and female could be infected by these endosymbionts during copulation since internal fertilization occurs in guitarfish. Khan (1972)

Table 1. Biometrical data (in µm) of *Trichodina rhinobatae* sp. n., *T. oviducti* Poljansky, 1955 and *T. rajae* Evdokimova, Kuznetsova and Stein, 1969

Trichodinid species	*Trichodina rhinobatae*	*Trichodina oviducti*	*Trichodina oviducti*	*Trichodina rajae*
Host	*Rhinobatos annulatus*	*Raja radiata*	*Raja radiata*	*Raja scabina*
Locality	Olifants River mouth, Southern Africa	Barents Sea	Coast of Newfoundland	Patagonian shelf, off coast of Argentina
Position in host	urogenital tract	oviducts	genital tract	oviducts
Reference	present study*	Poljansky (1955)	Khan (1972)	Evdokimova et al. (1969)
Body diameter	35.0-47.5 (41.6±3.3)	100-190	106-295 (168)	105
Adhesive disc diameter	29.5-41.5 (36.1±3.1)	up to 145	115-271 (156)	69-90
Border membrane width	2.0-3.5(2.9±0.5)145			
Denticle ring diameter	18.0-24.0 (21.3±1.9)	65-95	72-128 (98)	42-55
Denticle number	27-34 (30-32)	45-57 (51-54)	46-60(53)	34-41 (35-37)
Radial pins/denticle	7-9 (7,10)	12	5-7 (6)	10-12
Denticle length	4.0-5.5 (4.7±0.6)			
Blade length	3.0-4.5 (3.8±0.5)	5.4-7.2	5-17 (11)	9-12
Central part width	1.5-2.0 (1.6±0.2)			
Ray length	4.0-5.5 (4.4±0.5)	3.6-5.4	5-21 (11.9)	9-13.5
Denticle span	8.5-11.0 (9.9±0.8)			
Nuclear apparatus	C-shaped macronucleus			
Adoral spiral	410-420°	330-345°	300°	
N	15		100	

*Minimum and maximum values are given, followed in parentheses by the arithmetic mean and standard deviation. In the case of the number of denticles and radial pins, the mode is given instead of the arithmetic mean in the present study. Body diameter is measured from silver impregnated specimens as the adhesive disc plus border membrane. N - number of specimens measured.

could not clearly show the transmission route for *T. oviducti* in thorny skates, but concluded that their transmission was most likely venereal rather than via the water medium or transovarial. It would therefore seem that our findings and ideas of transmission support the theory put forward by Khan (1972). It will be necessary to examine male specimens of the lesser guitarfish to confirm our suggestion that transmission of these trichodinids possibly occurs only during the process of copulation.

REFERENCES

Basson L. (1989) An endoparasitic trichodinid (Ciliophora: Peritrichia) from the urinary system of *Barbus trimaculatus* Peters, 1852. *S. Afr. J. Zool.* **24:** 260-262

Basson L., Van As J. G., Fishelson L. (1990) A new species of *Trichodina* (Ciliophora: Peritrichia) from the intestine of the surgeonfish *Acanthurus xanthopterus*. *Int. J. Parasitol.* **20:** 785-787

Da Cunha M., Pinto C. (1928) *Trichodina fariai* n. sp. cilié peritriche endoparasite de Poisson Marin. *Comp. Rend. Soc. Biol.* **48:** 1570-1571

Evdokimova E. B., Kuznetsova I. G., Stein G. A. (1969) Parasitic ciliates of the family Urceolariidae (Peritricha, Mobilia) from some fish of the South-west Atlantic. *Zool. Zhur.* **48:** 1451-1455 (In Russian)

Khan R. A. (1972) Taxonomy, prevalence, and experimental transmission of a protozoan parasite, *Trichodina oviducti* Polyanski (Ciliata: Peritrichida) of the thorny skate, *Raja radiata* Donovan. *J. Parasitol.* **58:** 680-685

Li L., Desser S. S. (1985) The protozoan parasites of fish from two lakes in Algonquin Park, Ontario. *Can. J. Zool.* **63:** 1846-1858

Lom J. (1958) A contribution to the systematics and morphology of endoparasitic trichodinids from amphibians, with a proposal of uniform specific characteristics. *J. Protozool.* **5:** 251-263

Lom J. (1963) Discovery of a *Tripartiella* in the urinary tract of *Phoxinus phoxinus* L. *Acta Protozool.* **1:** 1-4

Lom J., Haldar D. P. (1976) Observations on trichodinids endocommensal in fishes. *Trans. Amer. Microsc. Soc.* **95:** 527-541

Luna L. G. (Ed.) (1968) Manual of Histological Staining Methods of the Armed Forces Institute of Pathology. 3 ed. McGraw-Hill Book Company, New York

Mueller J. F. (1931) A new species of *Cyclochaeta* from the ureters and urinary bladder of *Esox reticulatus*. *J. Parasitol.* **18:** 126

Mueller J. F. (1932) *Trichodina renicola* (Mueller, 1931) a ciliate parasite of the urinary tract of *Esox niger*. *Roosevelt wild Life Ann.* **3:** 139-154

Mueller J. F. (1938) A new species of *Trichodina* (Ciliata) from the urinary tract of the muskalonge, with a repartition of the genus. *J. Parasitol.* **23:** 251-258

Poljansky Yu. I. (1955) Additions to the parasites of the fish of the northern sea of the USSR. Parasites of the Barents Sea fishes. *Trudy zool. Inst., Leningr.* **19:** 5-170 (in Russian)

Van As J. G., Basson L. (1989) A further contribution to the taxonomy of trichodinid ciliophorans (Ciliophora: Peritrichia) and a review of the taxonomic status of some fish ectoparasites. *Syst. Parasitol.* **14:** 157-179

Van As J. G., Basson L. (1992) Trichodinid ectoparasites (Ciliophora: Peritrichida) of freshwater fishes of the Zambesi River system, with a reappraisal of host specificity. *Syst. Parasitol.* **22:** 81-109

Van As J. G., Basson L. (1993) On the biology of *Pallitrichodina rogenae* gen. nov., sp. n. and *P. stephani* sp. n. (Ciliophora: Peritrichida) mantle cavity symbionts of the giant African snail *Achatina* in Mauritius and Taiwan. *Acta Protozool.* **32:** 47-62

Vojtek J. (1957) Zur Kenntnis der Gattung *Trichodina* Ehrenberg 1830. *Vest. čsl. Spol. zool.* **21:** 173-180 (in Czech)

Received on 10th April, 1995; accepted on 29th August, 1995

ACTA
PROTOZOOLOGICA

Acta Protozoologica (1996) 35: 69 - 72

On the Sarcocysts of Two Further *Sarcocystis* Species Being New for the European Hare

Klaus ODENING, Hans-Henning WESEMEIER and Ingrid BOCKHARDT

Institute for Zoo Biology and Wildlife Research, Berlin, Germany

Summary. The sarcocysts reported from German hares (Witzmann) are described by means of light and electron microscopy (*Sarcocystis* sp. 1). They have no villar protrusions arising from the cyst wall. The bradyzoites are small and squatly fusiform. A sarcocyst of a further species is described from a Polish hare (*Sarcocystis* sp. 2). It has stub-like villar protrusions arising from the cyst wall, irregular in the outline, with variedly shaped osmiophilic condensations in the core which are attended by large granules. Thus in the European hare one *Sarcocystis* species was found in Germany and altogether 5 other species in Poland. *Sarcocystis cuniculorum* nom. nov. is proposed as replacement name for *S. cuniculi* Brumpt, 1913 nom. nud. Except this species the other 5 species from the European hare do not seem to be species-specific for this intermediate host.

Key words: host specificity, *Lepus europaeus*, *Sarcocystis cuniculorum* nom. nov. pro *S. cuniculi* nom. nud., *Sarcocystis* spp.

Abbreviations: LM - light microscopy, n - number of elements measured, PCW - primary cyst wall, s - standard deviation, TEM - transmission electron microscopy, x - mean value.

INTRODUCTION

Odening et al. (1994c) published the first description of the sarcocysts of 4 *Sarcocystis* species from European hares in Poland in detail by means of light (LM) and electron transmission microscopy (TEM). We knew only two reports on sarcocysts from *Lepus europaeus* from the time before which had not been described recognizably. One of these ranks among the first reports on the occurrence of sarcocysts: v. Hardenberg (in Ripping 1865), Central Europe. The others are statements from the German Länder Brandenburg and Thuringia (Witzmann 1982, Witzmann et al. 1983); this material exists in the form of paraffin blocks and histological preparations in our institute. We re-examined the sections and made ultrathin sections for TEM investigation after dewaxation, post-fixation and embedding into Epon of some samples. The result was the picture of a further *Sarcocystis* species, not found in the Polish hares investigated by Odening et al. (1994c). A further species new for *Lepus europaeus* was discovered during the re-examination of a sarcocyst from a Polish hare. Thus the number of the *Sarcocystis* species occurring in the European hare in Central Europe increases to 6.

MATERIALS AND METHODS

The methods applied to the Polish material were explained by Odening et al. (1994c). Regarding the German material, see Witzmann (1982) and Witzmann et al. (1983). For electron microscopy, tissues

Address for correspondence: K. Odening, IZW, PF 1103, D-10252 Berlin, Germany; Fax: (+49) 30-5126104

with sarcocysts were dewaxed, post-fixed or precontrasted in 2% osmiumtetroxid solution and embedded in Epon 812. Semithin and ultrathin sections were cut and examined with a Zeiss EM 902 A.

RESULTS

Sarcocystis sp. 1 (Figs. 1-3)

Locality: German Länder Brandenburg and Thuringia.

Site: muscle fibres (tongue, *M. masseter*, musculature of thigh).

Description: Sarcocysts oval to cigar-shaped, with inconspicuous compartmentation, on the sections up to 835 µm long and up to 138 µm wide. Cyst wall in the histological section appearing thin and smooth, up to ~ 1 µm wide, in the ultrathin section ~ 0.5 µm wide, without villar protrusions. The cyst wall was provided with the usual small invaginations in the region of the PCW (type 1 according to the classification of the ultrastructure of the cyst wall by Dubey et al. 1989). The cystozoites were squatly fusiform, small, 4-7 µm long (x = 5.6 µm, s = 1.125, n = 10) and 1.5-2.0 µm wide (x = 1.9 µm, s = 0.211, n = 10) (LM, on histological sections).

Sarcocystis sp. 2 (Figs. 4-6)

Locality: Poland (near Poznań).

Site: muscle fibre (tongue).

Description: one sarcocyst, elliptical, with inconspicuous compartmentation, 385 µm long and 135 µm wide. The cyst wall showed villar protrusions on the semithin section. The ground substance was 0.35-0.50 µm wide. On the ultrathin section the villar protrusions arising from the cyst wall were irregularly stub-shaped in the outline, up to 2.4 µm long and up to 3.6 µm wide. They contained many small and, in varied extent, some rows of large osmiophilic granules along osmiophilic, cord-like condensations. The cystozoites were fusiform, 9.0-11.5 µm long (x = 10.3 µm, s = 0.97, n = 5) and 2.5-3.0 µm wide (x = 2.8 µm, s = 0.27, n = 5) (LM, on the semithin section).

DISCUSSION

The occurrence of sarcocysts in the European hare is characterised by low prevalences and intensities. Out of 205 German hares 12.25% were infected according to Witzmann (1982) and Witzmann et al. (1983) (the prevalence varied in 4 hunting areas from 1.92% to 22.37%). Odening et al. (1994c) stated sarcocysts in 5% out of 219 Polish hares investigated. Among these a species occurred which is probably identical with "*Sarcocystis cuniculi*" from the rabbit (*Oryctolagus cuniculus*). The lower prevalence and intensity of this species in the hare could be connected with the fact that the definitive host is the cat and that wild felids are hardly present. The rabbit, invading the human housing areas and living there, is, however, more likely obtainable for the domestic cat (see Odening 1995). Besides the species "*S. cuniculi*", probably common to rabbit and hare, it is doubtful whether the other 5 *Sarcocystis* species found in the hare are specific for this host or for lagomorphs. The low infection values more likely suggest aberrant *Sarcocystis* species normally infecting other intermediate hosts. This is also indicated by the morphology of the corresponding species:

Sarcocystis sp. 1 Odening et al. 1994c (cyst wall type 7) is similar to *S. cruzi* from cattle and other Bovinae according to the size of the compartments (cf. Odening et al. 1995b). Experiments for transmitting *S. cruzi* to rabbits, however, were negative (see Dubey et al. 1989).

Sarcocystis sp. 2 Odening et al. 1994c (originally characterised as having remote resemblance to the type 21) is similar to *S. hirsuta* from cattle and other Bovinae (cf. Odening et al. 1995a).

Sarcocystis cf. *bertrami* of Odening et al. (1994c) (cyst wall type 11) is similar to a species from equids (cf. Odening et al. 1995a).

Sarcocystis sp. 1 of this paper (cyst wall type 1) is similar to *S.* cf. *sebeki* found by Odening et al. (1994a) in the European badger and by Stolte et al. (1996) in the raccoon (Germany). The sarcocysts of *S. sebeki* (Tadros and Laarman, 1976) occur in *Apodemus sylvaticus* and (experimentally) *Mus musculus*. *Strix aluco* is the definitive host. It is presumed that *S. sebeki* occurs also in intermediate hosts other than Muridae (Tadros and Laarman 1979, Odening et al. 1994a, Stolte et al. 1996). Tadros and Laarman (1982) wrote that lacking of villar protrusions of the cyst wall and a small size of the bradyzoites would suggest birds of prey as definitive hosts.

They mentioned this in connection with an undescribed *Sarcocystis* species in the Netherlands, occurring in "a scanty number of sarcocysts with thin cyst walls, devoid of cyst wall projections and with cystozoites 8-9 µm long", which "were occasionally encountered in naturally infected wild rabbits".

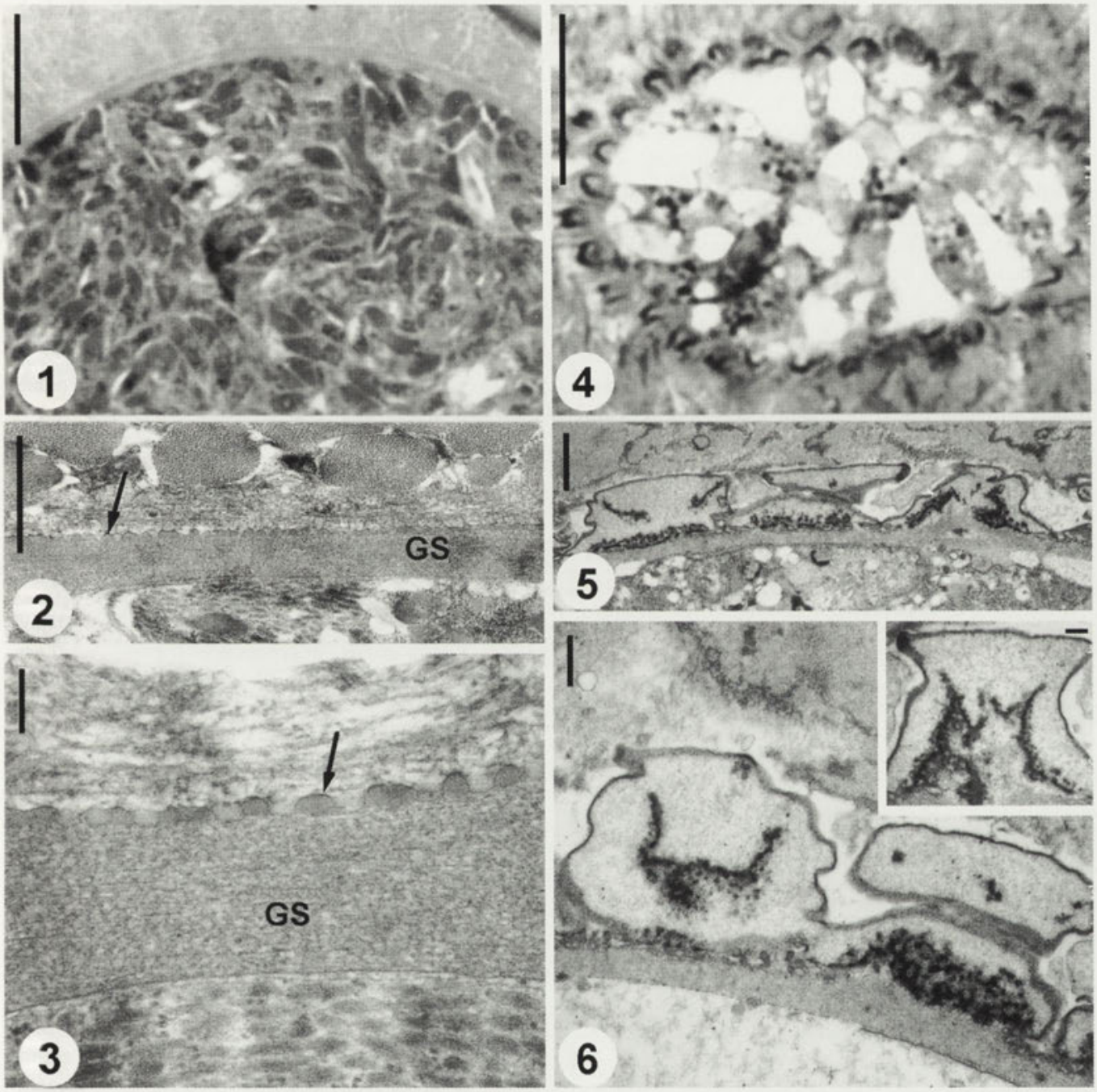

Figs. 1-3. *Sarcocystis* sp. 1 from German hares. 1 - part of a histological section (H and E) of a sarcocyst, bar - 10 µm. 2-3 - TEM micrographs of the cyst wall region; GS ground substance, arrows point to the small elevations of the PCW; bars: 2 - 1.1 µm, 3 - 0.15 µm

Figs. 4-6. *Sarcocystis* sp. 2 from a Polish hare. 4 - semithin section of a sarcocyst, bar - 10 µm. 5-6 - TEM micrographs of the cyst wall region and the villar protrusions (P); bars: 5 - 1.1 µm, 6 - 0.6 µm, inset - 0.25 µm

Sarcocystis sp. 2 of this paper is similar to *Sarcocystis* sp. (2) Odening et al. 1994b from the Mongolian gazelle (*Procapra gutturosa*) in Mongolia. This morphological conformity is perhaps the greatest puzzle in the evaluation of the *Sarcocystis* species in the European hare.

It is noteworthy that obviously only one *Sarcocystis* species has been found in German hares, in the Polish hares, however, 5 other ones.

Brumpt (1913) introduced the name *Sarcocystis cuniculi*. He wrote "Dans les muscles du Lapin domes-

tique (*L. domesticus*) et sauvage (*L. timidus*)". Accordingly, this was an indication of the localisation and of the host (*Oryctolagus cuniculus*). Both are not an "indication" in the sense of the International Code of Zoological Nomenclature (ICZN). The name is a nomen nudum, because it was not attended by any description. It is therefore not "available" in the sense of the ICZN, in spite of the name straying through the literature (see Odening et al. 1994c). The first description under this name was carried out by Tadros and Laarman (1977). Levine and Tadros (1980) and Levine (1986, 1988) listed the species as "*S. cuniculi* Brumpt, 1913 of Babudieri (1932)". But Babudieri (1932) had declared *S. cuniculi* as a synonym of the North American species *S. leporum* which was unjustified essentially and from the view point of priority. Levine's listing dealt with "*S. cuniculi* Brumpt, 1913 of Tadros and Laarman (1977)" from Europe. We propose *Sarcocystis cuniculorum* nom. nov. for replacement of *S. cuniculi* Brumpt, 1913 nom. nud. Description in Tadros and Laarman (1977, 1978, 1982), Odening et al. (1994c) and others.

Acknowledgement. We are grateful to Mrs. Doris Henne for kindly providing the material underlying the papers by Witzmann (1982) and Witzmann et al. (1983), to Mrs. Dagmar Viertel and Mrs. Marion Biering for specimen preparation for the electron microscopical investigation, and to Mrs. Susanne Auls and Mrs. Sigrid Holz for technical assistance.

REFERENCES

Babudieri B. (1932) I sarcosporidi e le sarcosporidiosi (Studio monografico). *Arch. Protistenkd.* **76:** 421-580

Brumpt E. (1913) Précis de parasitologie. Deuxième édition. Masson et Cie., Paris

Dubey J. P., Speer C. A., Fayer R. (1989) Sarcocystosis of animals and man. CRC Press, Inc., Boca Raton, Florida

Levine N. D. (1986) The taxonomy of *Sarcocystis* (Protozoa, Apicomplexa) species. *J. Parasitol.* **72:** 372-382

Levine N. D. (1988) The protozoan phylum Apicomplexa. Vol. I, II. CRC Press, Inc., Boca Raton, Florida

Levine N. D., Tadros W. (1980) Named species and hosts of *Sarcocystis* (Protozoa): Apicomplexa: Sarcocystidae). *Syst. Parasitol.* **2:** 41-59

Odening K. (1995) Natürliches Ökosystem, Zoo, Haustier- und menschliche Lebensstätten als Wechselwirkungsfelder von Parasiten. *Verh.ber. Erkrank. Zoo-Wildtiere (Berlin)* **37:** 399-407

Odening K., Stolte M., Walter G., Bockhardt I. (1994a) The European badger (Carnivora: Mustelidae) as intermediate host of further three *Sarcocystis* species (Sporozoa). *Parasite (Paris)* **1:** 23-30

Odening K., Stolte M., Lux E., Bockhardt I. (1994b) Cyst wall ultrastructure as compared with fresh state view in *Sarcocystis* from the Mongolian gazelle. 8th International Congress of Parasitology, 10-14 October 1994 Izmir-Turkey. Abstracts **2:** 252

Odening K., Wesemeier H.-H., Pinkowski M., Walter G., Bockhardt I. (1994c) European hare and European rabbit (Lagomorpha) as intermediate hosts of *Sarcocystis* species (Sporozoa) in Central Europe. *Acta Protozool.* **33:** 177-189

Odening K., Wesemeier H.-H., Walter G., Bockhardt I. (1995a) Ultrastructure of sarcocysts from equids. *Acta Parasitol.* **40:** 12-20

Odening K., Wesemeier H.-H., Walter G., Bockhardt I. (1995b) On the morphological diagnostics and host specificity of the *Sarcocystis* species of some domesticated and wild Bovini (cattle, banteng and bison). *Appl. Parasitol.* **36:** 161-178

Ripping L. H. (1865) Beiträge zur Lehre von den pflanzlichen Parasiten beim Menschen. III. Über die Miescherschen Schläuche. *Z. rationelle Med.* (Dritte Reihe) **23:** 139-142

Stolte M., Odening K., Bockhardt I. (1996) The raccoon as intermediate host of three *Sarcocystis* species in Europe. *J. Helminthol. Soc. Wash.* **63:** (in press)

Tadros W., Laarman J. J. (1977) The cat *Felis catus* as the final host of *Sarcocystis cuniculi* Brumpt, 1913 of the rabbit *Oryctolagus cuniculus*. *Proc. K. Nederl. Akad. Wet., Ser. C*, **80:** 351-352

Tadros W., Laarman J. J. (1978) A comparative study of the light and electron microscopic structure of the walls of the muscle cysts of several species of Sarcocystid Eimeriid Coccidia. I., II. *Proc. K. Nederl. Akad. Wet., Ser. C*, **81:** 469-491

Tadros W., Laarman J. J. (1979) Muscular sarcosporidiosis in the common European weasel, *Mustela nivalis*. *Z. Parasitenkd.* **58:** 195-200

Tadros W., Laarman J. J. (1982) Current concepts on the biology, evolution and taxonomy of tissue cyst-forming eimeriid Coccidia. *Adv. Parasitol.* **20:** 293-468

Witzmann H. (1982) Pathomorphologische Untersuchungen zum Sarkosporidienbefall beim Feldhasen (*Lepus europaeus*). Diploma Thesis Humboldt Univ., Vet. Med., Pathol., Berlin

Witzmann H., Ippen R., Henne D. (1983) Untersuchungen zum Sarkosporidienbefall beim Feldhasen (*Lepus europaeus*). *Verh. ber. Erkrank. Zootiere (Berlin)* **25:** 315-319

Received on 30th June, 1995; accepted on 15th July, 1995

ACTA
PROTOZOOLOGICA

Acta Protozoologica (1996) 35: 73 - 75

A New Species of *Isospora* (Apicomplexa) from Captive Pekin Robins, *Leiothrix lutea* (Passeriformes: Sylviidae), from the Dallas Zoo

Thomas E. McQUISTION[1], Chris T. McALLISTER[2], and Rita E. BUICE[3]

[1]Department of Biology, Millikin University, Decatur, Illinois; [2]Division of Natural and Applied Sciences, Cedar Valley College, Lancaster, Texas; [3]Veterinary Department, Dallas Zoo, Dallas, Texas, USA

Summary. A new species of coccidian (Apicomplexa, Eimeriidae) is described from the faeces of the pekin robin, *Leiothrix lutea,* from the Dallas Zoo. Oocysts of *Isospora leiothrixi* sp. n. were found in 2/3 adult birds and are ellipsoidal, 28.0 x 18.6 (24-32 x 15-21) µm, with a bilayered wall; shape index (length/width) 1.54. A micropyle and oocyst residuum are absent, but 1 or 2 polar granules are present. Sporocysts are ovoidal, 15.5 x 10.3 (12-20 x 7-12) µm, and possess a nipple-like Stieda body and a prominent substieda body; shape index 1.55. Each sausage-shaped sporozoite are loosely arranged side by side in the sporocyst and contained one posterior refractile body and a central nucleus.

Key words: Coccidia, *Isospora leiothrixi* sp. n., *Leiothrix lutea,* Muscicapidae, Passeriformes.

INTRODUCTION

The range of the Pekin Robin (*Leiothrix lutea),* extends from the Himalayas of southern Asia into northern India, Burma, Vietnam, southeastern Tibet and China. Found in dense, wet forests above 1200 meters elevation, *L. lutea* feed in the undergrowth on insects and fruit. The Pekin Robin was introduced on the Hawaiian Islands and has adapted well to the mountainous, dense forest environment (Sibley and Monroe 1990). Since no coccidian parasites have previously been described from *L. lutea,* herein we present a description of a new species of *Isospora.*

Address for correspondence: T. E. McQuistion, Department of Biology, Millikin University, 1184 West Main Street, Decatur, Illinois 62522, USA; Fax: (217) 424-3993; E-mail: tmcquistion@mail.millikin.edu

MATERIALS AND METHODS

During May 1994, faecal samples were obtained from 3 captive pekin robins housed at the Dallas Zoo. The samples were immediately placed in 2.5% (w/v) $K_2Cr_2O_7$ and maintained at 8°C in the laboratory. After the samples were forwarded to our laboratory, pellets were broken up with wood applicator sticks, and each sample was placed in a sterile Petri dish and the oocysts allowed to sporulate at 25°C for one week.

Sporulated oocysts were examined after flotation in Sheather's sugar solution (specific gravity 1.20). Measurements and photomicrographs were taken using a Nikon microscope with planapochromatic objectives, a Canon AE-1 camera, and a calibrated ocular micrometer. All measurements are in micrometers (µm) with size ranges in parentheses following the mean.

RESULTS

Two of three adult captive *L. lutea* from the Dallas Zoo were passing coccidian oocysts. Both birds were

passing hundreds of oocysts which appeared similar in morphological characteristics. Upon sporulation, these oocysts were found to represent a previously unreported species, which is described below.

***Isospora leiothrixi* sp. n. (Figs. 1-4)**

Description of oocysts: ellipsoidal, colorless, 28.0 x 18.6 (24-32 x 15-21) (N=15), with a smooth, bilayered wall *ca* 1.0 thick; shape index (length/width) 1.54 (1.33-1.81). Micropyle and oocyst residuum absent, 1-2 polar granules present, sometimes fragmented and consisting of 2-5 granules. Sporocysts ovoidal, 15.5 x 10.3 (12-20 x 7-12) (N=29) with smooth, thin wall *ca* 0.5 thick; shape index 1.55 (1.25-2.14); nipple-shaped Stieda body; prominent, substieda body. Sporocyst residuum present, 2 x 1, consisting of many coarse granules in a compact mass not bound by a membrane. Sporozoites sausage-shaped with blunted ends, centrally located nucleus and one terminal, refractile body, and arranged loosely, side by side in sporocyst.

Type host: *Leiothrix lutea* (Scopoli, 1786), Red-billed Leiothrix or Pekin Robin, alive and currently housed at the Dallas Zoo.

Type Locality: Dallas Zoo, Dallas County, Dallas, Texas, USA. The original collection site of the birds is not known but thought to be the Hawaiian Islands.

Type specimens: phototypes and buffered formalin preserved syntypes of *Isospora leiothrixi* have been deposited in the U.S. National Parasite Museum in Beltsville, Maryland as USNPC No. 84917 (phototypes) and USNPC No. 84918 (syntypes).

Fig. 1. Composite line drawing of sporulated oocyst of *Isospora leiothrixi* sp. n. from *Leiothrix lutea*. Bar -10 µm

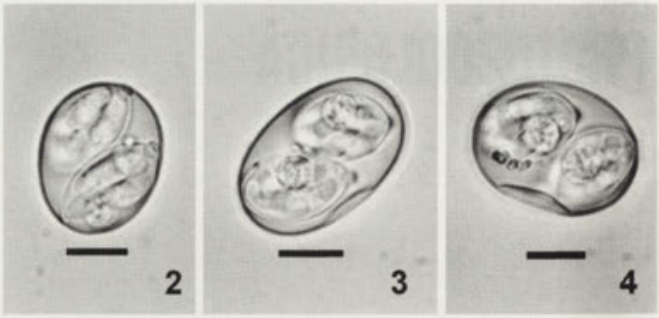

Figs. 2-4. Photomicrographs of sporulated oocysts of *Isospora leiothrixi* sp. n. 2 - note nipple-shaped Stieda body and prominent substieda body, 3 - full lateral view of oocyst with partially collapsed wall. Note subspherical sporocyst residuum and sporozoite with large central nucleus, 4 - partially collapsed oocyst with fragmented polar granule. Bars - 10 µm

Site of infection: unknown, oocyst recovered in faecal contents.

Prevalence: 2/3 *L. lutea* housed at the Dallas Zoo were passing oocysts.

Etymology: the specific epithet reflects the host genus.

DISCUSSION

Marquardt (1973) points out that some coccidiologists believe that members of the genus *Isospora* infecting birds have a lower degree of host specificity than do members of the genus *Eimeria*. Although reports of the same isosporan parasite infecting several different species of avian hosts are few, they usually show that the hosts sharing the same parasite are closely related genetically, occupying the same genus or family (Anwar 1966, Barré and Troncy 1974). Indeed, sympatric host subspecies have been shown to share the same coccidian parasite (McQuistion and Capparella 1992, 1994). Levine (1982) concluded that a coccidian species may be transmissible from one host species to another in the same genus, but until otherwise demonstrated, the parasite will not infect hosts of different genera within the same family. Consequently, sporulated oocysts of newly discovered coccidian species should be viewed with caution and routinely compared with oocyst descriptions of other coccidian species from the same host species or hosts living sympatric with the host species especially if the host species occupy the same family or genus.

Unfortunately, the capture location of *L. lutea* is not known. Most likely, it is the Hawaiian Islands because

Table 1. Isosporan Parasites from Passeriform Birds from Hawaii

Parasite	Host		Oocyst (µm)		Reference
Species	Genus	(Family)	Shape*	Avg. (Range)	
I. brayi	*Zosterops japonicus*	(Zosteropidae)	S-SS	27x26 (26-28x25-27)	Levine et al. 1980
I. manoaensis	*Zosterops japonicus*	(Zosteropidae)	S-SS	28x26.5 (26-31x23-29)	Upton et al. 1988
I. mejiro	*Zosterops japonicus*	(Zosteropidae)	S-SS	28.5x27 (25-32x25-30)	Upton et al. 1988
I. ivensae	*Lonchura punctulata*	(Passeridae)	S-SS	26x25 (N/A)	Levine et al. 1980
I. lyonensis	*Lonchura punctulata*	(Passeridae)	S-SS	24x23 (21-27x21-27)	Upton et al. 1988
I. cardinalis	*Cardinalis cardinalis*	(Fringillidae)	S-SS	24x23 (22-26x20-25)	Levine et al. 1980
I. loxopis	*Loxops virens*	(Fringillidae)	S-SS	26x23 (25-26x22-25)	Levine et al. 1980
I. phaeornis	*Phaeornis obscurus*	(Muscicapidae)	E	27x19 (25-28x18-20)	Levine et al. 1980
I. leiothrixi	*Leiothrix lutea*	(Sylviidae)	E	28x18.6 (24-32x15-21)	This study

* S-SS - spherical to subspherical, E - ellipsoidal, N/A - not available

they are one of the States in the United States, and *L. lutea* are abundant in Hawaii so the hosts would be easily available for the Dallas Zoo.

To date, 8 species of *Isospora* have been reported in birds that live sympatrically with *L. lutea,* all from Hawaii (Table 1). All the birds are members of different families than *L. lutea.* The sporulated oocysts of 7 isosporan species from Hawaiian birds are spherical to subspherical and contain sporocysts with very different Stieda bodies, substiedal bodies and sporozoites from those of *I. leiothrixi.* Although *I. phaeornis* is the only isosporan species with ellipsoidal oocysts and similar in size and shape with *I. leiothrixi. Isospora leiothrixi* has prominent nipple-shaped Stieda bodies on sporocysts with distinctly, large, substiedal bodies and a coarse residuum that does not appear to be membrane bound. These oocyst characteristics coupled with the fact that *I. leiothrixi* and *I. phaeornis* were found in hosts from different genera and families lead to the conclusion that these two isosporan parasites are distinct species.

Acknowledgments. We thank Mr. Scott Jenkins for the composite line drawing of *Isospora leiothrixi* and Ms. Marsha Funneman for her excellent technical assistance.

REFERENCES

Anwar M. (1966) *Isospora lacazei* (Labbe, 1893) and *I. chloridis* sp. n. (Protozoa: Eimeriidae) from the English sparrow (*Passer domesticus*), greenfinch (*Chloris chloris*) and chaffinch (*Fringilla coelebs*). *J. Protozool.* **13:** 84-90

Barré N., Troncy P. M. (1974) Note sur une coccidie rencontrés chez quelques Ploceidae du Tchad: *Isospora xerophila* n. sp. *Z. Parasitenk.* **44:** 139-147

Levine N. D. (1982) *Isospora passeris* n. sp. from the house sparrow *Passer domesticus, I. lacazei,* and related apicomplexan protozoa. *Trans. Am. Microsc. Soc.* **101:** 66-74

Levine N. D., Van Riper S., Van Riper C. III. (1980) Five new species of *Isospora* from Hawaiian birds. *J. Protozool.* **27:** 258-259

Marquardt W. C. (1973) Host and Site Specificity in the Coccidia. In: The Coccidia (Eds. D. M. Hammond, P. L. Long), University Park Press, London 23-43

McQuistion T. E., Capparella A. P. (1992) Two new coccidian parasites from the slate-colored grosbeak (*Pitylus grossus*) of South America. *J. Parasitol.* **78:** 805-807

McQuistion T. E., Capparella A. P. (1994) Two new species of *Isospora* (Apicomplexa: Eimeriidae) from ovenbirds (Passeriformes: Furnariidae) of South America. *Trans. Am. Microsc. Soc.* **113:** 90-95

Sibley C. G., Monroe B.L. Jr. (1990) Distribution and Taxonomy of Birds of the World. Yale University Press, London

Upton S. J., Marchiondo A. A., Williams R. N. (1988) New species of *Isospora* (Apicomplexa: Eimeriidae) from passeriform birds of Hawaii. *Syst. Parasitol.* **12:** 81-85

Received on 21st June, 1995; accepted on 10th August, 1995

ACTA
PROTOZOOLOGICA

Acta Protozoologica (1996) 35: 77 - 86

Three New Species of Septate Gregarines (Apicomplexa: Sporozoea) of the Genus *Gregarina* Dufour, 1828 from Insects

Tapas SENGUPTA* **and Durga Prasad HALDAR**

Protozoology Laboratory, Department of Zoology, University of Kalyani, Kalyani, W.B., India

Summary. This paper deals with the morphology and life history of three new species of septate gregarines (Apicomplexa: Sporozoea) under the genus *Gregarina* Dufour, 1828 in the gut of coleopteran, orthopteran and hemipteran insects collected from different economically important plants of West Bengal, India. The parasites are *Gregarina hyashii* sp. n. from *Coccinella transversalis*, *Gregarina vannucephala* sp. n. from *Gryllodes* sp. and *Gregarina coptosomae* sp. n. from *Coptosoma* sp.

Key words: *Apicomplexa, Gregarina*, Insecta, Sporozoea.

Abbreviations: TL - total length, LE - length of epimerite, LP - length of protomerite, LD - length of deutomerite, LN - length of nucleus,WE - width of epimerite, WP - width of protomerite, WD - width of deutomerite, WN - width of nucleus.

INTRODUCTION

In course of our studies on the cephaline gregarines from field pests of different parts of West Bengal with wide variations in their climatic conditions, we have obtained three different species of the genus *Gregarina* from insect pests of three separate orders collected from three economically important plants viz., Tea (*Camelia sinensis*) from hilly areas of Darjeeling and Bamboo (*Bambusa aurundinaceae*) and Mulberry plants (*Morus indica*) from Berhampore of West Bengal. The parasites differ markedly from each other and also from the ones described earlier under the same genus.

MATERIALS AND METHODS

The host insects were collected from different host plants and brought alive to the laboratory for investigations. The insects were decapitated, their guts carefully dissected out under a dissecting binocular and gently pressed for the parasites to come out from the gut lumen. Their smear preparations were fixed in Schaudinn's fluid and subsequently stained with Heidenhain's haematoxylin. Portions of midgut of infected hosts were fixed in Bouin's fluid and histological sections were studied for any intracellular developmental stage of the parasites. Cysts were collected from the hind gut of infected hosts and cultured in moist chamber for sporulation (Sprague 1941).

The ratios used in this paper are those of length of protomerite to total length (LP:TL) and width of protomerite to width of deutomerite (WP:WD). Measurements of all figures in the text, unless otherwise mentioned, are in micrometers (μm).

*Present address: Organon Research Centre, 7, Wood Street, Calcutta 700016 , India.

Address for correspondence: D. P. Haldar, Protozoology Laboratory, Department of Zoology, University of Kalyani, Kalyani 741235, West Bengal, India

Slides bearing the holotype and paratype materials are presently deposited at the Protozoology Laboratory, Department of Zoology, University of Kalyani and will later be submitted to the national collection of Zoological Survey of India, Calcutta.

RESULTS

Gregarina hyashii sp. n.

Host: *Coccinella transversalis*

Prevalence: 22% insect hosts are infected with this gregarine.

Development: earliest developmental stage has been detected in the epithelial cells of the midgut as a spherical body with a rounded nucleus having peripherally placed nucleolus. The infected cell shows a clear area around the parasite.

Trophozoite: solitary, ovoidal and opaque white in color when freshly viewed. It measures 31.9-57.5 in total length. The epimerite is a simple knob- or papilla-like structure (Fig. 1) measuring 2.2-6.2 x 1.3-5.7. The subspherical protomerite measures 6.7-10.8 x 10.8-16.2 while the deutomerite is obese in shape with a broadly rounded posterior extremity. The cytoplasm is finely granulated in protomerite and epimerite but moderately granulated in deutomerite. The pellicle is thin and epicyteal striations are not observable. The nucleus is spherical and the nucleoplasm is filled with masses of chromatin granules. Nucleus measures 5.4-10.5 x 6.7-9.4.

Sporadin and association: some sporadins (Figs. 4, 5) are elongated in shape with tongue-like protomerite, flat and elongated deutomerite with coarse granules and with ellipsoidal nucleus possessing heavy chromatin granules located in the middle of deutomerite. Other sporadins (Figs. 2, 3) are ovoidal in shape with hemispherical protomerite, obese deutomerite with rounded posterior end and the nucleus here is spherical with prominent nuclear membrane and a clear nucleolus located more anteriorly to the deutomerite. Cytoplasm is uniformly granulated throughout the proto- and deutomerite. Pellicle is thick and epicyteal striations are not discernable.

The association (syzygy) between two sporadins is always caudofrontal in nature (Figs. 6, 7). The contact between primite and satellite is very firm. The protomerite of the primite is hemispherical or conical while that of the satellite is flat.

Gametocyst and spore: freshly collected gametocyst (Fig. 8) is milky white in color. The cyst encloses two equal-sized gametocytes and appears as spherical, double-walled bodies measuring 370 x 351 in dimension. The gap between the two walls is 10.3. After 7 h of development inside the moist chamber the partition wall between the two gametocytes disappears and three blunt sporoducts develop through which after 54 h of development the spores are liberated. The double-walled, more or less rounded spores (Fig. 9) measure 5.9 x 5.4 in diameter. Thirteen hours after the release, 8 husk-shaped sporozoites are developed inside each spore and arranged in a circular fashion.

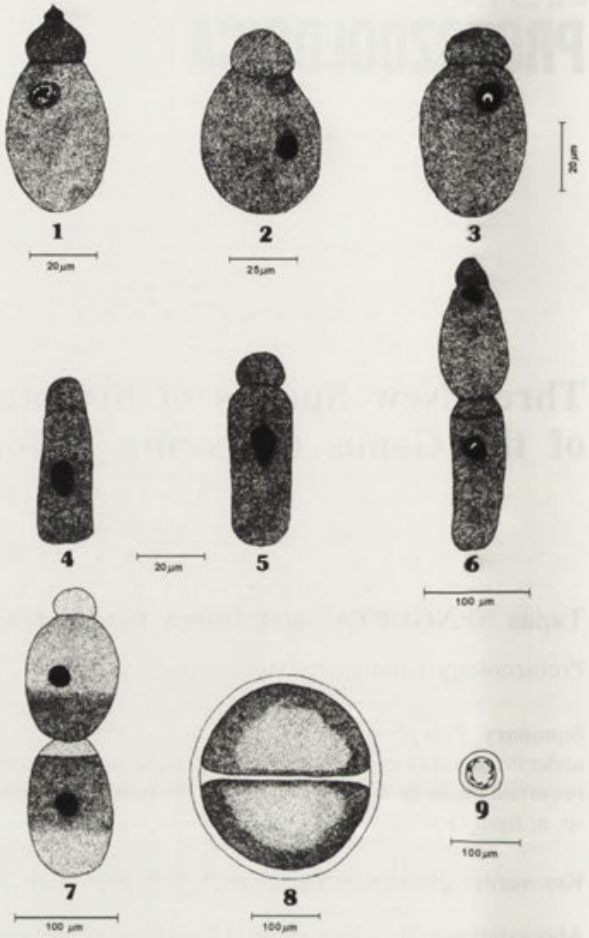

Figs. 1-9. Camera Lucida drawings of *Gregarina hyashii* sp. n. 1-trophozoite, 2-5 - sporadins of different shapes and sizes, 6-7 -sporadin in syzygy, 8 - gametocyst, 9 - spore

Measurements: Table 1 shows details of measurements of different parts of 20 individuals of *Gregarina hyashii* sp. n.

Holotype: of trophozoite on slide no. DB/IV, prepared by T. Sengupta on March 29, 1985.

Paratype: many on the above numbered slide and on other slides, prepared on different dates; other particulars are the same as for the holotype material.

Affinities: some of the characters of *G. ovata* Dufour, 1828 like shape of the epimerite, protomerite, nucleus, cyst and WP:WD ratio show similarities with those of the present form, but it differs, in having rounded spores, from *G. ovata* where these are cylindrical. It also has some affinities with *G. alcidessi* Haldar and Chakraborty, 1978 so far as the structures of epimerite, protomerite and LP:TL values are concerned. But in *G. alcidessi* both gametocyst and spores are ovoidal while in the newly reported form the cyst is spherical and the spore is rounded. The present form also bears similarities with *G. cocconellae* Lipa, 1967 in WP:WD ratios but differs widely in all other aspects. The differences, therefore, justify the creation of a new species and the name *Gregarina hyashii* sp. n. is proposed for it after the name of the eminent protozoologist Hyashi Hoshide (Table 3).

***Gregarina vannucephala* sp. n.**

Host: *Gryllodes* sp.

Prevalence: 27% insects are infected with this gregarine.

Development: extracellular.

Trophozoite: elongated, broadly ovoidal in shape measuring 21.3- 27.2 in total length. The epimerite is characteristically fanshaped with a small stalk at its base (Fig. 10) which is 0.5-1.6 x 0.8-2.1 in dimension. Protomerite is hat-shaped and slightly constricted at its base. The deutomerite is flat, elongated with greatly rounded posterior end. Posteriorly located nucleus is squarish in shape. Cytoplasm is finely to moderately granulated throughout the whole body. Pellicle is thick and epicyteal striations are not observable.

Sporadin and association: sporadins (Figs. 11, 12) are solitary as well as biassociative; elongated to conical in shape with broadly rounded or narrow posterior extremity measuring 24.4-58.7 in total length. The protomerite is flat to ellipsoidal in shape with irregular outline. It is 2.5 times broader than long and contains some condensed spots. The deutomerite is elongated or conical in shape with high amount of cytoplasm. Nucleus vary in shape and position. In caudo-frontal association (Figs. 13-15) the attachment is very firm. The satellite is larger than the primite. The protomerite of the primite is hemispherical to ellipsoidal while that of satellite is triangular or squarish in shape. The nucleus with condensed chromatin granules located anteriorly in primite and posteriorly in the satellite.

Gametocyst and spore: freshly collected gametocysts are yellowish white but with maturation, become greyish. Double-walled, rounded gametocyst (Fig. 16) measures

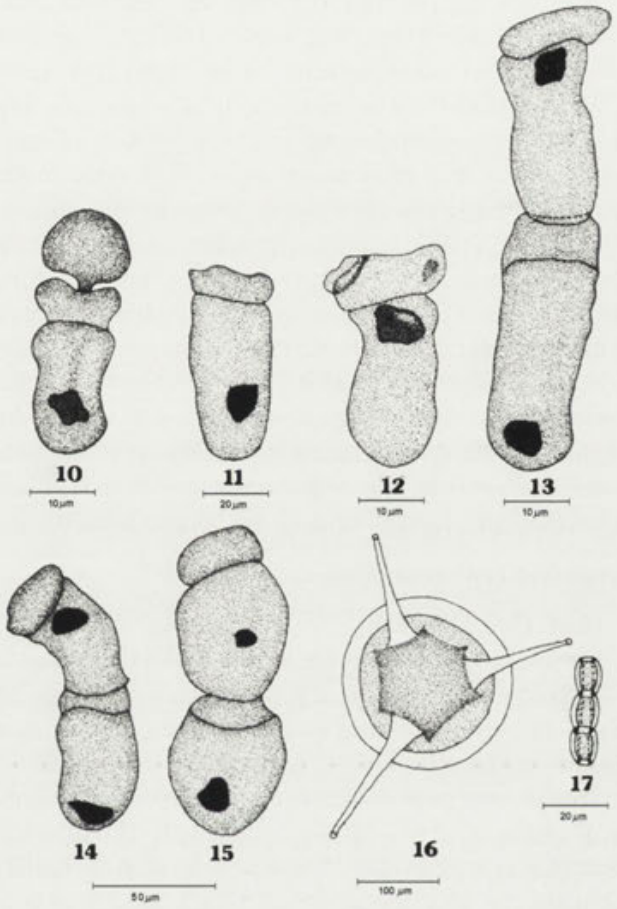

Figs. 10-17. Camera Lucida drawings of *Gregarina vannucephala* sp. n. 10 - a fully grown trophozote, 11-12 - elongated sporadins, 13-15 - sporadins in syzygy, 16 - gametocyst with three sporoducts, 17- barrel-shaped spores in chain

211.1 in diameter. At about 14 h of development inside the moist chamber three concave depressions appear on the cyst surface. Within next 12 h three sporoducts develop of which two are shorter each measuring 133.3 in length and the larger one measures 166.6 in length. After 46 h of development double-walled, barrel-shaped spores are liberated in chains and they measure 5.7 x 2.4 in dimension (Fig. 17). Eighteen hours after sporulation eight dot-like sporozoites are developed in each spore and arranged in two rows.

Measurements: Table 4 shows details of measurements of different parts of 20 individuals of *Gregarina vannucephala* sp. n.

Holotype: of trophozoite on slide no. OB/I, prepared by T. Sengupta on September 5, 1984.

Paratype: many, on the above-numbered slide and on other slides, prepared on different dates; other particulars are the same as for the holotype material.

Affinities: the present form possesses some similarities with *G. gryllodesii* Haldar and Sarkar, 1980 in having same host, extracellular development, barrel-shaped spores and in WP:WD ratio. But it differs widely in all other characters. This gregarine also possesses resemblance with *G. macrocephala* Labbé, 1899 in having a short neck in the epimerite-protomerite junction and also in the ratios of LP:TL and WP:WD, however, the differences between the two are marked in overall shape of the sporadin, gametocyst and spore as well as regarding host. Its shape of the spore and WP:WD ratio show some similarity with those of *G. kingi* Crawley, 1907, but it differs in all other aspects. It is therefore, considered as new to science for which the name *Gregarina vannucephala* sp. n. is given, for the characteristic fan-shaped epimerite which is hitherto undescribed in any species of the genus (Table 6).

***Gregarina coptosomae* sp. n.**

Host: *Coptosoma* sp.

Prevalence: 34% hosts are infected with this parasite.

Development: earliest stage of development is intracellular with a slightly elongated body containing a deeply-stained spherical nucleus located centrally.

Trophozoite: large-sized cylindrical trophozoites (Figs. 18, 19) measure 166.4-270.4 in total length. The spherical knob-like epimerite takes a deep stain with iron-alum haematoxylin and measures 12.5-18.7 x 12.5-14.6 in dimension. Petal-shaped protomerite bears a small notch on one side. The long cylindrical deutomerite ends in a sharply rounded base. A round or spherical nucleus with clear nuclear membrane and a hollow space at its centre is located at the posterior portion of the deutomerite. The epicyteal striations are not clearly seen in the deutomerite and it contains darkly-stained, dispersed cytoplasmic granules

Sporadin and association: sporadins are both solitary and biassociative. Former forms are cylindrical with bluntly rounded posterior extremity (Fig. 20) measuring 187.2-257.9 in total length. The subspherical protomerite measures 29.1-60.3 in length and 25-58.2 in width. The broadly obese deutomerite contains an ellipsoidal nucleus at its anterior part. The thick pellicle is uniformly granulated with coarse cytoplasmic granules. A thicker concave septum separates the deutomerite from the protomerite. Deutomerite measures 149.8-212.2 in length and 37.4-106.1 in width.

Association is always caudo-frontal (Figs. 21, 22). The protomerite of the primite and the deutomerite of the satellite are coarsely granulated with deeply-stained granules. The semilunar nucleus is located posteriorly in the deutomerite of both the partners. The primite and the satellite move in opposite directions and gradually assume rounded appearance ultimately leading to the formation of gametocyst (Figs. 23-26).

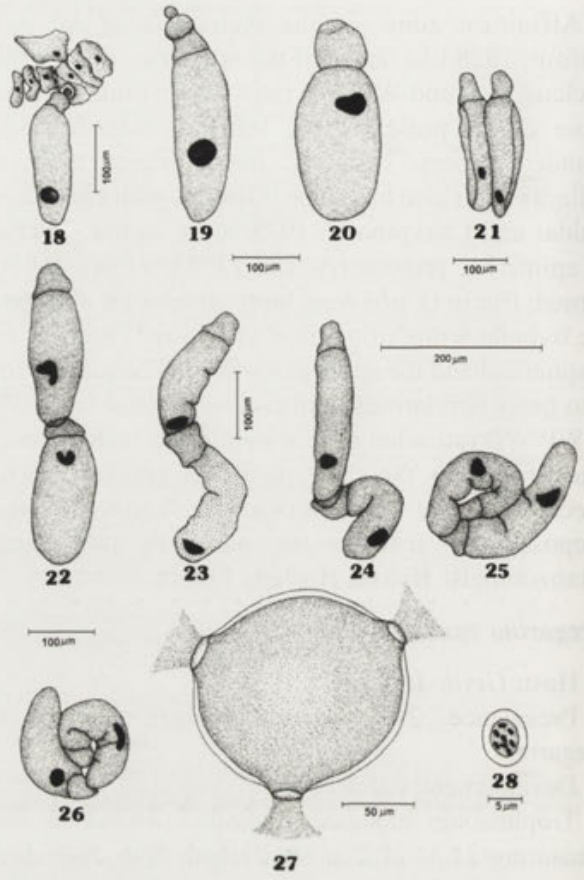

Figs. 18-28. Camera Lucida drawings of *Gregarina coptosomae* sp. n. 18, 19 - cylindrical trophozoites, 20 - mature sporadin, 21, 22 - sporadins in syzygy, 23-26 - movement of primite and satellite to form gametocyst, 27 - gametocyst with three distinct perforations, 28 - ovoidal spore

Gametocyst and spore: freshly collected gametocysts are opaque white in color with a distinct outer membrane. These are double-walled and spherical in shape measuring 156.6 in dimension (Fig. 27). The gap between the two walls is 6.2. After 82 h of development inside the moist chamber three distinct perforations are formed through which the spores are liberated at about 110 h of development. The diameter of each pore is 20.6 and these act as blunt sporoducts.

The ovoidal spores (Fig. 28) measure 7.7 x 3.9 in dimension. The gap between the two walls of the spore is 1.1-1.7. Each spore contains eight pea-shaped sporozoites arranged in an irregular fashion.

Measurements: Table 7 shows details of measurements of different parts of 20 individuals of *Gregarina coptosomae* sp. n.

Holotype: of trophozoite on slide no. AB/I, prepared by T. Sengupta on September 20, 1984.

Paratype: many, on the above-numbered slide and on other slides, prepared on different dates; other particulars are the same as for the holotype material.

Affinities: the occurrence of *Gregarina* spp. is very rare in hemipteran insects. So far, only one species of *Gregarina*, *G. lygeusi* Haldar, Ray and Gupta, 1982 has been reported from *Lygeus hospes* of the order Hemiptera. The present form exhibits some relationship with *G. lygeusi* in WP:WD ratio and in the shape of the epimerite, but it widely differs in all other aspects. It has also superficial similarities with *G. alcidesii* in LP:TL ratio, in the shape of the epimerite and the spore. But in *G. alcidesii* the gametocyst is ovoidal and the sporoducts are very long. Considering all these features it is concluded that the present gregarine is a new one for which it is designated as *Gregarina coptosomae* sp. n. after the name of its host insect, *Coptosoma* sp. (Tables 9, 10).

DISCUSSION

In majority of cases the systematics of septate gregarines, as established by various researchers, have been determined by certain parameters like measurements of trophozoites or gammonts, their ratios as well as type hosts. Richardson and Janovy (1990) for the first time showed the relationships between total length and other trophozoite measurements in terms of regression lines and correlation coefficients. Here also we have considered the same parameters (Tables 2, 5 and 8) and found that although measurements are positively and significantly correlated with total length, the different correlation coefficients indicate that most increases in size with age are because of the lengthening of the deutomerite.

So far as histopathological observations are concerned, the sections of the host's gut reveal certain features due to invasion of the parasites. In the cases of *G. hyashii* and *G. coptosomae*, where early development is internal, a clear 'halo' is observed around the parasite. The nuclei of the infected cells are displaced and there is increased basophilia thereby indicating some possibilities of the changes in the secretory habits of these cells. However, it is not known whether the infected cells recover these damages after the release of the intracellular parasites into the host gut lumen. Further research is therefore, needed to have some clear idea about the histopathological damage of the insect hosts due to gregarine infection which can throw some light in the possible role of gregarines on the biological control of insect pests.

Acknowledgements. The authors are grateful to the Council of Scientific and Industrial Research, New Delhi for awarding a fellowship to one of them (TS).

APPENDIX

Table 1. Showing details of measurements (in µm) of the different parts of 20 individuals of *Gregarina hyashii* sp. n.

Serial No.	TL	LE	LP	LD	LN	WE	WP	WD	WN	LP:TL	WP:WD
1.	51.8	2.7	10.8	38.3	8.6	5.4	16.2	29.4	9.4	1:4.8	1:1.8
2.	57.5	6.2	10.0	41.3	10.5	5.7	14.6	21.3	7.8	1:5.8	1:1.5
3.	31.9	2.2	6.7	22.9	5.4	1.3	10.8	13.5	6.7	1:4.7	1:1.2
4.	53.7	-	10.5	43.2	8.4	-	11.6	16.2	8.1	1:5.1	1:1.4
5.	48.6	-	11.1	37.5	5.1	-	13.2	27.3	5.9	1:4.4	1:2.1
6.	48.6	-	11.3	37.3	5.4	-	12.1	21.6	4.9	1:4.3	1:1.8
7.	51.0	-	12.1	38.9	5.9	-	14.8	27.0	4.9	1:4.2	1:1.8
8.	83.9	-	13.8	70.2	8.1	-	21.6	37.8	10.3	1:6.1	1:1.7
9.	91.0	-	14.3	76.7	11.3	-	21.9	45.6	10.8	1:6.4	1:2.1
10.	51.0	-	12.9	38.1	4.0	-	11.6	17.5	5.4	1:3.9	1:1.5
11.	52.6	-	8.1	44.5	6.5	-	13.2	15.7	5.9	1:6.5	1:1.2
12.	56.7	-	10.8	45.9	7.5	-	15.9	23.5	8.1	1:5.2	1:1.5
13.	56.7	-	9.4	47.2	6.7	-	16.2	21.6	10.5	1:6.0	1:1.3
14.	57.2	-	12.1	45.1	7.3	-	10.8	27.0	10.8	1:4.7	1:2.5
15.	89.1	-	19.4	69.7	13.5	-	23.2	44.0	13.5	1:4.6	1:1.9
16.	56.7	-	9.7	46.9	8.1	-	15.9	26.5	8.1	1:5.8	1:1.7
17.	56.7	-	12.1	44.5	7.0	-	14.8	28.6	9.4	1:4.7	1:1.9
18.	46.2	-	8.4	37.8	8.1	-	11.1	15.9	5.1	1:5.5	1:1.4
19.	49.9	-	9.4	40.5	3.5	-	10.8	21.6	4.3	1:5.3	1:2.0
20.	55.1	-	15.9	39.1	7.0	-	13.5	29.9	9.2	1:3.5	1:2.2

Table 4. Showing details of measurements (in μm) of the different parts of 20 individuals of *Gregarina vannucephala* sp. n.

Serial No.	TL	LE	LES	LP	LD	LN	WE	WES	WP	WD	WN	LP:TL	WP:WD
1.	27.7	8.1	1.6	4.9	13.0	5.7	8.1	2.1	8.1	9.8	5.2	1:5.7	1:1.2
2.	21.3	4.9	0.8	3.3	12.2	5.7	5.2	1.1	8.1	8.1	5.7	1:6.5	1:1.0
3.	28.2	4.9	0.5	8.1	14.7	5.9	5.7	0.8	10.9	9.8	4.1	1:3.5	1:0.9
4.	37.5	-	-	14.7	22.8	4.9	-	-	18.7	16.3	4.6	1:2.6	1:0.9
5.	39.1	-	-	7.3	31.8	7.3	-	-	17.4	14.3	4.7	1:5.3	1:0.8
6.	42.4	-	-	9.8	32.6	6.5	-	-	21.1	14.7	6.5	1:4.3	1:0.7
7.	50.5	-	-	9.8	40.7	6.8	-	-	23.1	22.0	4.1	1:5.2	1:0.9
8.	37.5	-	-	4.9	32.6	8.1	-	-	19.2	15.5	4.9	1:7.7	1:0.8
9.	40.4	-	-	9.8	30.6	7.3	-	-	21.2	14.7	3.3	1:4.1	1:0.7
10.	50.5	-	-	8.1	42.4	7.3	-	-	28.5	18.7	6.5	1:6.2	1:0.7
11.	40.4	-	-	8.1	32.6	6.2	-	-	14.7	13.0	4.9	1:5.0	1:0.9
12.	24.4	-	-	4.9	19.6	4.9	-	-	13.0	10.6	4.9	1:5.0	1:0.8
13.	47.3	-	-	8.9	38.3	8.1	-	-	23.6	18.7	4.9	1:5.3	1:0.8
14.	37.5	-	-	8.1	29.3	7.3	-	-	13.0	16.3	8.1	1:4.6	1:1.2
15.	56.2	-	-	9.8	46.4	4.9	-	-	21.2	26.9	6.5	1:5.7	1:1.3
16.	58.7	-	-	11.4	47.3	6.5	-	-	23.6	29.3	11.4	1:5.1	1:1.2
17.	39.1	-	-	8.1	30.9	4.9	-	-	22.0	17.1	5.2	1:4.8	1:0.8
18.	24.4	-	-	9.6	14.8	3.3	-	-	9.0	7.8	4.9	1:2.5	1:0.9
19.	47.3	-	-	11.4	35.9	6.5	-	-	31.8	26.1	5.9	1:4.1	1:0.8
20.	45.6	-	-	8.1	37.5	5.7	-	-	17.9	17.1	4.9	1:5.6	1:0.9

Table 7. Showing details of measurements (in μm) of the different parts of 20 individuals of *Gregarina coptosomae* sp. n.

Serial No.	TL	LE	LP	LD	LN	WE	WP	WD	WN	LP:TL	WP:WD
1.	166.4	18.7	38.3	109.4	15.8	14.6	41.6	62.4	19.9	1:4.3	1:1.5
2.	270.4	12.5	54.1	203.8	24.9	12.5	47.8	76.9	31.2	1:5.0	1:1.6
3.	257.9	-	60.3	197.6	22.9	-	58.2	106.1	30.3	1:4.3	1:1.8
4.	199.7	-	45.8	153.9	16.6	-	41.6	62.4	16.6	1:4.4	1:1.5
5.	228.8	-	54.1	174.7	24.9	-	36.4	56.2	21.6	1:4.2	1:1.5
6.	191.4	-	33.3	158.1	20.8	-	39.5	58.2	12.4	1:5.7	1:1.4
7.	228.8	-	58.2	170.6	24.9	-	41.6	58.2	23.3	1:3.9	1:1.4
8.	199.7	-	49.9	149.8	25.0	-	37.4	49.9	20.8	1:4.0	1:1.3
9.	249.6	-	38.4	212.2	20.8	-	45.8	66.6	23.7	1:6.7	1:1.5
10.	216.3	-	33.3	183.0	16.6	-	33.3	45.8	12.5	1:6.5	1:1.3
11.	232.9	-	37.4	195.5	18.7	-	37.4	54.1	16.7	1:6.2	1:1.6
12.	187.2	-	37.4	149.8	22.9	-	45.8	74.9	20.8	1:5.0	1:1.6
13.	232.9	-	37.4	195.5	10.4	-	41.6	58.2	14.6	1:6.2	1:1.4
14.	228.8	-	33.3	195.5	12.5	-	33.3	49.9	12.5	1:6.9	1:1.5
15.	228.8	-	29.1	199.7	12.5	-	37.4	66.6	18.7	1:7.9	1:1.8
16.	203.8	-	29.1	174.7	20.8	-	33.3	60.3	16.6	1:7.0	1:1.8
17.	208.0	-	37.4	170.6	16.6	-	25.0	37.4	14.6	1:5.6	1:1.5
18.	197.6	-	33.3	160.2	21.6	-	37.4	58.2	20.8	1:5.9	1:1.5
19.	191.4	-	29.1	162.2	21.2	-	33.9	47.8	16.6	1:6.5	1:1.4
20.	212.2	-	31.2	180.9	20.3	-	39.5	60.3	19.9	1:6.8	1:1.5

Table 3. Showing comparative characters of four species of *Gregarina* Dufour (in µm)

Characters	*Gregarina ovata*	*Gregarina coccinellae*	*Gregarina alcidessi*	*Gregarina hyashii* sp.n.
Total length	336-593	102-179	52.5-350	46.2-91
Epimerite	-	Large, papilla-like	Knob-like,length 5	Simple knob or papilla-like,length 3.7
Sporadin	Biassociative	Biassociative	Biassociative	Biassociative
Gametocyst	Oval,400-600 in diameter	Oval,115 in diameter	Ovoidal, sporoduct length 30	Spherical,with three blunt sporoducts
Spore	Cylindrical, 16x7.5	Spindle-shaped, 12x7, liberated in chains	Oval, 6x5, sporozoites ovoidal and arranged irregularly	Rounded, 5.9x5.4, huskshaped sporozoites arranged in circular fashion
LP : TL	1:8.6	1:7.3	1:5.5	1:5.1
WP : WD	1:1.9	1:1.7	1:1.2	1:1.7
Host	*Forficula auricularia* L.	*Coccinella septempunctata* L.	*Alcides leopardus* ol	*Coccinella transversalis*
Locality	France and Germany	Poland	Kalyani, India	Darjeeling, India
Reference	Dufour (1828)	Lipa (1967)	Haldar and Chakraborty (1978)	Present study

Table 6. Showing the comparative characters in different species of *Gregarina* Dufour, from gryllid hosts (in µm)

Characters	*G. macrocephala*	*G. kingi*	*G. tahitiensis*	*G. gryllodesii*	*G. vannucephala* sp. n.
Total length	-	-	Cephalin - 100, Sporadin - 250	Cephalin - 84, Sporadin - 400	Cephalin 21.3-28.2, Sporadin - 24.4-58.7
Epimerite	Large, hyaline, ovoidal	-	-	Small, conical	Characteristically fan-shaped
Syzygy	Biassociative	Biassociative	-	Biassociative	Biassociative, firm caudofrontal attachment
Nucleus	-	Small, spherical, endocyte not dense	-	Spherical	More or less squarish
Gametocyst	Spherical, dehisces by sporoduct	Spherical,maximum diameter 110, one sporoduct only	-	Spherical, 168 in diameter seven to ten short sporoducts	Rounded, 211.1 in in dimension, two short and one long sporoducts

Table 6 (cont.)

Spore	Dolioform	Barrel-shaped, 2.5x5 in dimension	-	Barrel-shaped, 8.7x6 in size, extruded in chains	Barrel-shaped, 5.7x2.4 in dimension, liberated in chains
LP:TL	1:5	1:3	-	1:5.7	1:2.5-7.7
WP:WD	1:1.2	1:1	-	1:1.1	1:0.7-1.3
Host	*Liogryllus campestris*	*Gryllus abbreviatus* Serv.	*Gryllodes sigillatus*	*Gryllodes* sp.	*Gryllodes* sp.
Locality	France	USA	France	India	India
Reference	Labbé(1899)	Crawley (1907)	Corbel (1968)	Haldar and Sarkar (1980)	Present study

Table 9. Showing comparative characters of *Gregarina coptosomae* sp. n. and other two related species of the genus *Gregarina* Dufour (in µm)

Characters	*Gregarina alcidesii*	*Gregarina lygeusi*	*Gregarina coptosomae* sp. n.
Total length	52.5-350	178.9-324.5	187.2-257.9
Epimerite	Knob-like, length 5	Globular, 13.2 in length	Spherical knob-like, 15.6 in length
Nucleus	Spherical	Spherical	Spherical or rounded
Sporadin	Biassociative	Biassociative	Solitary as well as biassociative
Gametocyst	Ovoidal, sporoducts 30 in length dehisces at about 36 hours of development	Ovoidal, fresh ones orange-coloured, four sporoducts, about 50 in length, dehisces at about 48 hours of development	Spherical, opaque white when freshly collected, three very blunt sporoductsdevelop, dehisces at about 110 hours of development
Spore	Oval, 6x5 in size, sporozoites form 8 hours after development	Dolioform, laterally compressed spores, sporozoites form 7 hours after dehiscence, spores come out in long chain	Ovoidal, 7.7x3.9 in size, eight pea-sharped sporozoites arranged in irregular fashion
LP:TL	1:5.5	1:6.1	1:5.7
WP:WD	1:1.2	1:1.6	1:1.5
Host	*Alcides* sp. nr. *leopardus* ol.	*Lygeus hospes* Fabricius	*Coptosoma* sp.
Locality	Kalyani, India	Kalyani, India	Berhampore, India
Reference	Haldar and Chakraborty (1978)	Haldar, Ray and Gupta (1982)	Present study

Table 10. Comparative characters of three new species of *Gregarina* Dufour, presented in this paper (in µm)

Characters	*Gregarina hyashii* sp. n.	*Gregarina vannucephala* sp. n.	*Gregarina coptosomae* sp. n.
Total length	46.2-91	24.4-58.7	187.2-257.9
Epimerite	Simple knob or papilla-like 2.2-6.2 in length	Fan-shaped, 4.9-8.1 in length	Spherical knob-like, 12.5-18.7 in length
Deutomerite	Obese with broadly rounded posterior extremity, no epicyteal striations	Elongated or conical, no epicyteal striation	Long cylindrical or obese
Nucleus	Spherical to ellipsoidal	Variable in shape	Spherical to ellipsoidal
Sporadin	Biassociative	Biassociative	Biassociative
Gametocyst	Spherical, milky white, dehiscence by three blunt sporoducts, 369.9x351 in dimension	Rounded, yellowish white, dehiscence by three sporoducts one long and two short, 211.1 in diameter	Spherical, opaque white, dehiscence by three highly blunt sporoducts, 156.6 in dimension
Spore	Rounded, 5.9x5.4 in dimension	Barrel-shaped, 5.7x2.4 in dimension	Ovoidal, 7.7x3.9 in dimension
LP:TL	1:3.6-6.5 (1:5.1)	1:2.5-7.7 (1:4.9)	1:3.9-7.9 (1:5.7)
WP:WD	1:1.8-2.5 (1:1.7)	1:0.7-1.3 (1:0.9)	1:1.3-1.8 (1:1.5)
Host	*Coccinella transversalis* (F)	*Gryllodes* sp.	*Coptosoma* sp.
Locality	Darjeeling, India	Berhampore, India	Berhampore, India

Table 2. Showing relationship between protomerite and deutomerite sizes and total length in *Gregarina hyashii* sp. n. (n = 20)

Y-axis	X-axis	Regression line	r = correlation coefficient
LP	TL	Y = 0.15x + 3.04	0.74*
WP	TL	Y = 0.23x + 1.35	0.89
LD	TL	Y = 0.87x - 4.56	0.99
WD	TL	Y = 0.54x - 5.19	0.88

* All r values are significantly different from zero ($p < 0.05$)

Table 5. Showing relationship between protomerite and deutomerite sizes and total length in *Gregarina vannucephala* sp. n. (n=20)

Y-axis	X-axis	Regression line	r = correlation coefficient
LP	TL	Y = 0.14x + 2.93	0.55*
WP	TL	Y = 0.51x - 2.13	0.51
LD	TL	Y = 0.99x - 9.42	0.97
WD	TL	Y = 0.53x - 4.71	0.92

*All r values are significantly different from zero ($p < 0.05$)

Table 8. Showing relationship between protomerite and deutomerite sizes and the total length in *Gregarina coptosomae* sp. n. (n = 20)

Y-axis	X-axis	Regression line	r = correlation coefficient
LP	TL	Y = 0.17x + 3.63	0.43*
WP	TL	Y = 0.13x + 14.94	0.42
LD	TL	Y = 0.85x - 8.74	0.89
WD	TL	Y = 0.23x + 9.89	0.42

*All r values are significantly different from zero ($p < 0.05$)

REFERENCES

Corbel J.C. (1968) Gregarines nouvelles parasites d'orthopteres. *Bull. Mus. natn. Hist. nat., Paris, 2e serie*, **39:** 992-996

Crawley H. (1907) The polycystid gregarines of the United States. *Proc. Acad. Nat. Sc. Phila.* **59:** 220-228

Dufour L. (1828) Note sur la gregarine nouveau genve de ver qui vit en tropeau dans les intestines de elivers insects. *Ann. Sci. Nat.* **13:** 366-368

Haldar D. P., Chakraborty N. (1978) Observations on three new species of cephaline gregarines (Protozoa:Sporozoa) from insects. *Acta Protozool.* **17:** 233-244

Haldar D. P., Sarkar N. K. (1980) Studies on three new species of cephaline gregarines of the genus *Gregarina* Dufour, 1828 from Indian gryllids. *Arch. Protistenk.* **123:** 61-71

Haldar D. P., Ray S. K., Gupta S. K. (1982) Studies in the morphology and life history of *Gregarina lygeusi* n. sp., a new cephaline gregarine (Apicomplexa:Sporozoea) from *Lygeus hospes* Fabricius. *J. Beng. Nat. Hist. Soc.* **1:** 17-22

Labbé A. (1899) Sporozoa. In: "Das Tierreich", Friedlander, Berlin, **5:** 1-180

Lipa J. J. (1967) Studies on gregarines (Gregarinomorpha) of arthropods in Poland. *Acta Protozool.* **5:** 97-179

Richardson S., Janovy J., Jr. (1990) *Actinocephalus carrilynnae* n. sp. (Apicomplexa: Eugregarinorida) from the blue damselfly *Enallagma civile* (Hagen). *J. Protozool.* **37:** 567-570

Sprague V. (1941) Studies on *Gregarina blattarum* with particular reference to the chromosome cycle. *Ill. Biol. Monogr.* **18:** 5-57

Received on 24th June, 1994; accepted on 15th January, 1995

INSTRUCTIONS FOR AUTHORS

ACTA PROTOZOOLOGICA publishes original papers embodying the results of experimental or theoretical research in all fields of protistology with the exception of faunistic notices of local character and purely clinical reports. Short (rapid) communications are acceptable but also long review articles. The papers should be as concise as possible, bewritten in English. Submission of a manuscript to ACTA PROTOZOOLOGICA implies that it has not been submitted for publication elsewhere and that it contains unpublished, new information. There are no page charges except colour illustration. Names and addresses of suggested reviewers will be appreciated. In case of any question please do not hesitate to contact Editor. Authors should submit papers to:

Miss Małgorzata Woronowicz
Managing Editor of ACTA PROTOZOOLOGICA
Nencki Institute of Experimental Biology,
ul. Pasteura 3
02-093 Warszawa, Poland
Fax:(48) 22 225342

Organization of Manuscripts

Submissions

Please enclose three copies of the text, one set of original of line drawings (without lettering!) and three sets of copies with lettering, four sets of photographs (one without lettering). In case of photographs arranged in the form of plate, please submit one set of original photographs unmounted and without lettering, and three sets of plates with lettering.

The ACTA PROTOZOOLOGICA prefers to use the author's word-processor disks (3.5"and 5.25" format IBM or IBM compatible, and MacIntosh 6 or 7 system on 3.5" 1.44 MB disk only) of the manuscripts instead of rekeying articles. If available, please send a copy of the disk with your manuscript. Disks will be returned with galley proof of accepted article at the same time. Please observe the following instructions:

1. Label the disk with your name: the word processor/computer used, e.g. IBM; the printer used, e.g. Laserwriter; the name of the program, e.g. Wordperfect 5.1; and any special characters used, and how you obtained them (i.e. dedicated key pressed or printer control codes used directly).
2. Send the manuscript as a single file; do not split it into smaller files.
3. Give the file a name which is no longer than 8 characters.
4. Create and /or edit your manuscript, using the document mode (or equivalent) in the word-processor program.
5. If necessary, use only italic, bold, underline, subscript and superscript. Multiple font, style or ruler changes, or graphics inserted the text, reduce the usefulness of the disc.
6. Do not right-justify and use of hyphen at the end of line.
7. Avoid the use of footnotes.
8. Distinguish the numerals 0 and 1 from the letters O and l.

Text (three copies)

The text must be typewritten, doublespaced, with numbered pages. The manuscript should be organized into Summary, Key words, Abbreviations used, Introduction, Materials and Methods, Results, Discussion, Acknowledgments, References, Tables and Figure Legends. The Title Page should include the full title of the article, first name(s) in full and surname(s) of author(s), the address(es) where the work was carried out, page heading of up to 40 characters. The present address for correspondence, Fax, and E-mail should also be given.

Each table must be on a separate page. Figure legends must be in a single series at the end of the manuscript. References must be listed alphabetically, abbreviated according to the World List of Scientific Periodicals, 4th ed. (1963). Nomenclature of genera and species names must agree with the International Code of Zoological Nomenclature, third edition, London (1985) or International Code of Botanical Nomenclature, adopted by XIV International Botanical Congress, Berlin, 1987. SI units are preferred.

Examples for bibliographic arrangement of references:

Journals:

Häder D-P., Reinecke E. (1991) Phototactic and polarotactic responses of the photosynthetic flagellate, *Euglena gracilis*. *Acta Protozool.* **30:** 13-18

Books:

Wichterman R. (1986) The Biology of Paramecium. 2 ed. Plenum Press, New York

Articles from books:

Allen R. D. (1988) Cytology. In: Paramecium, (Ed. H.-D. Görtz).Springer-Verlag, Berlin, Heidelberg, 4-40

Zeuthen E., Rasmussen L. (1972) Synchronized cell division in protozoa. In: Research in Protozoology, (Ed. T. T. Chen). Pergamon Press, Oxford, **4:** 9-145

Illustrations

All line drawings and photographs should be labeled, with the first author's name written on the back. The figures should be numbered in the text as arabic numerals (e.g. Fig. 1). Illustrations must fit within either one column (86 x 231 mm) or the full width and length of the page (177 x 231 mm). Figures and legends should fit on the same page. Lettering will be inserted by the printers and should be indicated on a tracing-paper overlay or a duplicate copy.

Line drawings (three copies + one copy without lettering)

Line drawings should preferably be drawn about twice in size, suitable for reproduction in the form of well-defined line drawings and should have a white background. Avoid fine stippling or shading. Computer printouts of laser printer quality may be accepted, however *.TIF, *.PCX, *.BMP graphic formats on disk are preferred.

Photographs (three copies + one copy without lettering)

Photographs at final size should be sharp, with a glossy finish, bromide prints. Photographs grouped as plates (in size not exceeding 177 x 231 mm **including legend**) must be trimmed at right angles accurately mounted and with edges touching and mounted on firm board. The engraver will then cut a fine line of separation between figures. Magnification should be indicated. Colour illustration on transparent positive media (slides 60 x 45mm, 60 x 60mm or transparency) are preferred.

Proof sheets and offprints

Authors will receive one set of page proofs for correction and are asked to return these to the Editor within 48-hours. Fifty reprints will be furnished free of charge. Orders for additional reprints have to be submitted with the proofs.

Indexed in Chemical Abstracts Service, Current Contents (Agriculture, Biology and Environmental Sciences), LIBREX-AGEN, Protozoological Abstracts.

ACTA
PROTOZOOLOGICA

1996 FEBRUARY
VOLUME 35 NUMBER 1